Etude Multi-couches dans le système HSDPA

Mohamad Assaad

Thèse

présentée pour obtenir le grade de Docteur de

l'Ecole Nationale Supérieure Des Télécommunications

Mohamad ASSAAD

ETUDE MULTI-COUCHES DANS LE SYSTEME HSDPA

soutenue le 06 Mars 2006 devant le jury composé de:

Prof. Jean-Claude Belfiore	Président	ENST Paris, France
Prof. Khaled Ben Letaief	Rapporteur	University of Science and Technology, Hong Kong
Prof. Hamid Aghvami	Rapporteur	King's College, Londres
Prof. Hikmet Sari	Examinateur	Supélec, France
Dr. Mongi Marzoug	Examinateur	Orange, France
Prof. Djamal Zeghlache	Directeur de thèse	INT Evry, France

Département Réreaux et Services Multimédia Mobiles

Institut National des Télécommunications (INT)

Evry - France

Dissertation

presented in partial fulfillment of the requirements for the degree of

DOCTOR OF PHILOSOPHY

of

Ecole Nationale Supérieure Des Télécommunications

Mohamad ASSAAD

CROSS LAYER STUDY IN HSDPA SYSTEM

The committee in charge is formed by:

Prof. Jean-Claude Belfiore	Committee chair	ENST Paris, France
Prof. Khaled Ben Letaief	Reviewer	University of Science and Technology, Hong Kong
Prof. Hamid Aghvami	Reviewer	King's College, London
Prof. Hikmet Sari	Examiner	Supélec, France
Dr. Mongi Marzoug	Examiner	Orange, France
Prof. Djamal Zeghlache	Thesis Director	INT Evry, France

Mobile Networks and Multimedia Services Department

Institut National des Télécommunications (INT)

Evry - France

March 2006

"To My Family"

Acknowledgements

The work on this thesis has been an inspiring, exciting and interesting experience. First and foremost, I would like to express my deepest sense of gratitude to my supervisor Prof Djamal Zeghlache for his encouragement, support and excellent advice over the past years. His valuable technical helps and constructive suggestions were a source of inspiration and motivation all along my way. Our hours-lasting discussions on technical and non-technical issues have enriched my experience and paved my way to the finish line. Thanks Djamal for your nice humanitarian attitude and your friendship that I want to last for many more years.

I am greatly grateful to Professors Khaled Ben Letaief and Hamid Aghvami to accept to review this thesis despite their busy routine. They have enriched my knowledge with their valuable comments and exceptional insights into the telecommunications. Many thanks go also to Dr Mongi Marzoug and professors Hikmet sari and Jean-Claude Belfiore who honored me by their participation to my thesis committee.

I am really indebted to all the members of the Mobile Networks and Multimedia Services department at INT for the convivial and family environment within the department. I can not omit mentioning our angel Isabelle who ran to our help especially when we had difficulties with the *French Bureaucracy*. Over the past three years, I built a friendship with my office colleague Wajdi Louati. Special thanks to you Wajdi for your support, help and everything we shared especially during the famous "pauses café". It is now your turn to defend your PhD. Good luck!

This paragraph would certainly be incomplete if I did not mention my family who gave me unconditional support and love. I express my profound gratitude to them for being helpful and supportive all along my way.

Abstract

The increased use of Internet and data services motivates the evolution of cellular networks from second to third generation and beyond. The UMTS (Universal Mobile for Telecommunications System) has prepared for this evolution in successive releases within the third generation partnership project (3GPP). In this context, HSDPA (High Speed Downlink Packet Access) has been developed in releases 5 and 6 by introducing a number of additional enhancements (Hybrid ARQ, Adaptive Modulation and Coding or AMC and fast scheduling over time shared channels) into the standard to enable flexible and adaptive packet transmissions and to offer Internet and multimedia based services. The efficiency of these introduced features depends essentially upon the interactions of these techniques with the higher and lower layers (physical, transport, application,...). Cross layer interactions can have a drastic impact on overall throughput and capacity. This thesis focuses on the analysis and modeling of these cross layer interactions between the new MAC-hs entity (Medium Access Control high speed) of HSDPA and the upper and lower layers. The objective is to find the best configuration of this new entity to minimize the negative interaction between layers and optimize the performance of HSDPA. Consequently, this thesis provides comprehensive modeling studies covering the following topics or aspects:

- Analysis and modeling of the effect of wireless channel (shadowing, fast fading,...) on the HSDPA system performance and efficiency for various scheduling algorithms. Several uncorrelated and correlated fading models are considered in this study.

- Analysis and modeling of the effect of Circuit Switched (CS) services transmitted on the UMTS Release 99 (R99) Dedicated Physical Channels (DPCHs). This analysis can serve to provide guidelines for the UMTS planning process when resources are dynamically shared between circuit and packet services.

- Characterization and modeling of the interaction between TCP protocol and the MAC-hs layer resulting from the introduction of Hybrid-ARQ and scheduling features into the network. A new scheduler is suggested to reduce this interaction and improve the system performance and efficiency.

- Characterization of the interaction of the MAC-hs with the streaming services. A new opportunistic scheduler is proposed to achieve better trade-off between fairness and cell capacity, in other words to guarantee stringent QoS constraints (delay, jitter,...) of streaming services without losing much cell capacity.

System simulations using NS2 (Network Simulator) are used to assess the accuracy of the analytical conducted studies.

Résumé

L'augmentation de l'utilisation de l'Internet et des services de données motive l'évolution des réseaux cellulaires de la deuxième à la troisième et "après troisiéme" générations (3G and beyond en anglais). L'UMTS (Universal Mobile for Telecommunications System) a été préparé pour cette évolution à travers les versions successives (releases) de la norme développées au sein du 3GPP (third generation partnership project). Dans ce contexte, HSDPA (High Speed Downlink Packet Access) a été développé dans les releases 5 et 6 pour poursuivre l'volution du mode "paquet" de l'UMTS. Ce système utilise de nouvelles technologies telles que le Hybrid-ARQ (Automatic Repeat Request), la modulation adaptative en présence d'une adaptation de lien et l'ordonnancement rapide (fast Scheduling) pour permettre de véhiculer des débits plus élevés sur l'interface radio et d'augmenter la capacité. En deuxième phase, la technologie Multi-antennes MIMO (Multiple Input Multiple Output) est prévue d'être utilisée afin d'accroître la capacité radio et permettre d'intégrer des services à des débits plus élevés. L'éfficacité et les performances des techniques utilisées dans HSDPA dépendent essentiellement des interactions entre les différentes couches physique, transport, application, etc. Ces interactions peuvent affecter le débit de chaque utilisateur et avoir, par la suite, des conséquences sur la capacité et l'éfficacité globales du système. Cette thèse se focalise sur l'analyse et la modélisation des interactions entre la couche MAC-hs (Medium Access Control - high speed) de HSDPA et les autres couches (physique, transport). L'objectif est de trouver la configuration optimale de cette entité MAC-hs afin de réduire les interactions "négatives" entre-couches et optimiser les performances de HSDPA. Par conséquent, cette thèse fournit des études et des modélisations analytiques couvrant les aspects suivants:

- Analyse et modélisation de l'impact du canal radio (shadowing, fast fading,...) sur l'efficacité et les performances du système HSDPA dans le cas où plusieurs algorithmes d'ordonnancement sont utilisés. Plusieurs modèles de "fading" correlés et d-correlés sont considérés dans cette étude.

- Analyse et modélisation de l'effect des services "Circuit" CS (Circuit Switched) sur les performances de HSDPA. Ces services sont véhiculés sur les canaux dédiés DPCHs (Dedicated Physical Channels) de l'UMTS (release 99) et partagent simultanément les mêmes ressources cellulaires que HSDPA. Cette étude pourra servir dans la plannification de l'UMTS où les ressources sont partagées dynamiquement et simultanément entre les services "circuit" et "packet".

- Charactérisation et modélisation de l'interaction entre le protocole TCP et l'entité MAC-hs. Cette interaction est due essentiellement à l'utilisation des techniques Hybrid-ARQ et ordonnancement (scheduling) dans le système. Une nouvelle stratégie d'ordonnancement est proposée dans cette partie de la thèse afin de réduire cette interaction et améliorer les performances du système.

- Charactérisation de l'interaction entre l'entité MAC-hs et les services streaming ayant de fortes contraintes de QoS (Quality of Service). Une nouvelle stratégie d'ordonnancement dite opprotunistique est proposée afin d'atteindre un meilleur compromis entre l'équité et la capacité de la cellule, autrement afin de garantir les contraintes sévères de QoS (délai, gigue,...) des services streaming sans trop perdre de capacité cellulaire.

Une simulation "système" utilisant le logiciel NS2 (Network Simulator) a été utilisée pour valider les études analytiques menées tout au long de cette thèse.

Publications of the author

Book

1. Mohamad Assaad and Djamal Zeghlache, TCP over UMTS-HSDPA Systems, To be published by CRC Press, Francis and Taylor Auerbach Publications, New York, ISBN: 0849368383, 224 pages, (expected 19/07/2006).

Journals

1. Mohamad Assaad and Djamal Zeghlache, "Effect of Circuit Switched Services on HSDPA Cell Capacity ", IEEE Transactions on Wireless Communications, Vol. 5, Issue 5, May 2006, pp. 1044-1054.

2. Mohamad Assaad and Djamal Zeghlache, "Cross Layer Design in HSDPA System ", IEEE Journal on Selected Areas in Communications (JSAC), Vol. 24, No. 3, March 2006, pp. 614-625.

3. M. Assaad and D. Zeghlache, "How to minimize the TCP Effect in a UMTS-HSDPA System", Wiley Wireless Communications and Mobile Computing (WCMC), June 2005, vol. 5 issue 4, pp. 473-485.

4. M. Assaad, B. Jouaber and D. Zeghlache, "TCP Performance over UMTS-HSDPA System", Kluwer on Telecommunication Systems 27:2-4, 371-391, 2004.

5. Mohamad Assaad and Djamal Zeghlache, "A Simple SIR Distribution For Correlated Dense Multipath Channel And Its Application to HSDPA Cell Capacity Analysis," IEEE transactions on wireless communications Letters, second round review.

6. Mohamad Assaad and Djamal Zeghlache, "Opportunistic Scheduler for HSDPA System ", IEEE Transactions on Wireless Communications, submitted.

7. Mohamad Assaad and Djamal Zeghlache, "Resource Allocation for Circuit Switched and Packet Switched Services in a Combined UMTS R99/HSDPA System", IEEE Transactions on Vehicular Technology, submitted.

8. Mohamad Assaad and Djamal Zeghlache, "HSDPA Performance Under Nakagami Fading Channel", IEEE Transactions on Wireless Communications, second round review.

Conferences

1. M. Assaad, B. Jouaber and D. Zeghlache, "Effect of TCP on UMTS/HSDPA System Performance and Capacity", IEEE Global Telecommunications Conference, GLOBECOM '04, Dallas. Volume: 6 , 29 Nov.-3 Dec., 2004, Pages:4104 - 4108.

2. M. Assaad and D. Zeghlache, "Scheduler Study in HSDPA System", IEEE PIMRC 2005, Sep. 2005.

3. M. Assaad and D. Zeghlache, "On the Capacity of HSDPA System", Global Telecommunications Conference, 2003. GLOBECOM '03. IEEE ,Volume: 1, 1-5 Dec. 2003, Pages: 60 - 64.

4. M. Assaad and D. Zeghlache, "Comparison between MIMO techniques in a UMTS-HSDPA System", IEEE International Symposium on Spread Sprectrum Techniques and Applications ISSSTA, 30 Aug.-2 Sept. 2004, Sydney, Pages 874-878.

5. M. Assaad and D. Zeghlache, "Fast Scheduling in HSDPA System: A Trade-off Between Fairness and Efficiency", IEEE WPMC 2005, Sep. 2005.

6. M. Assaad and D. Zeghlache, "MIMO/HSDPA with Fast Fading and Mobility: Capacity and Coverage Study", 15th IEEE International Symposium on Personal, Indoor and Mobile Radio Communications, PIMRC 2004, Volume: 3 , 5-8 Sept. 2004, Barcelona, Pages:2181 - 2186.

7. M. Assaad, B. Jouaber and D. Zeghlache, "TCP Performance over UMTS-HSDPA System", ICN'04 Guadeloupe, French Caribbean, March 2004, Vol.2, (Gosier, February-Mars 2004), p. 874-878.

8. M. Assaad and D. Zeghlache, "Opportunistic Scheduler for Streaming Services in HSDPA system," to appear in IEEE PIMRC 2006, Helsinki, Finland, 11-14 September, 2006.

Description générale des travaux menés dans cette thèse

Depuis le début des années 1990, les services de communications cellulaires connaissent un développement sans précédent, rendu possible par l'existence de technologies numériques dites de 2e génération, le GSM étant l'une des plus populaires. Les systèmes mobiles de 2e génération sont conus pour offrir des services de transmission de la voix et des données de faible débit. Cependant, Le mode de fonctionnement " données " est en train de prendre du terrain sur le mode " voix ". Pour permettre la création de nouveaux services et d'offrir aux usagers une véritable itinérance à l'échelle mondiale, il était devenu nécessaire d'effectuer un saut technologique et de franchir le pas vers les réseaux cellulaires de 3e génération. Le nom UMTS (Universal Mobile for Telecommunication System) a été choisi par l'organisme de standardisation de télécommunication européenne ETSI (European Telecommunication Standard Institute) pour les systèmes de troisième génération. La technique CDMA (Code Division Multiple Access) est adoptée comme mode d'accès et de partage de la ressource. L'UMTS utilise sur l'interface radio deux modes : UTRA FDD (UMTS Terrestrial Radio Access Frequency Division Duplex) basé sur la technique WCDMA pur (Wideband Code Division Multiple Access) et UTRA TDD (UMTS Terrestrial Radio Access Time Division Duplex) basé sur la combinaison TDMA-CDMA (Time Division Multiple Access Code Division Multiple Access).

Les systèmes futurs de communications mobiles large bande sont appelés à fournir la capacité d'accès suffisante à un nombre croissant d'utilisateurs combiné à une densification du trafic de type " Internet mobile ". Vu que la capacité du système UMTS, comme tous les systèmes utilisant le CDMA, est limitée par la sensibilité du CDMA aux interférences, les études se sont concentrées depuis la fin de l'année 2000 sur l'évolution de l'interface radio de l'UMTS dans le but de répondre au défi ci dessus. HSDPA (High Speed Downlink Packet Access) est l'une des solutions proposées. Ce système utilise de nouvelles technologies telles que le Hybrid-ARQ, la modulation adaptative en présence d'une adaptation de lien et l'ordonnancement rapide (fast Scheduling) pour permettre de véhiculer des débits plus élevés sur l'interface radio et d'augmenter la capacité. En deuxième phase, la technologie Multi-antennes MIMO (Multiple Input Multiple Output) est prévue d'être utilisée afin d'accroître la capacité radio et permettre d'intégrer des services à des débits plus élevés. En effet, l'utilisation de modulations d'ordre élevé permet d'atteindre des débits plus élevés sur la voie descendante. Par contre, Ceci peut dégrader les performances du système surtout en absence de contrôle de puissance. Pour y faire face, on procède à une adaptation rapide de lien combinée à un mécanisme de HARQ. Ce mécanisme permet de retransmettre les paquets erronés jusqu'à réception de l'information. Une combinaison dite "douce"

des différentes retransmissions est utilisée en HSDPA afin de diminuer le nombre de retransmissions. Le but est d'envisager une augmentation du débit du canal et par la suite d'accroître la capacité jusqu'à 14.4 Mbps par secteur.

Les contributions essentielles des travaux de recherche dans cette thèse s'inscrivent dans le contexte de l'étude des interactions entre les couches physique, MAC, Transport et application. Le but est de trouver l'apport de ces interactions sur la capacité totale et les performances des systèmes mobiles. Ces études ont été menées analytiquement en utilisant des outils mathématiques et statistiques. Une simulation dite " système " est ensuite utilisée pour valider les algorithmes et modèles analytiques proposés. Les travaux de recherche menés tout au long de cette thèse peuvent divisés en quatre majeures parties:

1. Effet du canal radio sur les performances des algorithmes d'ordonnancement (chapitre 3)
2. Interaction des services voix de l'UMTS Release 99 avec les services Data de HSDPA (chapitre 4)
3. Interaction de la couche MAC-hs avec le protocole TCP de la couche transport (chapitre 5)
4. Interaction de la couche MAC-hs avec les services streaming (chapitre 6)

Cette thèse est divisée en sept chapitres. Les contributions essentielles sont décrites dans les chapitres 3 à 6. Chapitre 1 présente une introduction générale aux problématiques abordées en décrivant les motivations et les contributions apportées. Chapitre 2 présente une description générale du système HSDPA. Les conclusions et les éventuelles perspectives sont présentées dans le chapitre 7.

1. Effet du canal radio sur les performances de HSDPA (chapitre 3)

En HSDPA, le couplage de " Adaptation de lien " / " ordonnancement (Scheduling) " contrôle les allocations d'accès en mode paquet. Il permet de partager le canal de transport des données, dit HS-DSCH, entre les utilisateurs et de gérer la charge du système. En effet, le Scheduler décide à quel utilisateur le canal HS-DSCH sera dédié dans le prochain slot. L'adaptation de lien utilisant la technique AMC (Adaptive Modulation and Coding) est utilisée ensuite afin d'adapter les paramètres de transmissions aux variations rapides (fast fading) du canal radio. L'allocation de ressources (AMC+scheduling) doit tenir compte des conditions radios de chaque utilisateur ainsi que du délai toléré par chaque service. Plusieurs stratégies d'ordonnancement peuvent être utilisées dans ce cas. La stratégie Max C/I consiste à allouer le canal à l'utilisateur qui a les meilleures conditions radios ce qui permet d'utiliser des

modulations et des codages d'ordre plus élevé et d'accroître ainsi la capacité du système. Ce genre d'ordonnancement risque de bloquer des utilisateurs situés en bordure de la cellule et dont le lien radio n'est pas toujours le plus favorable. Une autre stratégie consiste à allouer le canal aux utilisateurs de telle faon à avoir une répartition équitable de ressources entre les utilisateurs autrement dit à avoir le même débit final par utilisateur (dit Fair Throughput). Cette stratégie respecte les contraintes temporelles des services mais ne permet pas d'optimiser la capacité. Dans la littérature, plusieurs algorithmes d'ordonnancement ont été proposés afin de trouver un compromis entre la maximisation de la capacité et le respect des contraintes temporelles. Citons par exemple, le Proportional Fair (PF) et le Score Based (SB). La maximisation de la capacité et la performance de l'allocation de ressources en général dépendent de plusieurs facteurs : les conditions radios et plus précisément l'environnement radio (e.g. macro, micro, shadowing, fast fading,), le récepteur utilisé (e.g. Rake) ainsi le type des services utilisés. Cette partie de la thèse présente des études statistiques sur l'effet du canal radio (plusieurs modèles de fast fading et des canaux multi-trajet avec et sans corrélation) sur les performances de HSDPA en présence de plusieurs algorithmes d'ordonnancement et d'un récepteur de type " Rake ". Ces études se sont concentrées sur les trafics FTP uniquement (services non temps réel). Une simulation système utilisant le logiciel NS2 est utilisée pour valider les études analytiques élaborées.

2. Interaction des services "circuit" de l'UMTS Release 99 avec les services Data de HSDPA (chapitre 4)

Les services " données " offerts par HSDPA seront utilisés en parallèle avec les services " circuit " de l'UMTS Release 99. L'effet de ces derniers sur la capacité de HSDPA n'a pas eu assez d'attention des les études déjà existantes dans la littérature. Les services voix " speech " ont toujours la priorité par rapport aux services données à cause de leurs contraintes temporelles sévères. Ces services " circuit " utilisent le même arbre de code que les utilisateurs HSDPA. En plus, ils consomment une partie de la puissance du node B et exercent une interférence supplémentaire sur le canal HS-DSCH de HSDPA. Par conséquent, il faut trouver la capacité que peut offrir HSDPA en présence des services circuits (e.g. voix, services données à contrainte faible LCD ou Low Constraint Data). Dans cette partie, on propose un modèle permettant de calculer la capacité du HSDPA en présence des services " circuit ". Les mêmes algorithmes étudiés dans la phase précédente ont été étudiés à nouveau en présence des services " circuit " afin de trouver l'effet de ces derniers sur les performances de HSDPA dans plusieurs environnements

radio. Les études analytiques menées dans cette partie ont été validées par une simulation système utilisant le logiciel NS2.

3. Interaction de la couche MAC-hs (Medium Access Control - high speed) de HSDPA avec le protocole TCP de la couche transport (chapitre 5)

TCP (Transport Control Protocol) est un protocole qui assure une transmission fiable des données et un contrôle de flux au niveau de la couche transport. Ceci est assuré par l'utilisation d'un mécanisme de transmission à fenêtre glissante couplé avec un mécanisme de retransmission des segments TCP erronés et un contrôle de la taille de la fenêtre de transmission en fonction des congestions dans les réseaux. TCP est utilisé comme protocole de transport dans la majorité des services véhiculés sur Internet (presque 90%) et il est prévu d'occuper une large partie des services " données " véhiculés dans les réseaux mobiles de troisième génération. Dans les réseaux sans fil, les erreurs sur l'interface radio sont interprétées par TCP comme étant des congestions ce qui entraîne une retransmission des segments TCP contenant les erreurs et une baisse de la taille de la fenêtre de transmission. Ceci entraîne une baisse de la capacité totale du système et une perte d'efficacité dû à une baisse de la fenêtre sans qu'il y ait de congestion (autrement sans un réel besoin de cette baisse). L'utilisation de Hybrid-ARQ résout en partie ce problème. En effet, ARQ retransmet les paquets erronés au niveau de la couche MAC-hs empêchant ainsi le transfert des erreurs à la couche transport. Par conséquent, les erreurs causées par l'interface radio seront transparentes par rapport à la couche transport. Cependant, le mécanisme Hybrid-ARQ génère un délai de réception dû aux retransmissions fréquentes des paquets. Si ce délai est important (ce qui est le cas malheureusement à cause des erreurs fréquentes sur l'interface radio), un phénomène de " timeout " surgit (i.e. un timer déclenché au moment de la transmission du segment TCP expire sans recevoir un acquittement du récepteur indiquant la réception du segment sans erreur). TCP mal interprète ce délai comme étant dû à une congestion et déclenche un mécanisme de retransmission suivi d'une baisse de la fenêtre de transmission jusqu'à sa valeur initiale entraînant ainsi une perte d'efficacité et une baisse de la capacité totale du système. Dans cette partie de la thèse, on a développé une analyse mathématique de ce problème en proposant un modèle analytique capable de déterminer quantitativement l'effet des algorithmes d'ordonnancement (étudiés précédemment) sur les performances services TCP véhiculés sur HSDPA. Un nouvel algorithme d'ordonnancement est proposé

afin de minimiser l'aspect négatif de cette interaction entre les couches TCP et MAC-hs et améliorer ainsi les performances de HSDPA dans le cas des services non temps réel utilisant TCP comme couche de transport. Ces études analytiques sont ensuite validées par simulation système sou NS2.

4. Interaction de la couche MAC-hs avec les services streaming (chapitre 6)

Cette partie décrit les études menées pour analyser l'interaction entre la couche MAC-hs (AMC+scheduling+
et les services streaming ayant des contraintes temporelles plus sévères que les services non temps réel. Le but est de voir si l'on peut faire passer des services streaming sur HSDPA avec un minimum de coût, autrement dit sans trop perdre de capacité. En effet, une caractéristique fondamentale des services streaming est de maintenir la gigue sous un certain seuil. Ce seuil dépend essentiellement du débit du trafic et de la capacité de stockage du récepteur. L'utilisation d'un buffer à la réception permet de lisser la gigue du trafic et réduire ainsi la sensibilité de l'application aux délais.

Dans cette thèse, on s'est concentré uniquement sur les services streaming à débit constant égal à 128kbps (Constant Bit Rate ou CBR). Les résultats ont montré que les schedulers traditionnels tels que le Proportional Fair ne sont adaptés aux contraintes des services streaming. La variation du débit durant la connexion ne permet pas d'offrir des services streaming à un grand nombre d'utilisateurs dans la cellule. Cette partie s'est aboutie à une proposition d'un nouvel algorithme d'ordonnancement capable de véhiculer du streaming sur HSDPA sans trop perdre de capacité cellulaire. Autrement dit, cet algorithme permet d'atteindre un meilleur compromis entre " la capacité cellulaire " et " l'équité" que les schedulers traditionnels.

Contents

List of Figures

List of Tables

Chapter 1

General Introduction and Thesis Contribution

1.1 General Introduction

The increased use of Internet and data services motivated the evolution of cellular systems from second to third generation. The UMTS system (Universal Mobile for Telecommunications System) in Europe has prepared for this evolution in successive releases within the third generation partnership project (3GPP) that standardizes and specifies the UMTS air interface, the access and core network architectures. Various advanced radio technologies are being introduced through the various releases in order to convey mass market multimedia services in UMTS networks.

Release 99 of UMTS, the first release, relies mostly on the introduction of CDMA based radio and access technologies. This step in the evolution remains insufficient to achieve full compatibility with IP. The air interface as specified in release 99 does not provide the needed higher data rates either. Therefore, releases 5 and 6 introduce a number of additional enhancements into the standard to enable flexible and adaptive packet transmissions and to offer Internet based services.

HSDPA (High Speed Downlink Packet Access) is the umbrella of these evolutions on the downlink. HSDPA has been introduced in the standards essentially in release 5. Release 6 contains some enhancements to this technology in order to improve performance. The major introduced evolutions are at the physical and data link layers.

The techniques introduced in HSDPA are adaptive modulation and coding (AMC) to achieve better spectral efficiency, link adaptation to mitigate radio channel impairments, Hybrid ARQ (Automatic

Repeat Request) to retransmit erroneously received radio blocs and to increase link reliability and scheduling to enable intelligent allocation of resources to improve capacity and offer packet based multimedia services. Scheduling over shared channels must take into account radio channel conditions, mobile location in the cell and service type to provide tangible throughput, capacity and delay benefits. Scheduling must also ensure fairness with respect to users and applications.

At the data link layer (Radio Link Control and Medium Access Control) and the radio resource control, another major enhancement was the addition of the downlink shared channels next to the release 99 dedicated channels. The dedicated channels are suitable for real time services but are inadequate for packet services. The introduction of shared channels results in power savings, interference mitigation and system capacity improvements.

Besides, Multiple transmit and receive antennas can also be used to achieve higher data rates and improve system capacity. The introduction of multiple antennas is planned for the last phases of the UMTS architecture enhancements.

The introduction of new features in networks to improve data rates and enhance reliability of data transmission over the air interface can have nevertheless an impact on end to end performance and efficiency. Retransmission mechanisms relying on ARQ interact with higher layer protocols, especially the Transport Control Protocol (TCP) used in conjunction with IP to offer non real time services. Real time services are typically offered using UDP/IP and streaming services using RTSP/RTP/IP. Cross layer interactions can have a drastic impact on overall throughput and capacity. Care must be taken to characterize these interactions and suggest ways of preventing or at least reducing any negative effects resulting from the introduction of ARQ and other techniques in wireless networks that unavoidably interact with congestion control mechanisms in Internet networks (when TCP protocol is used) and generate additional delay in receiving data which can affect the efficiency of HSDPA for services with stringent delay constraints (e.g., streaming).

1.2 Thesis Objectives

This thesis focuses on the analysis and modeling of cross layer interaction between the new MAC-hs (MAC high speed) of HSDPA system and other layers (physical, transport and application layers). The objective is to find the best configuration of this layer to minimize the negative interaction between layers and optimize the performance of HSDPA. The studies in this thesis are conducted to answer the following objectives:

- Characterize the effect of wireless channel (shadowing, fast fading,..) on the performance of HSDPA. The Adaptive Modulation and coding, fast link adaptation and fast scheduling techniques introduced in HSDPA are tightly coupled to adapt the transmission parameters to the continuous varying channel and optimize the resource management by allocating the HS-DSCH channel to the user having favorable channel conditions. In this context, the channel variations (especially short term variations) have an important impact on the efficiency of the system performance. To the best of our knowledge, this topic has not been studied yet in the literature. Therefore, the first objective of this thesis is to model analytically the effect of the wireless channel on the performance of the HSDPA system. Several channel models are considered (Rayleigh fading channel, Nakagami fading channel,..). Results obtained from this analysis are of interest to assess the efficiency of the schedulers used in HSDPA and the impact of the wireless environment on the HSDPA performance.

- Characterize the interaction between the MAC-hs and the data link layer of the UMTS R99 (Release 99). Since HSDPA has been conceived for packet switched services, the UMTS R99 will still be used, in parallel to HSDPA, to convey speech and circuit switched services. The interaction between these two service classes that use the same wireless bandwidth and CDMA code tree must be assessed to determine the impact of the UMTS R99 capacity on the HSDPA capacity. This topic has not been addressed in the literature. The challenge consists not only in characterizing this interaction between R99 services and HSDPA connections but also in modeling analytically this interaction for various schedulers used in HSDPA and various wireless fading channel models.

- Characterize analytically the interaction between the MAC-hs layer and the Transport Control Protocol (TCP). As described herein, the introduction of new features in HSDPA such as Hybrid ARQ and fast scheduling unavoidably interact with congestion control mechanisms in the Internet. TCP misinterprets the delay generated by HARQ and scheduling techniques and triggers unnecessary timeout mechanisms resulting in congestion window shrinking and drastic throughput degradation. The challenge in this case is to characterize analytically these interactions and suggest ways of preventing or at least reducing any negative effects to improve the performance of TCP over HSDPA (e.g., introduce of a new scheduler that reduces these negative interactions). Although the performance of TCP over wireless networks has been studied widely in the literature, few studies are conducted in the case of HSDPA. These studies are essentially based on

simulation. Moreover, the majority of studies on TCP over wireless systems propose modification of TCP implementations which is not desirable. Relying on scheduling to minimize interactions of lower layer protocols with TCP and achieve capacity benefits without breaking the IP paradigm is a more appropriate alternative.

- Characterize the interaction between the MAC-hs layer and the streaming Quality of Service (QoS) constraints. Streaming is one of the emerging services that are expected to occupy a large share of the wireless system capacity. Streaming services are characterized by stringent QoS constraints (delay, jitter,...). Transmitting the streaming services over shared channels using the existing schedulers results in cell throughput degradation due to the jitter constraints. Consequently, characterizing the interaction of streaming services with the MAC-hs is needed to conceive an appropriate scheduler to convey these services over HSDPA without losing much cell capacity. The challenge in this case is to design an opportunistic scheduler achieving a trade-off between fairness and cell capacity, in other words guaranteeing the required streaming QoS constraints without losing much cell capacity. Few studies on this topic are available in the literature.

1.3 Thesis Contributions

The contributions of this thesis can be classified into four major analyses that mirror the challenges described earlier on the effect of the environment, of other protocols and other UMTS channels on the HSDPA system capacity:

- Effect of radio channel models on HSDPA performance (chapter 3);
- Interaction of HSDPA services with R99 Circuit Switched services transmitted (chapter 4);
- Interaction of MAC-hs and schedulers with TCP protocol (chapter 5);
- Interaction of MAC-hs and schedulers with Streaming services (chapter 6).

These studies are conducted using analytical and statistical analysis. A network system simulation is also used to assess the accuracy of the proposed models. In the fourth contribution, only a fraction of the proposed solutions and simulation results is reported in this thesis. Other contributions related to a research contract are not reported for confidential reasons.

Chapter 2 provides background information on the HSDPA system to introduce the context of the conducted studies in this thesis.

Chapter 7 concludes the manuscript by summarizing the studies and presents perspectives to pursue and extend the thesis.

1.3.1 Effect of radio channel models on HSDPA performance (chapter 3)

As indicated above, HSDPA relies on several advanced technologies such as AMC, HARQ and scheduling to improve the system capacity and allow the introduction of new high bit rate services. These techniques are tightly coupled and benefit from the shared time nature of the transport channel (the so-called HS-DSCH) to allocate the HS-DSCH channel to the adequate user at the right moment and to adapt its transmission parameters to the short term radio channel variations. In this context, the role of the scheduling is essential for the improvement of system efficiency and performance. The scheduling should maximize as much as possible the cell throughput and offer to each user enough resources to achieve the desired Quality of Service (QoS) for each application. Consequently, the efficiency of the scheduler depends essentially upon the conveyed traffic characteristics and the wireless channel model. A cross layer study between the wireless channel (modeled by path loss, shadowing, fast fading, correlation between channel paths,...), the MAC-hs layer (HARQ, AMC, scheduling) and the application QoS constraints is essential to estimate the performance of HSDPA, find a good configuration of the MAC-hs (find a good scheduler,...) and optimize the planning of the HSDPA system.

This thesis studied analytically the effect of wireless fading on the performance of various schedulers in HSDPA. This study has been conducted using statistical models of the wireless channel fading. The proposed analytical models estimate cell throughput and user bit rate and enable performance comparisons between schedulers.

The user bit rate and cell capacity estimation requires the introduction into the model of the techniques used in HSDPA, in particular AMC, HARQ and scheduling. In addition, derivation of the analytical expressions requires the description of the channel model, the receiver type and an approximate expression of SIR (Signal to Interference Ratio). Several statistical channel models are considered in the study. The cases of composite uncorrelated and correlated multipath/shadowing channels with path amplitude following Rayleigh and Nakagami distributions are investigated. The case of composite dense uncorrelated and correlated multipath/shadowing channel is also studied. This last case considers a Wide-sense Stationary channel, constant Power Dispersion Profile (PDP) and frequency selective fading following a Rayleigh distribution.

Finally, results obtained from the analytical models are verified by a system simulation conducted

using the Network Simulator NS2. Note that the conducted studies in this part of the thesis assume the use of non real time data in particular FTP traffic.

1.3.2 Interaction of HSDPA services with Circuit Switched services transmitted on UMTS R99 dedicated channels (chapter 4)

Since HS-DSCH is reserved only for non real time data services, CS services will be transmitted as before on downlink dedicated channels known as DPCH channels (Dedicated Physical Channel). The DPCH channel, normalized by the 3GGP in Release 99, supports fast power control and soft handover.

In the case of multiple services, policies to set priorities between the various services are required to achieve adequate throughput and service differentiation and to offer each service their required bit rate and QoS. The scenario of interest in this part of the thesis corresponds to the simultaneous presence of circuit switched (CS) services (e.g., speech) on the DPCH channel and of HSDPA packet services on the HS-DSCH channel. The priority between CS users and HSDPA users can be found by analyzing the effect that CS services have on the capacity of HSDPA. To assess interaction between CS and HSDPA packet services, an analytical model is proposed to estimate the capacity of HSDPA in the presence of CS users on the DPCH channels. A network level simulation, implemented in NS-2, is used to evaluate the accuracy of the proposed model.

CS services consume part of the code tree resources and the node B power and exert interference on the HSDPA packet services. The entire left over node B power is used to serve HSDPA packet services. Estimating, approximating or lower bounding the capacity of the HSDPA system requires prior analysis of CS services. The basic analytical expression for HSDPA capacity includes terms related to HARQ, fast scheduling and the selected AMC combination according to radio link conditions. Consequently, the derivation of the analytical model requires prior assessment of CS services behavior in terms of total power consumption (including soft handover aspects), the relationship that exists between codes used by CS services and those left for HSDPA users, the scheduling used and the ensuing AMC combination for HSDPA users. The derivation of the analytical model proposed in the contribution to estimate the capacity of HSDPA considers as in the previous analyses (presented above i.e. without the presence of CS services) several scheduling algorithms under various wireless channel model (cases of composite uncorrelated and correlated multipath/shadowing channels with path amplitude following Rayleigh and Nakagami distributions, case of composite dense uncorrelated and correlated multipath/shadowing channel with Wide-sense Stationary channel, constant Power Dispersion Profile (PDP) and frequency

selective fading following a Rayleigh distribution).

The accuracy of the obtained results are also assessed by a system simulation using NS2.

1.3.3 Interaction of MAC-hs and schedulers with the TCP protocol (chapter 5)

The interaction between radio link control mechanisms and TCP has been identified early in the scientific community that has since provided many variants for TCP to reduce and possibly eliminate interactions when random errors over the air interface are mistakenly taken by TCP as congestion in the fixed network segments. Even if some approaches propose link layer solutions, most tend to break the end to end IP paradigm when TCP is modified in an attempt to alleviate the experienced negative cross layer effects due to errors occurring over the radio link. Among the proposed solutions, only a few are actually used in practice. Split TCP has been used in public land mobile networks (PLMNs) at gateways located at the edge of wireless core networks to separate the Internet from the PLMNs and thereby avoiding interactions between TCP and the radio link errors and recovery mechanisms. Some TCP versions have also become de facto standards because they have been extensively deployed in the Internet during the quest for alternatives to the standard or the original TCP. This thesis will consequently focus on the more common and popular versions of TCP (TCP Reno) to conduct the analysis of interactions between Hybrid ARQ, scheduling and TCP congestion mechanism. In addition, this thesis goes further as it clearly contends that systems using scheduling over the air interface are better off taking advantage of scheduling itself to alleviate the RLC/TCP interactions rather than violating the end to end IP paradigm. An analytical model is proposed to assess the cell throughput for HSDPA using several scheduling algorithms and the de facto TCP Reno congestion control algorithm. The results reported in chapter 5 indicate that wireless systems can rely on scheduling to minimize interactions of lower layer protocols with TCP and achieve capacity benefits without breaking the IP paradigm. An analytical expression of cell throughput provides insight on capacity behavior. A new scheduler has been proposed in this part of the thesis (chapter 5) to improve the performance of TCP over the HSDPA system and minimize the negative interaction between TCP and the reliable data link layer.

1.3.4 Interaction of MAC-hs and schedulers with Streaming services (chapter 6)

Streaming applications are supposed to occupy a large share of the third generation system bandwidth. The fundamental characteristic of this application class is to maintain traffic jitter under a specific threshold. Jitter relates to the time relation between received packets. This threshold depends on the

application, the bit rate and the buffering capabilities at the receiver. The use of a buffer at the receiver smoothes traffic jitter and reduces the delay sensitivity of the application.

In this thesis, we have conducted a study on the scheduling algorithms for streaming services in the UMTS HSDPA system. The objective is to see if basic scheduling algorithms are suitable for streaming services. In other words, can these algorithms achieve an acceptable cell capacity while offering streaming services with fixed reading rates (i.e. Constant Bit Rate or CBR typically at target bit rate of 128kbps). Selected sources in the analysis operate consequently at 128 kbps as CBR streaming traffic. The entire end to end path from the applications in the User Equipment (UE) to the source side (in the network) is considered.

This study has been conducted in the context of a research project with France Telecom Research and Development (FTR&D). Consequently, only a fraction of the proposed schedulers and results will be reported in this public document. The results in this manuscript correspond to presence of composite uncorrelated multipath/shadowing channel with amplitude following a Rayleigh distribution.

Results show that basic schedulers (e.g., Proportional Fair,...) are not suitable for streaming traffic. The bit rate fluctuations over time do not allow offering streaming services with acceptable cell capacity. At the end of this thesis, a new scheduler, more appropriate for handling streaming services, has been consequently suggested to alleviate the weaknesses observed and encountered for the basic schedulers. Simulations assess the performance of this new scheduler and show that it can outperform other existing schedulers in terms of capacity and fairness.

Chapter 2

High Speed Downlink Packet Access (HSDPA)

The UMTS system proposed for third generation cellular networks in Europe, is meant to provide enhanced spectral efficiency and data rates over the air interface. The objective for UMTS, known as WCDMA in Europe and Japan, is to support data rates up to 2Mbps in indoor/small-cell-outdoor environments and up to 384 Kbps in wide-area coverage for both packet data and circuit-switched data. The 3GPP, responsible for standardizing the UMTS system, realized early on that the first releases for UMTS would be unable to fulfill this objective. This was evidenced by the limited achievable bit rates and aggregate cell capacity in release 99. The original agenda and schedule for UMTS evolution has been modified to meet these goals by gradual introduction of advanced radio, access and core network technologies through multiple releases of the standard. This phased roll out of UMTS networks and services would also ease the transition from second generation to third generation cellular for manufacturers, network and service providers. To meet in addition the rapidly growing needs in wireless Internet applications, studies initiated by 3GPP since 2000 not only anticipated this needed evolution but also focused on enhancements of the WCDMA air interface beyond the perceived third generation requirements.

The High Speed Downlink Packet Access (HSDPA) system [1-5] has been proposed as one of the possible long term enhancements of the UMTS standard for downlink transmission. It has been adopted by the 3GPP and will be used in Europe starting in 2006/2007. HSDPA introduces, first, adaptive modulation and coding, retransmission mechanisms over the radio link and fast packet scheduling and, later on, multiple transmit and receive antennas. This chapter describes the HSDPA system and some

of these related advanced radio techniques. Once the multiple antenna systems envisaged in HDSPA are integrated, UMTS networks will be able to achieve aggregate cell throughput in the 10 to 20 Mbps range.

2.1 HSDPA Concept

Interference control and management is key in increasing cell capacity in CDMA based systems. This can be performed at the link level by enhanced receiver structures such as Multi User Detection (MUD) used to minimize the level of interference at the receiver. At the network level, a good management of the interference can be provided by an enhanced power control and associated Call Admission Control (CAC) algorithms.

This philosophy of simultaneously managing the interference at the network level for dedicated channels leads to limited system efficiency. Fast power control used to manage the interference increases the transmission power during the received signal fades. This causes peaks in the transmission power and subsequent power rises that reduce the total network capacity. Power control imposes provision of a certain "*headroom*" or margin in the total Node B transmission power to accommodate variations [6]. Consequently, system capacity remains insufficient and unable to respond to the growing need in bit rates due to the emergence of Internet applications. A number of performance enhancing technologies must be included in the UMTS standard to achieve higher aggregate bit rates in the downlink and to increase the spectral efficiency of the entire system. These techniques include Adaptive Modulation and Coding (AMC), fast link adaptation, Hybrid ARQ and fast scheduling. Multi User Detection (MUD) and Multiple Input Multiple Output (MIMO) antenna solutions can also be included, but this is expected in later releases of UMTS to further improve system performance and efficiency.

The use of higher order modulation and coding increases the bit rate of each user but requires more energy to maintain decoding performance at the receiver. Hence, the introduction of fast link adaptation is essential to extract any benefit from introducing higher order modulation and coding in the system. The standard link adaptation used in current wireless system is power control. However, to avoid power rise as well as cell transmission power headroom requirements, other link adaptation mechanisms to adapt the transmitted signal parameters to the continuously varying channel conditions must be included. One approach is to tightly couple AMC and Scheduling. Link adaptation to radio channel conditions is the baseline philosophy in HSDPA which serves users having favorable channel conditions. Users with bad channel conditions should wait for improved conditions to be served. HSDPA

adapts in parallel the modulation and the coding rates according to the instantaneous channel quality experienced by each user.

AMC still result in errors due to channel variations during packet transmission and feedback-delays in receiving channel quality measurements. A Hybrid-ARQ scheme can be used to recover from link adaptation errors. With Hybrid-ARQ, erroneous transmissions of the same information block can be combined with subsequent retransmission before decoding. By combining the minimum number of packets needed to overcome the channel conditions, the receiver minimizes the delay required to decode a given packet. There are three main schemes for implementing HARQ : Chase combining (retransmissions are a simple repeat of the entire coded packet), Incremental redundancy IR (additional redundant information is incrementally transmitted) and self decodable IR(additional information is incrementally transmitted but each transmission or retransmission is self decodable).

The link adaptation concept adopted in HSDPA implies the use of time shared channels. Therefore, scheduling techniques are needed to optimize the channel allocation to the users. Scheduling is a key feature in the HSDPA concept and is tightly coupled to fast link adaptation. Note that the time-shared nature of the channel used in HSDPA provides significant trunking benefits over DCH for bursty high data rate traffic.

The HSDPA shared channel does not support soft handover due to the complexity of synchronizing the transmission from various cells. Fast cell selection can be used in this case to replace the soft handover. It could be advantageous to be able to rapidly select the cell with the best Signal to Interference Ratio (SIR) for the downlink transmission.

HSDPA can be seen as "*an umbrella of enhancement techniques applied on a combined CDMA-TDMA (Time Division Multiple Access) channel shared by users*" [6]. This channel, called High Speed Downlink Shared Channel (HS-DSCH), is divided into slots called Transmit Time Intervals (TTIs) each one equal to 2ms. The signal transmitted during each TTI uses the CDMA technique. Since link adaptation is used, the variable spreading factor is deactivated because its long-term adjustment to the average propagation conditions is not required anymore. Therefore, the spreading factor is fixed and equal to 16. The use of relatively low spreading factor addresses the provision for increased applications bit rates.

Finally, the transmission of multiple spreading codes is also used in the link adaptation process. However, a limited number of Wash codes is used due the low spreading adopted in the system. Since all these codes are allocated in general to the same user, Multi User Detector (MUD) can be used at the

User Equipment (UE)to reduce the interference between spreading codes and to increase the achieved data rate. This is in contrast to traditional CDMA systems where MUD techniques are used in the uplink only.

2.2 Channels Structure

HSDPA consists of a time shared channel between users and is consequently suitable for bursty data traffic. HSDPA is basically conceived for non real time data traffic. Research is actually ongoing to handle streaming traffic over HSDPA using improved scheduling techniques.

In addition to the shared data channel, two associated channels, called High Speed Shared Control Channel (HS-SCCH) and High Speed Dedicated Physical Control Channel (HS-DPCCH), are used in the downlink and the uplink to transmit signalling information to and from the user. These three channels in HSDPA : HS-DSCH, HS-SCCH and HS-DPCCH are described in more details.

2.2.1 HS-DSCH Channel

The fast adaptation to the short term channel variations requires handling of fast link adaptation at the node B. Therefore, the data transport channel HS-DSCH is terminated at the node B. This channel is mapped onto a pool of physical channels called High Speed Physical Downlink Shared Channel (HS-PDSCH) to be shared among all the HSDPA users on a time and code multiplexed manner [7, 8]. Each physical channel uses one channelization code, of fixed spreading factor equal to 16, from the set of 15 spreading codes reserved for HS-DSCH transmission. Multi-code transmission is allowed, which translates to mobile user being assigned multiple codes in the same TTI, depending on the User Equipment (UE) capability. Moreover, the scheduler may apply code multiplexing by transmitting separate HS-PDSCHs to different users in the same TTI.

The transport channel coding structure is reproduced as follows: One transport block is allocated per TTI, so that no transport block concatenation (such as in UMTS DCH based transmission) is used. The size of transport block changes according to the Modulation and Coding Scheme (MCS) selected using the Adaptive Modulation and Coding (AMC) technique. To each transport block, a Cyclic Redundancy Check (CRC) sequence with 24 bits is added. Since errors occur in bursts, one CRC sequence per transport block (i.e. per TTI) is sufficient. Once the CRC sequence is attached, the transport block bits are bit scrambled and segmented into blocks to apply Turbo block encoding. The code block size depends upon the turbo coding rate and can reach a maximum value of 5114 bits [9]. The coding

rate changes according to the MCS scheme selected by the link adaptation technique. At the turbo encoder output, rate matching is applied by the physical layer HARQ functionality. After matching the number of bits to the number of bits in the allocated HS-DSCH physical channels, segmentation divides the resulting bits among the HS-DSCH physical channels. The bit sequence obtained for each physical channel is then interleaved using one step interleaver with fixed size 32×30 (i.e. 32 rows and 30 columns) [9]. Finally, the resulting bit sequence is modulated using 16-ary Quadrature Amplitude Modulation (16QAM) or Quadrature Phase Shift Keying (QPSK) according to the MCS scheme selected [10,11].

2.2.2 HS-SCCH Channel

The downlink signalling related to the HS-DSCH is transmitted over the High Speed Shared Control Channel (HS-SCCH). The signalling information carried by the HS-SCCH contains essentially the Transport Format Resource Indicator (TFRI) and the HARQ information of the HS-DSCH channel. The TFRI includes the channelization codes used by the HS-DSCH, the modulation scheme and the transport block size. The HARQ information consists of the HARQ new data indicator, the HARQ process identifier and the redundancy and constellation version. Since the HS-DSCH channel is shared among users, the UE Identity (ID) is sent over the HS-SCCH to indicate the identity of the user for which the HS-DSCH is allocated during the TTI. Note that the UE ID is given by the 16 bits HS-DSCH Radio Network Temporary Identifier (H-RNTI) defined by the Radio Resource Controller (RRC) [12, 13].

Finally, this channel can be transmitted at a fixed power or can use power control. The decision to use power control is entirely left to the implementation.

2.2.3 HS-DPCCH Channel

In the uplink, signalling information has to be transmitted for the HARQ acknowledgment and the feedback measurement. The use of fast link adaptation on the HS-DSCH channel requires knowledge of the channel quality during the transmission. The UE measures the channel quality on the Common Pilot Indicator Channel (CPICH) and sends the result to the node B. The use of HARQ requires an acknowledgment message from the user to the node B, so that the node B retransmits the erroneously received packet or a new packet.

This signalling information is carried by the HS-DSCH associated uplink dedicated control channel (HS-DPCCH). This channel is spread, with a spreading factor of 256 (i.e. 30 bits per TTI), and code multiplexed with the existing dedicated uplink physical channels (DPCH). The H-ARQ acknowledgment

is a 1-bit Ack/Nack indication repeated 10 times and transmitted in one slot. The H-ARQ acknowledgement field is gated off when there is no ACK/NACK information being sent. The measurement feedback information contains Channel Quality Indicator (CQI) that may be used to select transport format and resource by HS-DSCH serving Node-B, according to CQI tables specified in [11]. It is an essential information needed for fast link adaptation and scheduling. The channel quality information, consisting of 5 bits, is coded using a (20,5) code transmitted over two slots.

2.3 MAC-hs

The use of fast adaptation to the short term channel variations requires handling of the HSDPA transport channels by the node B. Therefore, a Medium Access Control-high speed (MAC-hs) entity has been introduced in the node B. This entity has the responsibility of handling the HARQ process, scheduling and the selection of the transport format (due to AMC) [14]. The MAC-hs also stores the user data to be transmitted across the air interface. This imposes some constraints on the minimum buffering capabilities of the Node B.

2.4 Fast Link Adaptation

The wireless channel in cellular systems is a composite multipath/shadowing channel. The radio waves follow several paths from the transmitter to reach the destination. Fading occurs when many paths interfere, adding up to a composite signal exhibiting short time signal power variations at the receiver. This power could be weaker or stronger than the required power needed to achieve a given user Quality of Service (QoS). The link quality between the transmitter and the receiver is also affected by slow variations of the received signal amplitude mean value due to shadowing from terrains, buildings, and trees.

To deal with the problems caused by multipath fast fading, the existing wireless systems use diversity techniques such as long interleaving, robust channel coding, frequency hopping, and direct sequence spread spectrum. These techniques are based on one concept: averaging the temporary fading effect over all the transmission time and the bandwidth, so that bad conditions are compensated by good conditions. The spread spectrum technique (frequency hopping and direct sequence) spread the signal bandwidth over a wider frequency spectrum so that only a part of the spectrum is affected by the fading. Interleaving can be seen as spreading technique over time. By reordering the bits before transmission,

the information message is spread out over time. Therefore, bursty errors caused by the fading channel are spread out in time so the decoder receives distributed non bursty random errors that are easier to detect and correct. The channel coding includes redundancy in the transmitted signal to increase robustness against errors. Introducing more redundancy increases robustness but decreases effective information bit rate. In current systems, the channel coding rate is fixed to deal with the worst case and the transmission power is adapted to the channel conditions in order to achieve the application QoS [15].

Since fading results from the addition of different waves from multiple paths, it can potentially be predicted. Channel parameters (amplitude, phase, frequency), remain stationary for time windows of the order of half a wavelength. For example, at a carrier frequency of 2GHz (case of UMTS) and a mobile speed of 36 Km/h, the fading pattern could be predicted for a time window of approximately 7.5 ms. Estimation of the channel is feasible over a few ms and power can be consequently adjusted over such time scales.

In the UMTS R99, channel estimation is used to adapt the transmission power of each user, every slot (corresponding to a rate of 1500 Hz), to the short term channel variations. This is achieved at the cost of some power rise and higher interference as previously explained in section 2.2.

In HSDPA, the idea is to avoid power adaptation and hence power control by approaching the radio resource allocation and sharing from a different angle. Why continue using averaging techniques such as long interleaving and a fixed channel coding rate to counteract the fast fading if these techniques require high performance power control? Instead one can use AMC tightly coupled with fast scheduling so that modulation orders and coding rates are adapted according to estimated channel fading. In addition, the HS-DSCH channel can be allocated to the user with favorable channel conditions. To this avail, a Channel Quality Indicator (CQI) has been introduced in HSDPA (for details, see next section)to enable such intelligent allocation of resources to users.

The idea is to measure the channel quality over the Common Pilot Indicator Channel (CPICH) and to transmit the measurement report over the HS-DPCCH channel to the node B, so that scheduling and AMC can act according to the CQI and hence optimize channel resource allocation. The time window between the channel conditions measurement and the resource allocation should not exceed half a wavelength as indicated previously. In the 3GPP specifications [11], 30 CQIs have been standardized as described in the next section. The time window between the channel measurement and the start of the transmission over the HS-DSCH channel is 7 timeslots. By considering the transmission time of the

HS-DSCH channel (1 TTI), the overall delay between the radio channel measurement and the end of the packet transmission over the HS-DSCH channel is 10 timeslots. Therefore, HSDPA is suitable for urban area when mobile users move at low speed (less than 40 Km/h). For mobile at higher speeds, the environment conditions change rapidly. "*Fortunately, in this case the mobiles have a low degree of randomness since they move along known paths (traveling by train, driving down a freeway, etc..). Therefore, special solutions can be performed to predict the channel fading pattern in these cases*" [15].

In the 3GPP R6 (Release 6), enhancements are added to the CQI reporting method by introducing tuneable reporting rates through additional CQI reports during periods of downlink activity and fewer reports at other times [4]. These additional CQIs can be initiated on demand of fast layer 1 signalling. In addition, a certain number of successive CQI values may be averaged with respect to channel quality at the UE. The averaged value is reported and used with the instantaneous CQI measured to select the Modulation and Coding Scheme (MCS). The motivation for this technology is to improve the selection of MCS, so that the delay due to HARQ retransmissions can be reduced. In addition, the UL signalling overhead may be reduced and this decreases the uplink interference. Finally, the use of the feature requesting extra CQI transmissions by fast layer 1 signalling improves the performance of the first packets of a packet call.

2.5 Adaptive Modulation and Coding

As explained earlier, the link adaptation in HSDPA is performed by the use of Adaptive Modulation and Coding. According to the channel quality, the modulation and the coding assigned to the user change, so that higher peak data rate and average throughput can be provided. A Channel Quality Indicator (CQI) has been introduced to inform the system about the channel conditions. In order to guarantee a Block Error Rate (BLER) greater than 10% on the HS-PDSCH, each CQI is mapped onto a specific Modulation and Coding Scheme (MCS) corresponding to a given transport format. The selection of the transport format is performed by the MAC-hs located in the node B. Each transport format or MCS is defined by a [11]:

1. Modulation format, which can be either QPSK or 16QAM

2. Turbo encoder rate, which varies between 0.17 and 0.89. The encoding rate depends upon the User Equipment (UE) capabilities (maximum number of HS-DSCH codes that the UE can handle) and the desired Transport Block Size (TBS). The different code rates are obtained through puncturing

of bits in the turbo encoder of rate 1/3.

3. Number of HS-PDSCH codes allocated to the user, which ranges from 1 to the maximum number of codes supported by the UE (depends on UE category). Note that for any UE category, this number can not exceed 15 codes. In fact, the spreading factor used in HSDPA is fixed at 16. Therefore, 16 branch codes are available from which at least one code branch is reserved for signalling and control channels. Thus, leaving a maximum of 15 codes to allocate to a given user at best.

In the 3GPP specifications [11], 12 UE categories are defined according to the maximum number of HS-DSCH that the UE can handle simultaneously. The transport formats and the corresponding CQIs for all UE categories can be found in [11].

2.6 Hybrid-ARQ

Fast link adaptation provides the flexibility to match the MCS to the short term channel variations for each user. However, link adaptation is sensitive to measurement errors, delays in the CQI procedure and unexpected channel variations. Therefore, the use of ARQ, which is insensitive to CQI measurement errors, is indispensable to tolerate higher error rates in order to save cell resources, use higher order MCS and increase the user and the average cell throughput.

The ARQ technique used in UMTS is Selective Repeat (SR). The retransmissions are performed by the RLC layer in the RNC. Introducing ARQ induces delays in receiving error free information and interacts unfortunately with higher layer protocols such as the Transmission Control Protocol (TCP) used to handle end to end IP packcet communications between end hosts. If these interactions are not addressed and handled properly, drastic degradation in applications flow rates will be experienced. These interactions and means to reduce their negative effects on overall system throughput are addresses in chapters 6 and 7.

In HSDPA, the ARQ protocol is performed by the MAC-hs entity in the node B. HSDPA uses the ARQ protocol combined with Forward Error Correction (FEC) code so that an erroneous packet is not discarded but softly combined with its retransmissions in order to reduce the average delay in receiving error-free information. In addition, the tight coupling of Hybrid-ARQ and fast link adaptation limits the excessive use of ARQ (in other words the delay) since retransmissions occur if link adaptation fails to cope with the instantaneous channel conditions.

2.6.1 Hybrid-ARQ types

In HSDPA, three types of HARQ have been studied and standardized in the 3GPP specifications [1,14,16-20]: Chase combining, Incremental Redundancy (IR) and self decodable IR.

In [17], D. Chase has shown that the sequence resulting of combining two copies of the same sequence presents a lower error rate than the original sequences. Therefore, instead of discarding erroneous packets, the UE proceeds to soft combining (called Chase combining) of multiple retransmissions of the same packets before decoding. This concept, developed and standardized in the 3GPP specifications (Release 5) [1], reduces the delays compared to the ARQ used in the UMTS R99. This HARQ algorithm does not interact optimally with the AMC and the fast link adaptation since the multiple retransmissions are the same copies of the first one, i.e. the same MCS is used even if the channel conditions change. Consequently, enhanced HARQ algorithms have been introduced in the 3GPP specifications [1,14]. These new schemes rely on on Incremental redundancy (IR).

In HARQ IR, instead of retransmitting the same copy of the erroneous packet, redundant information is incrementally added to retransmissions copies. This represents a better protection of the information packets and copes more with channel conditions and AMC. In this type of HARQ, only a fraction of the information sequence is sent in the retransmission packet (according to the redundancy degree). The retransmitted packet is not self decodable and should be combined with the first transmission before decoding. To counteract this problem, a IR scheme that is self decodable has been studied and developed by the 3GPP [1,14]. To obtain a self decodable scheme, incremental redundant information is added to the first sequence and incremental puncturing is also used so that the receiver can reconstruct the information sequence and decode each retransmission before soft combining the retransmissions in case of unsuccessful decoding.

2.6.2 HARQ Protocol

The increase in complexity and in requirements of the HARQ SR leads to the adoption of simpler HARQ strategies. The Stop and Wait (SW) ARQ protocol is quite simple to implement but since it is inefficiency, a trade-off between between the simple SW and the SR, called N-Channel SW, has been developed and standardized for HSDPA [1,14].

The N-Channel SW consists of activating N HARQ processes in parallel, each one using the SW protocol. Hereby, one HARQ instance (process) can transmit data on the HS-DSCH while other instances are waiting for the acknowledgment on the uplink. Using this strategy, the retransmission process be-

haves as if the SR HARQ were employed. The advantage of the N-channel SW strategy with respect to the SR protocol is that a persistent failure in a packet transmission affects only one channel, allowing data to be transmitted on the other channels. In addition, compared to the simple SW, the N-Channel SW provides to the MAC-hs entity the flexibility to allocate the HS-DSCH channel to the same user if the radio conditions are favorable.

2.7 Packet Scheduling

The shared time structure of the HS-DSCH channel supports the use of time scheduling. Fast link adaptation based on AMC tightly coupled with scheduling provides higher transmission rates and average throughput. By allocating the HS-DSCH channel to the user with favorable channel conditions, higher order MCS are selected and higher achievable data rate and average throughput are provided. Introducing the MAC-hs entity in the node B for scheduling and using low TTI value of 2 ms allow better tracking of the short term variations of the radio channel. Users with temporary good channel conditions are more easily selected.

With the growing demand on data application services (especially non real time services such as interactive and background), HSDPA, such as any wireless system, should provide the capability of supporting a mixture of services with different quality of service requirements. Even if the interactive and background services are seen as best effort services with no service guarantees, these users still expect to receive data within a certain period of time. The starvation of these users can have a drastic effect on the performance of higher layers such as the Transport Control Protocol (TCP) layer. Therefore, a minimum service guarantee should be introduced for these services and HSDPA should achieve some "Fairness" in sharing resources among users and services. The "Fairness" can be defined as "meeting the data rate and the delay constraints of the different applications".

Consequently, the scheduler has two tasks to accomplish: increasing the average throughput by allocating the HS-DSCH channel to the user having favorable channel conditions and achieving fairness between services. These two objectives are in contradiction and there is a risk in achieving one at the expense of the other. A trade-off between fairness and efficiency (e.g. increasing the cell throughput) should be performed by the scheduler.

The scheduling over a time shared channel has been addressed widely in the literature and many proposals have been elaborated. The most famous algorithms are: Max C/I and Proportional Fair (PF) proposed in [21-22]. In Max C/I, the node B tracks the channel quality of each user by measuring the SIR

(Signal to Interference Ratio) on the CPICH channel (Common Pilot Indicator Channel) and allocates the HS-DSCH channel to the user with the best SIR. This algorithm maximizes the cell capacity but presents a problem of fairness between users especially for users at the cell border. In this context, work in [23] presents a performance comparison of several scheduling algorithms concluding that algorithms that provide the highest throughput per sector also tend to present the largest variations in throughput per user. To alleviate this problem, PF scheduling has been proposed. PF which realizes a reasonable trade-off between efficiency and fairness, consists in transmitting to the user with the highest data rate relative to its currently achieved mean data rate. This scheduler, studied in [21,22,24-28], is widely used in currently developed systems. In addition, many other algorithms have been proposed. In [29], six packet scheduler algorithms are analyzed to assess the inherent trade off among cell capacity and user fairness. In [30], an opportunistic transmission-scheduling policy, that maximizes the network throughput given a resource sharing constraint, is presented. A study in [31] illustrates a method to provide user QoS guarantees in terms of minimum data rates, while at the same time achieving some user diversity gain. Many other proposals, based on the queuing management and the channel state, have been analyzed in order to achieve fairness. A non exhaustive list of schedulers is given for reference: CSDPS (Channel state dependent packet scheduling) [32], IWFQ (Idealized Wireless Fair Queuing Algorithm) [33], CIF-Q (Channel-Condition Independent Fair Queueing) [34], SBFA (Server Based Fairness Algorithm) [35], I-CSDPS (Improved channel state dependent packet scheduling) [36], CAFQ (Channel adaptive fair queueing) [37], MLWDF (Modified Largest Weighted Delay First) [38], CDGPS (Code-division generalized processor sharing) [39], and DSDFQ (Delay-sensitive Dynamic Fair Queueing) [40].

2.7.1 Scheduling Constraints and Parameters

In HSDPA, the MAC-hs entity in the node B handles the scheduling functionality using estimated radio channel conditions to enhance cell throughput while satisfying user QoS. Certain constraints concerning the radio channel conditions, the physical available resources in the cell and user QoS have to be considered in the scheduler design. These constraints are (see [6] for details):

- The available Physical resources, which include:

    - The HSDPA reserved power: This is the power reserved by the RNC (Radio Network Controller) to the HSDPA system. The selected MCS, which determines the user data rate, depends directly upon the power reserved for HSDPA.

  - The number of spreading codes reserved by the RNC to HSDPA since this limits the available MCSs.
  - The number of available HS-SCCH channels. They represent an overhead power. In addition, code multiplexing the users in the same TTI, to increase the scheduler flexibility, depends on the number of available HS-SCCH reserved by the RNC.

- radio channel conditions, reported on the CQI each TTI, so that the scheduler selects the user with favorable channel conditions.

- QoS constraints, which include:

  - Amount of data in the node B buffer: It represents a significant parameter especially for services with limited tolerable jitter.
  - Guaranteed bit rate for certain services (such as streaming)
  - Tolerated Delay Jitter.
  - Services priority: allows the node B to prioritize flows relative to other flows. It is indicated by the parameter SPI (Scheduling Priority Indicator) set by the RNC.
  - Allocation and Retention Priority (ARP): allows the node B to determine the priority of a bearer relative to other UMTS bearers.
  - Discard Timer: This parameter is of significant relevance for streaming services. In fact, the data flows transferred from the RNC to the MAC-hs in the node B, through the Iub interface, are in the form of MAC-d PDUs (Protocol Data Units). Once arrived at the node B, a QoS discard timer is set on these PDUs in order to limit their maximum queuing. If a given MAC-d PDU is not served before the timer expiration, this PDU is discarded. This parameter should be introduced in the tolerated delay jitter constraint.
  - HARQ status knowledge: The scheduler should know if the packet to transmit is a new or a retransmitted packet. According to this knowledge, a priority indicator can be introduced to prioritize the retransmitted packets in order to satisfy the QoS delay constraints.

2.7.2 Selected Scheduling algorithms

As already mentioned, many scheduling proposals have been analyzed in the literature in order to share a channel in a time manner. In this section, five most popular and relevant schedulers are described:

the Round Robin (RR), the Fair Throughput (FT), the Max C/I, the Proportional Fair (PF) and the Score Based (SB) [41]. These schedulers are used in the modeling of cell capacity described in the next chapter.

Round Robin

The round Robin (RR) algorithm allocates the channel to the users in a cyclic order offering a fair time resource sharing among users. Since this scheduler ignores the radio channel conditions, it does not provide a fair throughput between users. The absence of the scheduling adaptation to the short term channel variations counteracts the fast link adaptation introduced in HSDPA. Consequently, this scheduler provides low cell throughput. The only advantage of using this algorithm is its implementation simplicity.

Fair Throughput

The Fair Throughput (FT) scheduler allocates the HS-DSCH channel to the users in order to achieve fair sharing of the entire cell throughput among users. During each TTI, the channel is allocated to the user who has the lowest average received data rate over previous TTIs. This algorithm provide fair resource sharing but does not exploit the instantaneous channel information. Therefore, this scheduler neglects and defeats the fast link adaptation of HSDPA and results in poor average cell throughput.

Max C/I

This scheduler is perfectly suited to the fast adaptation to the instantaneous channel variations. During each TTI, the HS-DSCH channel is allocated to the user having the best channel conditions. In fact, the node B uses the Channel Quality Indicator (CQI) reported by the link adaptation procedure and allocates the HS-DSCH channel to the user with the best SIR (Signal to Interference Ratio). In the ideal situation when channel conditions of the users present the same statistics, this strategy maximizes the total capacity of the system and the throughput of individual users. In reality, the statistics are not symmetrical since the users can be closer to the base station with a better average SIR or at the cell border with relatively bad conditions, stationary or moving at high speed, in a rich scattering environment or with no scatterers around them. Therefore, by using the Max C/I strategy in practice, the channel is always allocated with higher order MCS (i.e. higher average transmission rate) but induces starvation of users with relatively bad channel conditions. Consequently, this algorithm maximizes the

cell capacity but presents a problem of fairness between users especially for users at the cell border. In addition, the QoS constraints (e.g. the throughput in a given time scale and not the long term average throughput) of different services are not considered in this scheduler which can have a drastic effect on higher layers such as TCP or on certain services such as streaming.

Proportional Fair

As explained above, the FT algorithm performs a fair sharing of the average cell throughput among users independently of the channel conditions. This causes loss in average throughput per user and per cell. The Max C/I strategy prioritizes users with good channel conditions and thus maximizes the cell throughput but at the expense of users at the cell border. A problem of fairness is therefore observed. To achieve a trade-off between fairness and efficiency, the Proportional Fair strategy has been proposed [21-22]. It consists in transmitting to the user with the highest data rate relative to its current mean data rate. During each TTI, the channel is allocated to the user having max(r/S. variable r is the transmission rate in the current TTI (according to the transmission scheme selected) and S is the average bit rate transmitted in the previous TTIs and evaluated through an exponentially weighted low pass filter. S is evaluated through the following equation:

$$S(n+1) = \begin{cases} (1-\frac{1}{t_c})S(n) + \frac{1}{t_c}r(n) & \text{if the TTI } n \text{ is allocated to the user} \\ (1-\frac{1}{t_c})S(n) & \text{elsewhere} \end{cases} \quad (2.1)$$

This strategy keeps track of the average throughput S of each user in a past window of length t_c where t_c is a parameter varying between 800 and 1000 in general.

In the literature, there are several versions of the Proportional fair. Some versions propose to evaluate the mean bit rate R through an exponentially smoothed average when others increase the influence of the instantaneously transmission rate by using the user selection condition: $max(r^c/S)$ where c is a parameter depending on the channel conditions [42-43]. These algorithms increase the fairness at the expense of cell throughput and vice versa. The selected algorithm is entirely up to the implementer and the operator strategy. The PF algorithm can be considered as a reasonable trade-off between fairness and capacity.

Score Based

The Score Based (SB) scheduler, proposed by Bonald in [41], consists of allocating the channel to the user having the maximum transmission rate relative to its past rate statistics. This algorithm can be explained as follows: Let us consider a HSDPA system with two active users. Let "$r_{1,v}$" and "$r_{2,v}$" where v=1..n be the past transmission rates for each user (even when the TTI is not attributed to this user) observed over a window size n. The idea is to classify the past rates of each user in decreasing order and to give a rank for each rate (for example rank 1 for the highest rate). During the TTI "$n+1$", if the possible rate of user 1 "$r_{1,n+1}$" is classified in rank 1 relative to his own rate statistics and the rate of user 2 "$r_{2,n+1}$" is classified in rank 3 relative to his own rate statistics, in this case the channel is allocated to user 1 even if $r_{2,n+1} > r_{1,n+1}$. This algorithm has the advantage of not suffering from asymmetric fading and data rate constraint which is not the case of the Proportional Fair algorithm.

Bibliography

[1] 3GPP TS 25.308 V6.3.0 (2004-12), "HSDPA Overall Description", stage 2, (Rel. 6).

[2] 3GPP TR 25.858 V5.0.0 (2002-03), "High Speed Downlink Packet Access, Physical layer aspects", (Rel. 5).

[3] 3GPP TR 25.877 V5.1.0 (2002-06), "High Speed Downlink Packet Access (HSDPA) Iub/Iur protocol aspects", (Rel. 5).

[4] 3GPP TR 25.899 V6.1.0 (2004-09), "High Speed Download Packet Access (HSDPA) enhancements", (Rel. 6).

[5] Harri Holma and Antti Toskala, WCDMA for UMTS. Radio Access for Third Generation Mobile Communications, Third Edition, John Wiley and Sons, England, 2004, ISBN 0470870966.

[6] P.J. Ameigeiras Gutierrez, "Packet Scheduling And QoS in HSDPA", Ph.D. Thesis, Aalborg University, Oct. 2003, ISBN: 8790834380.

[7] 3GPP TS 25.201 V6.2.0 (2005-06), "Physical layer - General description", (Rel. 6).

[8] 3GPP TS 25.211 V6.6.0 (2005-09), "Physical channels and mapping of transport channels onto physical channels (FDD)", (Rel. 6).

[9] 3GPP TS 25.212 V6.6.0 (2005-09), "Multiplexing and channel coding (FDD)", (Rel. 6).

[10] 3GPP TS 25.213 V6.4.0 (2005-09), "Spreading and modulation (FDD)", (Rel. 6).

[11] 3GPP TS 25.214 V6.5.0 (2005-03), "Physical layer procedures (FDD)", (Release 6).

[12] 3GPP TS 25.331 V6.7.0 (2005-09), "Radio Resource Control (RRC) Protocol Specification", (Release 6).

[13] R. Tanner and J. Woodard, WCDMA Requirements and Practical Design, John Wiley & Sons Ltd, 2004, ISBN 0470861770.

[14] 3GPP TS 25.321 V6.5.0 (2005-06), "Medium Access Control (MAC) protocol specification", (Release 6).

[15] N. C. Ericsson, "On Scheduling and Adaptive Modulation in Wireless Communications", Technical Licentiate Thesis, UPPSALA University, Sweden, June 2001.

[16] 3GPP TSG RAN WG1#28, Tdoc R1-02-1084, "Duration of CQI Measurement", Philips, Seattle, USA, Aug. 2002.

[17] D. Chase, "Code Combining–A Maximum-Likelihood Decoding Approach for Combining an Arbitrary Number of Noisy Packets", Communications, IEEE Transactions on [legacy, pre - 1988] , Volume: 33 Issue: 5 , May 1985.

[18] 3GPP TSG RAN WG1#18, Tdoc R1-01-0048, "Clarifications on Dual-Channel Stop-and-Wait HARQ", Motorola, 2001.

[19] 3GPP TSG RAN WG1#18, Tdoc R1-01-0007, "Considerations on HSDPA HARQ concepts", Nokia, 2001.

[20] 3GPP TSG RAN WG1#20, Tdoc R1-01-0553, "Further buffer complexity and processing time considerations on HARQ", Nokia, Busan, Korea, May 2001.

[21] J.M. Holtzman, "CDMA forward link waterfilling power control," In Proc. of IEEE VTC Spring, 2000.

[22] A. Jalali, R. Padovani, and R. Pankaj, "Data Throughput of CDMA-HDR a high efficiency-high data Wireless personal communication system", in Proc. 50th annual Int. VTC, vol. 3, Tokyo, May 2000, pp. 1854-1858.

[23] R. C. Elliott and W. A. Krzymien, "Scheduling Algorithms for the CDMA2000 Packet Data Evolution," IEEE Vehicular Technology Conference, VTC 2002 Fall, Volume 1, pp. 304-310.

[24] J.M. Holtzman, Asymptotic analysis of Proportional Fair algorithm. Proc. of 12th IEEE PIMRC, 2001.

[25] S. Borst, "User-Level Performance of Channel-Aware Scheduling Algorithms in Wireless Data Networks", Proc. to IEEE INFOCOM 2003.

[26] Mohamad Assaad and Djamal Zeghlache, " Cross Layer Design In HSDPA System", IEEE Journal On Selected Areas In Communications (JSAC), to appear in 2006.

[27] Mohamad Assaad and Djamal Zeghlache, "Scheduling Study in HSDPA System," In Proc. of the 16th Annual IEEE International Symposium on Personal Indoor and Mobile Radio Communications (PIMRC 2005), Berlin, Sep. 2005.

[28] Mohamad Assaad and Djamal Zeghlache, "Fast Scheduling in HSDPA System: A Trade-off Between Fairness and Efficiency," In Proc. of the Eigth International Symposium on WirelessPersonal Multimedia Communications (WPMC'05), Aalborg, Sep. 2005.

[29] T. Kolding ,F. Frederiksen, and P. Mogensen,"Performance Aspects of WCDMA Systems with High Speed Downlink Packet Access (HSDPA)," IEEE semi annual Vehicular Technology Conference, 2002, VTC 2002 Fall, Volume 1, pp. 477- 481.

[30] Xin Liu, Edwin K. P. Chong, and Ness B. Shroff, "Opportunistic Transmission Scheduling With Resource-Sharing Constraints in Wireless Networks," IEEE Journal on Selected Areas in Communications, Volume 19, Oct 2001, pp 2053-2064.

[31] P. Hosein, "QoS Control for WCDMA High Speed Data," 4th International Workshop on Mobile and Wireless Communications Network, September, 2002, pp. 169-173.

[32] C. Fragouli, V. Sivaraman, and M. Srivastava, "Controlled mul-timedia wireless link sharing via enhanced class-based queueing with channel-state dependent packet scheduling," in Proc. of INFOCOM98, vol. 2, Mar. 1998, pp. 572580.

[33] S. Lu and V. Bharghavan, "Fair scheduling in wireless packet net-works," IEEE/ACM Trans. Networking, vol. 7, no. 4, pp. 473489, 1999.

[34] T. S. Eugene Ng, I. Stoica, and H. Zhang, "Packet fair queueing algorithms for wireless networks with locationdependent errors," in Proc. of INFOCOM98, Mar. 1998, pp. 11031111.

[35] P. Ramanathan and P. Agrawal, "Adapting packet fair queueing algorithms to wireless networks," in Proc. ACM MOBICOM98, Oct. 1998.

[36] J. Gomez, A. T. Campbell, and H. Morikawa, "The Havana frame-work for supporting application and channel dependent QoS in wireless networks," in Proc. ICNP99, Nov. 1999, pp. 235244.

[37] Li Wang, Yu-Kwong Kwok, Wing-Cheong Lau, and Vincent K. N. Lau, Channel Capacity Fair Queueing in Wireless Networks: Issues and A New Algorithm, ICC 2002, April, 2002, New York, U.S.A.

[38] M. Andrews, K. Kumaran, K. Ramanan, A. Stolyar, P. Whiting, and R. Vijayakumar, Providing quality of service over a shared wireless link, IEEE Communications Magazine, vol. 39, no. 2, Feb. 2001, pp. 150154.

[39] L. Xu, X. Shen, J. Mark, "Dynamic bandwidth allocation with fair scheduling for WCDMA systems," IEEE Wireless Communications, April, 2002.

[40] Huai-Rong Shao, Chia Shen, Daqing Gu, Jinyun Zhang, Philip Orlik, "Dynamic Resource Control for High-Speed Downlink Packet Access Wireless Channel," In Proceedings of the 23 rd IEEE International Conference on Distributed Computing Systems Workshops (ICDCSW03), May 2003, pp. 838-843.

[41] Thomas bonald, "A score-based opportunistic scheduler for fading radio channels," in Proc. of European Wireless 2004.

[42] H. Kim, K. Kim, Y. Han and J. Lee, An Efficient Algorithm for Qos in Wireless Packet Data Transmission, In Proc. of the IEEE International Symposium on Personal Indoor and Mobile Radio Communications (PIMRC2002), vol. 5, September 2002, pp. 22442248.

[43] G. Aniba and S. Aissa, "Adaptive proportional fairness for packet scheduling in HSDPA," IEEE Global Telecommunications Conference (GLOBECOM 2004), Vol. 6, Nov./Dec. 2004, pp. 4033-4037.

Chapter 3

Scheduling of Non-real Time Data: Analytical Studies

3.1 Introduction

The evolution of the mobile communication market is expected to bring a major increase in data traffic demands combined with high bit rate services. Recent 3G standardization (3GPP) and related technologies development reflect the need for high-speed packet data wireless system. In this context, The 3GPP introduces a "beyond 3G" system denominated High Speed Downlink Packet Access (HSDPA). The HSDPA concept appears as an umbrella of some new technologies introduced to increase the user peak data rates up to 14.4 Mbps and to improve the spectral efficiency for downlink packet data services. HSDPA consists of a new downlink time shared channel HS-DSCH (High Speed Downlink Shared Channel) that supports a 2ms Transmission Time Interval (TTI), Adaptive Modulation and coding (AMC), Multi-code transmission and fast physical layer Hybrid ARQ (Automatic Repeat Request). The link adaptation and packet scheduling functionalities are executed directly from the node B, which enables them to acquire knowledge of the instantaneous radio channel quality of each user. This knowledge allows advanced packet scheduling techniques that increase user bit rate and system capacity.

AMC and fast scheduling are tightly coupled to allocate the HS-DSCH channel to the adequate user and to adapt its transmission parameters to the short term radio channel variations. Therefore, wireless channel model has a capital effect on the scheduling behavior, AMC selection and consequently on the HSDPA performance capacity.

In this chapter, we have studied analytically the effect of wireless fading on the performance of

various schedulers in HSDPA system. This study has been conducted using statistical models of the wireless fading channel. The analytical proposed models estimate the cell throughput and the user bit rate to compare the performance of schedulers.

The user bit rate and cell capacity estimation requires the introduction into the model of the techniques used in HSDPA, in particular AMC, HARQ and scheduling. In addition, derivation of the analytical expressions requires the description of the channel model, the receiver type and an approximate expression of SIR (Signal to Interference Ratio). Several statistical channel models are considered in the conducted study in this chapter, in particular the cases of uncorrelated and correlated multipath/shadowing channels with path amplitude following Rayleigh or Nakagami distributions. The case of composite dense uncorrelated and correlated multipath/shadowing channel considers the presence of Wide-sense Stationary channel, constant Power Dispersion Profile (PDP) and frequency selective fading following a Rayleigh distribution.

This chapter is divided as follows: Section 3.2 presents an approximate expression of the SIR, at the user, derived in the case of multipath channel and Rake receiver. Section 3.3 provides description of the analytical proposed models. The HARQ effect on the cell and user throughput is modeled in section 3.3.1. In section 3.3.2, the effect of the fast cell selection on the cell capacity is presented. The AMC models are derived in section 3.3.3. Introduction of scheduling in the models is described in section 3.3.4. The schedulers considered in modeling are the Round Robin (RR), Fair Throughput (FT), Max C/I, Proportional Fair (PF) and Score Based (SB). The final expressions of the user and cell throughput are then obtained.

3.2 Signal to Interference Ratio (SIR) expression

3.2.1 Transmitted signal

In HSDPA, a quadrature-Amplitude (4-QAM or 16QAM)-modulated symbol stream is spread by a real-valued channelization code followed by a complex scrambling code. The signals of various user codes are then linearly combined and transmitted over the wireless channel. While the channelization codes of different users are different and orthogonal to each other, the same scrambling code is shared by all the users in a cell. The baseband representation of the signal transmitted on the downlink is given by:

$$s(t) = \sum_{i=1}^{N_c} \sqrt{P_i} b_i(t) \sum_j c_j^i \psi(t - jT_c) \tag{3.1}$$

where N_c is the number of intracell downlink codes used during the TTI t, b(t) is the normalized QPSK/16QAM symbol stream of user code i, c_j^i is the j^{th} chip sequence of the complex channelization code concatenated with the scrambling code and $\psi(t)$ is the chip pulse shape. The HSDPA downlink uses a root raised cosine (RRC) pulse for $\psi(t)$ with a roll off factor of 0.22 [1].

3.2.2 Channel model

Wireless signals transmitted over the wireless propagation channel are subject to a number of impairments and phenomena including:

- Path loss due to distance between the transmitter and receiver.
- Shadowing effects due to the immediate environment around the user that influence the average received signal energy over several hundreds of wavelengths.
- Fast fading in the signal envelope manifest via random signal amplitude, phase, energy and power variations. These variations are observed on time scales of the order of half a wavelength.
- Doppler effects due to user or terminal mobility. This is a frequency spreading phenomenon proportional to vehicle or terminal speed.

In the literature, several analyses have been conducted to characterize the radio propagation channel in time and frequency domain (see [2-7]). Since this thesis focuses on scheduling study and cell capacity estimation, only the channel impulse response in the time domain will be considered.

The impulse response of the channel, as seen by user code i, can be modeled as [2]:

$$h(t,\tau) = \sqrt{G_i}\sum_{l=1}^{N_T}\alpha_l(t)\delta(t-\tau_l) \tag{3.2}$$

where $\alpha_l(t) = |\alpha_l(t)|e^{j\varphi(t)}$ is the complex time-varying path gain, N_T is the number of resolvable multipath components, τ_l is the time delay of path l, and G_i is the mean channel loss, including the shadowing (described in the next section, "Path loss and shadowing model") . The 3GPP standard specifies several channel profiles, e.g., typical urban (TU), rural area (RA), and hilly terrain (HT) [1, 10]. Each profile is described by a given number of paths, with the l^{th} path having average power $E[|\alpha_l(t)|^2]$ and relative delay τ_l.

The amplitude and phase distribution of the received signal depend primarily on the presence or not of a Line Of Sight (LOS) component [2-7]:

- When the receiver is located in a rich scattering channel and there is no line of sight (LOS) between the transmitter and the receiver, the signal is impinging the receiver antenna from many directions and is the sum of a large number of uncorrelated components. The composite signal can be decomposed in Cartesian coordinates into an in phase and quadrature component each approximated by Gaussian random variables of equal variance . The resulting received signal envelope follows consequently a Rayleigh distribution:

$$f(\alpha) = \frac{2\alpha}{\Omega} e^{-\frac{\alpha^2}{\Omega}}, \alpha \geq 0 \tag{3.3}$$

  Assuming uncorrelated quadrature components, the received signal phase is uniformly distributed in the interval [0,2π].

- In practice, however, there is occasionally a dominant incoming wave which can be a LOS component or a strong specular component. In these situations, the received signal envelope obeys the well known Rician distribution:

$$f(\alpha) = \frac{\alpha}{\Omega} I_0\left(\frac{\alpha\rho}{\Omega}\right) e^{-\frac{\alpha^2+\rho^2}{2\Omega}}, \alpha \geq 0 \tag{3.4}$$

  where I_0 is the zero-th order modified Bessel function of the first kind. The average power is given by:

$$E(|\alpha|^2) = \rho^2 + 2\Omega \tag{3.5}$$

  The parameter $K = \rho^2/2\Omega$ gives the ratio between the power in the direct line of sight component to the power of all other delayed paths. When $K = 0$ the channel exhibits a Rayleigh fading behavior. For $K \to +\infty$, the channel does not exhibit fading at all since the LOS component is dominant. Due to the presence of the LOS component, the phase is no longer uniformly distributed:

$$f_\Phi(\phi) = \frac{1}{2\pi} e^{-\frac{\rho^2}{2\Omega}} \left[1 + \sqrt{\frac{\pi}{2}} \frac{\rho cos\phi}{\sqrt{\Omega}} e^{\frac{\rho^2 cos^2\phi}{2\Omega}} \left(1 + erf\left(\frac{\rho cos\phi}{\sqrt{2\sqrt{\Omega}}}\right)\right)\right], |\phi| \leq \pi \tag{3.6}$$

- A purely empirical model that matches more closely experimental data than the Rayleigh or Rician

fading models is the Nakagami model. The Nakagami distribution is given by:

$$f(\alpha) = \frac{2m_m \alpha^{2m-1}}{\Gamma(m)\Omega^m} e^{-\frac{m\alpha^2}{\Omega}}, \alpha \geq 0, m \geq 1/2 \tag{3.7}$$

where $\Omega = E(|\alpha|^2)$ and $\Gamma(.)$ is the Gamma function.

For m=1/2, the Nakagami distribution gives the Rayleigh distribution. For $m = (K+1)^2/(2K+1)$, it provides a good approximation of the Rician distribution.

When $m \to +\infty$, the Nakagami distribution becomes an impulse and indicates the absence of fading. The Nakagami model is often used in analytical modeling and analysis not only because it reflects experimental data well but also because it embeds both the Rayleigh and Rician models as specific cases.

Path loss and shadowing model

In addition to the fast fading, the link quality is also affected by slow variation of the mean signal level due to the shadowing from terrain, building, and trees. This shadowing is modeled in general by a log-normal variable [8].

In general, the path loss and shadowing effect on the signal received by user i can be modeled as $G_i = d_{ij}^{-\mu} 10^{s/10}$. d_{ij} is the distance between user i and the node B of cell j, μ is the path loss slope ($\mu = 3,4$ in macro cell and $\mu = 2$ in micro cell) and s corresponds to log-normal shadowing with zero mean and standard deviation σ (σ^2 between 8 and 12 dB). The shadowing loss s is correlated between the BSs [8].This effect is usually modeled by considering the shadowing as a sum (in dB) of a component common to all base stations, s_c and a component s_{sj} specific to base station j noted BS_j. The shadowing loss expression is given as:

$$s_j = a s_c + b s_{sj} \tag{3.8}$$

where $a^2+b^2 = 1$. A reasonable assumption is $a^2 = b^2 = 1/2$. The mean and variances of the log-normal variables are:

$$\begin{cases} E(s_j) = E(s_c) = E(s_{sj}) = 0 \\ var(s_j) = var(s_c) = var(s_{sj}) = \sigma^2 \\ E(s_{sj} s_{sk}) = 0 \qquad\qquad j \neq k \end{cases} \tag{3.9}$$

3.2.3 Receiver output

The receiver used is a Selective Rake receiver with N_F fingers. The signal at the input of the receiver can be given by:

$$r(t) = \sqrt{G}\sum_{l=1}^{N_T}\sum_{i=1}^{N_c}\sqrt{P_i}\alpha_l(t)b_i(t-\tau_l)\sum_j c_j^i\psi(t-\tau_l-jT_c) + n(t) \tag{3.10}$$

Note that the signals of all the downlink codes face the same multipath channel gains and delays. For each user code i, the output of its receiver after despreading is:

$$O_i = \sum_{n=1}^{N_F}\int_{\tau_n}^{\tau_n+T_s} r(t)\omega_n^*(t)\Big(\sum_j c_j^i\psi(t-\tau_l-jT_c)\Big)dt \tag{3.11}$$

where $\omega_n(t) = |\omega_n(t)|e^{j\theta(t)}$ is the n^{th} Rake finger weight at time t, N_F is the number of Rake fingers in the receiver, and T_s is the symbol duration. Note that the channel gain is assumed to be constant over the duration of a symbol. The receiver output O_i can be written as follows:

$$O_i = S_i + \sum_{j\neq i} S_j + W \tag{3.12}$$

where S_i is the signal component, S_j is the interference component due to the j^{th} code, and W is the noise component. S_i is given by:

$$S_i = (SF)\sqrt{P_iG_i}b_i\sum_{n=1}^{N_F}\alpha_n\omega_n^* \tag{3.13}$$

where SF is the spreading factor. Therefore, the signal power at the output of the receiver is:

$$|S_i|^2 = (SF)^2P_iG_ib_i|\sum_{n=1}^{N_F}\alpha_n\omega_n^*|^2 \tag{3.14}$$

For the interfering signals, the expression is much more complicated and it depends on the cross correlation expressions. If x is the time shift between 2 PN sequences scrambling codes, the interference from code j to code i is given by the following equation [9, 10]:

$$S_j = \sqrt{P_iG_i}\sum_{n=1}^{N_F}\sum_{l\neq n}^{N_T}\alpha_l\omega_n^*\Big[b_{-1}^jR_{i,j}(x,\tau_l-\tau_n) + b_0^j\widehat{R}_{i,j}(x,\tau_l-\tau_n)\Big] \tag{3.15}$$

where

$$R_{i,j}(x,\tau) = \int_0^{\tau} \Big(\sum_k c_k^i \psi(t + xT_c - \tau - kT_c)\Big)^* \Big(\sum_k c_k^j \psi(t + xT_c - kT_c)\Big) dt \tag{3.16}$$

$$\widehat{R}_{i,j}(x,\tau) = \int_{\tau}^{T_s} \Big(\sum_k c_k^i \psi(t + xT_c - \tau - kT_c)\Big)^* \Big(\sum_k c_k^j \psi(t + xT_c - kT_c)\Big) dt \tag{3.17}$$

$$b^j(\tau) = \begin{cases} b_{-1}^j & -T_s \leq \tau < 0 \\ b_0^j & 0 \leq \tau < T_s \end{cases} \tag{3.18}$$

It is easy to verify that the intra cell interference power is given by:

$$I_{intra} = E\Big[\sum_{j \neq i}^{N_c} \|S_j\|^2\Big] \tag{3.19}$$

By averaging over all the channelization and scrambling codes, the time shift x, the amplitudes and the phases of the multipath gains, and the fractional chip delays between the multipaths, the interference power can be approximated by:

$$I_{intra} = \beta(P_{cell} - P_i) G_i SF \Big(\sum_{n=1}^{N_T} |\alpha_n|^2\Big)\Big(\sum_{n=1}^{N_F} |\omega_n^*|^2\Big) \tag{3.20}$$

where P_{cell} is the total cell power and β is loss of orthogonality of CDMA codes approximated to 40% in macro cell environment and 6% in micro cell environment [1].

3.2.4 SIR expression

Using the three previous sections, the Signal to Interference Ratio (SIR) of user i in cell j can be evaluated using the following expression:

$$SIR_i = \frac{SF}{log_2(M)\tau} \frac{\frac{\delta P_j - N_{c,i} P_{sig}}{N_{c,i}} G_{ij} \Big(|\sum_{n=1}^{N_F} \alpha_n \omega_n^*|^2\Big)}{\Big[\beta\Big(P_j - \frac{\delta P_j - N_{c,i} P_{sig}}{N_{c,i}}\Big) G_{ij} \Big(\sum_{l=1}^{N_T} |\alpha_l|^2\Big) + I_{inter} + \eta_0\Big]\Big(\sum_{n=1}^{N_F} |\omega_n^*|^2\Big)} \tag{3.21}$$

where P_j is the transmitted power of cell j, η_0 is the noise power, δ is the fraction of power allocated to data channels (HS-DSCH) approximately equal to 0.8 and P_{sig} is the transmitted power of SCCH associated to HS-DSCH. I_{inter} is the inter cell interference approximated in general to $\sum_{k \neq j} P_k G_{ik}$ where P_j is the transmitted power of cell k and G_{ik} is the path loss (including the shadowing) between cell k and user i. Since the noise power η_0 has a small value compared to the interference (-99 dBm) it

is neglected in the analysis conducted in this thesis (see [1, 8]).

3.3 HSDPA analytical models

In order to compare between several scheduling algorithms in HSDPA, we propose in this section analytical models capable of evaluating the cell throughput and the bit rate of each user in the cell. These models considers the enhanced techniques used in HSDPA such as AMC, HARQ and scheduling as well as fast cell selection. Full Rake receiver is assumed to be used at the mobile user. The radio channel used is a correlated multipath channel with shadowing following log-normal distribution. The amplitude module of each path follows Rayleigh or Nakagami distributions.

3.3.1 Hybrid-ARQ

In this thesis, the Hybrid Automatic Repeat Request (HARQ) used is the multi-channel "Stop and Wait" ARQ protocol, called N-channel SAW. Erroneous packet retransmissions are combined softly using the Chase algorithm. The HARQ affects the user bit rate and the cell throughput since erroneous packets are retransmitted several times. To assess the effect of HARQ on HSDPA users, we provide in this section an analytical estimation of the mean number of packets (blocks) transmissions in HSDPA.

In modeling HARQ, let P_e be the probability of errors after decoding the information block by FEC. Let P_{s2} be the probability of errors after soft combining two successive transmissions of the same information block and more generally P_{sj} be the probability of errors after soft combining j successive transmissions. It is assumed that all the errors are detected thanks to a CRC. According to [11, 12], the effective code rate after soft combining j blocks is τ/j where τ is the coding rate. For a given target BLock Error Rate BLER (SIR target), the value of P_{sj} is extracted from the curve of link level simulation by having the same SIR given by the curve corresponding to (modulation M, coding τ) in [13].

Lemma

The mean number of transmissions is given by the following equation:

$$N_s \approx \frac{1 + P_e - P_e P_{s2}}{1 - P_e P_{s2}} - \frac{P_e^3 P_{s2}}{1 - P_e P_{s2}} + \frac{P_e^3 P_{s2} P_{s3}}{1 - P_e P_{s4}} \tag{3.22}$$

The factor $\frac{1+P_e-P_eP_{s2}}{1-P_eP_{s2}}$ in (3.22) represents the mean number of transmissions when the soft combining involves only two transmissions.

Proof

Since fast link adaptation is used, the received SIR of each transmission scheme (modulation and coding) can be assumed fairly constant. Consequently, the probability to properly decode the block and be error free after j transmissions is:

$$P_j = (P_e)^{j-1}(P_{s2}P_{s3}..P_{s(j-1)})(1-P_{sj}) \tag{3.23}$$

The required mean number of transmissions ($\sum jP_j$), after several manipulations, is given by:

$$N_s = 1 + P_e\Big(\sum_{i=0}^{\infty} P_e^i P_{s2}^i\Big) + P_e^3 P_{s2}^2\Big(\sum_{i=0}^{\infty} P_e^i P_{s2}^i\Big) + P_e^3 P_{s2}P_{s3}\Big(1 + \sum_{i=2}^{\infty} P_e^i \underbrace{P_{s4}...P_{s(3+i)}}_{iterms}\Big) \tag{3.24}$$

For i varying from 2 to infinity, $\underbrace{P_{s4}...P_{s(3+i)}} \leq P_{s4}^i$. Hence, (3.24) can be upper bounded after several manipulations:

$$N_s \leq \frac{1+P_e-P_eP_{s2}}{1-P_eP_{s2}} - \frac{P_e^3P_{s2}}{1-P_eP_{s2}} + \frac{P_e^3P_{s2}P_{s3}}{1-P_eP_{s4}} \tag{3.25}$$

The difference between N_s and the upper bound, noted ε, can be upper bounded using the following equation:

$$\varepsilon \leq P_e^5 P_{s2}P_{s3}P_{s4}\Big(\frac{P_{s4}}{1-P_eP_{s4}} - \frac{P_{s5}}{1-P_eP_{s6}}\Big) \tag{3.26}$$

ε has a very low value and can be neglected. Hence, the mean number of transmissions can be approximated by its upper bound as in equation 3.22.

3.3.2 Fast cell selection

The HS-DSCH channel does not support soft handover. However, a fast cell selection procedure is applied in each TTI which could be seen as a substitute for handover. Fast cell selection affects the interval of variation of the shadowing parameter (this point will be described more in the next section when evaluating the distribution function of the SIR in order to get the probability of use of different MCSs). The mobile user measures the "mean" received power of the CPICH channel of the various cells

and chooses the cell to which it would be connected. The choice is governed by the following equation:

$$P_{CPICH,j} d_j^{-\mu} 10^{s_j/10} \geq P_{CPICH,l} d_l^{-\mu} 10^{s_l/10} \quad (for \ \ l \neq j) \tag{3.27}$$

$P_{CPICH,j}$ is the transmitted power of the CPICH channel in cell j. The cell selection depends on the mean received power and not on the instantaneous power which explains the fact that the fast fading is not included in the analysis of cell selection. Note that the HS-DSCH in HSDPA does not support fast power control. No fast power control is used either on the control channel. Hence, the transmitted power of the node B is constant and all the available power at the node B is assumed as used (43dBm). Consequently, the CPICH transmitted power is the same in all the cells. By replacing s_j by its value $as_c + bs_{sj}$ and using the condition in (3.27) the following inequality is obtained after several manipulations:

$$s_{sl} < s_{sj} - \frac{10\mu log10(d_j/d_l)}{b} \quad (for \ \ l \neq j) \tag{3.28}$$

3.3.3 Adaptive Modulation and Coding (AMC)

To track the variation of the channel conditions, AMC is used in HSDPA where a Modulation and Coding Scheme (a modulation order M, a coding rate τ and a number of HS-DSCH codes N), denoted by MCS, is selected on a dynamic basis according to the value of SIR (Signal to Interference Ratio). Note that N is at maximum equal to 15 codes.

Modeling AMC consists of evaluating analytically the percentage (or the probability) of use of each modulation and coding scheme for each user. Let k_{mcs} be the probability of selection of modulation and coding scheme mcs and γ_{mcs} be the target SIR of this transmission scheme (i.e. CQI). $k_{mcs} = Prob(SIR \geq \gamma_{mcs})$ for the highest order modulation and coding scheme (the 30^{th} CQI) and $kmcs = Prob(\gamma_{mcs} \leq SIR < \gamma_{mcs+1})$ for the other transmission schemes. The probability $Prob(\gamma_{mcs} \leq SIR < \gamma_{mcs+1})$ can be evaluated through $[Prob(SIR \geq \gamma_{mcs}) - Prob(SIR > \gamma_{mcs+1})]$.

$$k_{mcs} = \begin{cases} Prob(SIR \geq \gamma_{mcs})) & \text{highest order } (M, \tau, N)_m \\ Prob(SIR \geq \gamma_{mcs}) - Prob(SIR > \gamma_{mcs+1}) & \text{other } (M, \tau, N)_m \end{cases} \tag{3.29}$$

The SIR expression depends upon the radio environment (i.e. path loss model, shadowing, correlation between paths and fast fading distribution e.g. Rayleigh and Nakagami) and the number of Rake receiver fingers. In this section, we consider full rake receiver with correlated and identically distributed

fast fading paths. The cases of Rayleigh and Nakagami fast fading are studied and the probabilities of use of MCS schemes are derived analytically in each case.

For full rake receiver and Rake finger weight ω equal to the time-varying path gain α (which is in general the case), the probability $Prob(SIR \geq \gamma_{mcs})$ can be written as follows:

$$\left(\sum_{l=1}^{N_T} |\alpha_l|^2\right) X \geq \frac{\gamma_{mcs}}{A_{mcs} - \gamma_{mcs} B_{mcs}} \tag{3.30}$$

where:

$$A_{mcs} = \frac{SF}{log_2(M)\tau} \frac{\delta P_j - N_{c,i} P_{sig}}{N_{c,i}} \tag{3.31}$$

$$B_{mcs} = \beta\left(P_j - \frac{\delta P_j - N_{c,i} P_{sig}}{N_{c,i}}\right) \tag{3.32}$$

$$X = \frac{10^{bs_{sj}/10}}{\sum_{l \neq j}\left(P_l \left(\frac{d_l}{d_j}\right)^{-\mu} 10^{bs_{sl}/10}\right)} \tag{3.33}$$

Distribution function of parameter X

The expression $\sum_{l \neq j}\left(P_l \left(\frac{d_l}{d_j}\right)^{-\mu} 10^{bs_{sl}/10}\right)$ is the sum of independent log-normal variables. According to [14], using the approximation of Fenton-Wilkinson, the sum of a finite number of log-normal variables can be approximated to a log-normal variable. Hence, X can be considered as the division of two correlated log-normal variables which is equivalent to a log-normal variable (the correlation is interpreted by the relation between s_{sj} and s_{sl} due to the effect of handover as we have shown in the condition of equation 3.28).

To evaluate the parameters of the equivalent log-normal variable, i.e. the mean value μ_f and the variance σ_f^2, we need to consider the effect of fast cell selection (hard handover) which limits the interval of variation of parameter s_{sj} (see equation 3.28).

To get the mean value μ_X and the variance σ_X^2 of the equivalent log-normal variable, we use the Fenton-Wilkinson (FW) approximation which is quite accurate for correlated identically log-normal components with standard deviation up to 12dB [15]. In this thesis, we add to the FW approximation the fast cell selection condition (equation 3.28) as follows:

We evaluate the mean value and the variance of the expression
$(1/X) = \sum_{l \neq j} P_l \left(\frac{d_l}{d_j}\right)^{-\mu} \left[10^{b(s_{sl} - s_{sj})/10}; s_{sl} < s_{sj} - \frac{10\mu log10(d_j/d_l)}{b}\right]$, E1 and V1 given by equations 3.34 and 3.35, where σ^2, the variance of s_j, equals 8 to 12 dB in general [1, 8] and $E(d_j, d_l, d_{l'})$ is given

by equation 3.36.

$$E1 = e^{(b\beta\sigma)^2/2} \sum_{l \neq j} \left(\frac{d_j}{d_l}\right)^{\mu} P_l Q\left(b\beta\sigma - \frac{10\mu log10(d_l/d_j) - bs_{sj}}{b\sigma}\right) \tag{3.34}$$

$$V1 = e^{(b\beta\sigma)^2}\Bigg[e^{3(b\beta\sigma)^2} \sum_{l \neq j} P_l^2 (\frac{d_j}{d_l})^{2\mu} Q(2\sqrt{2}b\beta\sigma + \frac{10\mu log10(\frac{d_j}{d_l})}{\sqrt{2}b\sigma}) + \sum_{l \neq j} \sum_{l' \neq l,j} P_l P_{l'} (\frac{d_j}{d_l})^{\mu} (\frac{d_j}{d_{l'}})^{\mu} E(d_j, d_l, d_{l'}) - e^{(b\beta\sigma)^2} \left(\sum_{l \neq j} P_l (\frac{d_j}{d_l})^{\mu} Q(\sqrt{2}b\beta\sigma + \frac{10\mu log10(\frac{d_j}{d_l})}{\sqrt{2}b\sigma})\right)^2\Bigg] \tag{3.35}$$

$$E(d_j, d_l, d_{l'}) = \frac{1}{\sqrt{2\pi}\sigma} \int_{-\infty}^{+\infty} \left[e^{-2\beta b s_{sj}} e^{-\frac{s_{sj}^2}{2\sigma^2}} Q(b\beta\sigma + \frac{10\mu log10(\frac{d_j}{d_l}) - bs_{sj}}{b\sigma}) Q(b\beta\sigma + \frac{10\mu log10(\frac{d_j}{d_{l'}}) - bs_{sj}}{b\sigma})\right] ds_{sj} \tag{3.36}$$

The parameters μ_X and σ_X^2 are then given by:

$$\mu_X = -\epsilon \ln\left(\frac{E1^2}{\sqrt{V1 + E1^2}}\right) \tag{3.37}$$

$$\sigma_X^2 = \epsilon^2 \ln\left(\frac{V1 + E1^2}{E1^2}\right) \tag{3.38}$$

where $\epsilon = 10/ln10$.

Uncorrelated Rayleigh distribution

In this section, we have considered the case of uncorrelated multipath channel with envelope amplitude following a Rayleigh distribution. The distribution function of the expression $u = \sum_{l=1}^{N_T} |\alpha_l|^2$ can be given by [2]:

$$pdf(u) = \sum_{l=1}^{N_T} \frac{(\Omega_l)^{N_T - 2}}{\prod_{r \neq l}^{N_T} (\Omega_l - \Omega_r)} e^{-u/\Omega_l} \tag{3.39}$$

The expression $v = (\sum_{l=1}^{N_T} |\alpha_l|^2) X$ has then the following distribution:

$$pdf(v) = \int_0^{\infty} \frac{\epsilon}{\sqrt{2\pi}\sigma_X \omega} e^{-\frac{(10log\omega - \mu_X)^2}{2\sigma_X^2}} \frac{1}{\omega} \sum_{l=1}^{N_T} \frac{(\Omega_l)^{N_T - 2}}{\prod_{r \neq l}^{N_T} (\Omega_l - \Omega_r)} e^{-v/\omega\Omega_l} d\omega \tag{3.40}$$

Using the following approximation [16]

$$\int_0^\infty \frac{1}{\omega} e^{-v/\omega} \frac{\epsilon}{\sqrt{2\pi}\sigma_X \omega} e^{-\frac{(10log\omega - \mu_X)^2}{2\sigma_X^2}} d\omega \approx \frac{\epsilon}{\sqrt{2\pi}\sigma_f v} e^{-\frac{(10logv - \mu_f)^2}{2\sigma_f^2}} \tag{3.41}$$

the distribution of $v = (\sum_{l=1}^{N_T} |\alpha_l|^2)X$ can then be approximated by:

$$pdf(v) = \sum_{l=1}^{N_T} \frac{(\Omega_l)^{N_T-2}}{\prod_{r\neq l}^{N_T}(\Omega_l - \Omega_r)} \frac{\epsilon}{\sqrt{2\pi}\sigma_f v} e^{-\frac{(10logv - 10log\Omega_l - \mu_f)^2}{2\sigma_f^2}} \tag{3.42}$$

where $\mu_f = -\epsilon C + \mu_X$ and $\sigma_f^2 = \epsilon^2\zeta(2) + \sigma_X^2$. C=0.5772 is the Euler constant and $\zeta(2) = \pi^2/6$ is the Riemann-Zeta function. This approximation can be interpreted by the fact that the product or the sum of a log-normal variable with other variables of sharper frequency distributions (e.g., exponential, etc.) is dominated at the higher order moments by the log-normal distribution with largest logarithm variance [17].

The probability $Prob(SIR \geq \gamma_{mcs})$ is then given by:

$$Prob(SIR \geq \gamma_{mcs}) = \sum_{l=1}^{N_T} \frac{(\Omega_l)^{N_T-2}}{\prod_{r\neq l}^{N_T}(\Omega_l - \Omega_r)} Q\Big[\frac{ln\Big(\frac{\gamma_{mcs}}{A_{mcs} - \gamma_{mcs}B_{mcs}}\Big) - (10log\Omega_l + \mu_f)/\epsilon}{\sigma_f/\epsilon}\Big] \tag{3.43}$$

The probability of use of the modulation and coding scheme mcs is then given by 3.29.

Correlated Rayleigh distribution

In the case of correlated multipath channel with envelope amplitude following a Rayleigh distribution, the distribution function of the expression $u = \sum_{l=1}^{N_T} |\alpha_l|^2$ has been studied widely in the literature. To get the distribution function we proceed as follows:

Let $\rho_{l,l'} = \frac{Cov(\omega_l, \omega_{l'})}{\sqrt{Var(\omega_l)Var(\omega_{l'})}}$ be the correlation parameter between the paths l and l' where $\omega_l = \alpha_l^2$. The Moment Generation Function (MGF) of u ($M_u(s) = E_u[e^{su}]$) can be expressed as:

$$M_u(s) = det(\underline{I} - s\underline{DC})^{-1} = \prod_{l=1}^{N_T}(1 - s\lambda_l)^{-1} \tag{3.44}$$

where λ_l, l = 1,...,N_T are the eigenvalues of the matrix $\underline{DC}$. $\underline{D}$ and $\underline{C}$ are the $N_T \times N_T$ path power and

covariance matrices given by:

$$\underline{D} = \begin{pmatrix} \Omega_1 & 0 & ... & 0 \\ 0 & \Omega_2 & ... & 0 \\ . & . & . & . \\ . & . & . & . \\ 0 & 0 & ... & \Omega_{N_T} \end{pmatrix} \tag{3.45}$$

$$\underline{C} = \begin{pmatrix} 1 & \sqrt{\rho_{12}} & ... & \sqrt{\rho_{1N_T}} \\ \sqrt{\rho_{21}} & 1 & ... & \sqrt{\rho_{2N_T}} \\ . & . & . & . \\ . & . & . & . \\ \sqrt{\rho_{N_T1}} & \sqrt{\rho_{N_T2}} & ... & 1 \end{pmatrix} \tag{3.46}$$

The $M_u(s)$ has a similar form as the MGF of independent gamma variates. Hence, by inverting the MGF $M_u(s)$ (for example using the inversion method described by Moschopoulos in [18]), one can get the distribution function of u:

$$pdf(u) = \frac{1}{\prod_{l=1}^{N_T} \lambda_l} \sum_{l=1}^{N_T} \frac{e^{-u/\lambda_l}}{\prod_{r \neq l}^{N_T} (\frac{1}{\lambda_r} - \frac{1}{\lambda_l})} \tag{3.47}$$

Using the same method as in the uncorrelated Rayleigh multipath, the distribution function of $v = (\sum_{l=1}^{N_T} |\alpha_l|^2)X$ can be expressed as:

$$pdf(v) = \frac{1}{\prod_{l=1}^{N_T} \lambda_l} \sum_{l=1}^{N_T} \frac{1}{\prod_{r \neq l}^{N_T} (\frac{1}{\lambda_r} - \frac{1}{\lambda_l})} \frac{\epsilon}{\sqrt{2\pi}\sigma_f v} e^{-\frac{(10logv - 10log\lambda_l - \mu_f)^2}{2\sigma_f^2}} \tag{3.48}$$

where $\mu_f = -\epsilon C + \mu_X$ and $\sigma_f^2 = \epsilon^2 \zeta(2) + \sigma_X^2$. The probability of use of the modulation and coding scheme mcs is then expressed as in 3.29 where the probability $Prob(SIR \geq \gamma_{mcs})$ is given by:

$$Prob(SIR \geq \gamma_{mcs}) = \frac{1}{\prod_{l=1}^{N_T} \lambda_l} \sum_{l=1}^{N_T} \frac{1}{\prod_{r \neq l}^{N_T} (\frac{1}{\lambda_r} - \frac{1}{\lambda_l})} Q\Big[\frac{ln\Big(\frac{\gamma_{mcs}}{A_{mcs} - \gamma_{mcs} B_{mcs}}\Big) - (10log\lambda_l + \mu_f)/\epsilon}{\sigma_f/\epsilon}\Big] \tag{3.49}$$

Uncorrelated Nakagami distribution

In the case of uncorrelated Nakagami multipath fading channel, the expression $u = \sum_{l=1}^{N_T} |\alpha_l|^2$ has a distribution function determined by the Moschopoulos theorem in [18]:

$$pdf(u) = \prod_{l=1}^{N_T} \left(\frac{\Omega_{min}}{\Omega_l} \right)^m \sum_{k=0}^{\infty} \delta_k \frac{1}{\Omega_{min}^{mN_T+k} \Gamma(mN_T + k)} u^{mN_T+k-1} e^{-u/\Omega_{min}} \tag{3.50}$$

where $\Omega_{min} = min(\Omega_l)$, l = 1,...,N_T and δ_k is a parameter obtained recursively by the following expression:

$$\begin{cases} \delta_0 = 1 \\ \delta_{k+1} = \frac{m}{k+1} \sum_{i=1}^{k+1} \left[\sum_{j=1}^{N} \left(1 - \frac{\Omega_{min}}{\Omega_j} \right)^i \right] \delta_{k+1-i} \end{cases} \tag{3.51}$$

The distribution of $v = (\sum_{l=1}^{N_T} |\alpha_l|^2) X$ is then given by:

$$pdf(v) = \prod_{l=1}^{N_T} \left(\frac{\Omega_{min}}{\Omega_l} \right)^m \sum_{k=0}^{\infty} \delta_k \frac{1}{\Omega_{min}^{mN_T+k} \Gamma(mN_T + k)} \int_0^{\infty} \left(\frac{v}{t} \right)^{mN_T+k-1} e^{-v/(t\Omega_{min})} \frac{1}{t} \frac{\epsilon}{\sqrt{2\pi}\sigma_X t} e^{-\frac{(10logt-\mu_X)^2}{2\sigma_X^2}} dt \tag{3.52}$$

Using the following approximation [16]

$$\int_0^{\infty} \left[\left(\frac{m}{u} \right)^m \frac{(v)^{m-1}}{\Gamma(m)} exp\left(-m\frac{v}{x} \right) \frac{\epsilon}{\sqrt{2\pi}\sigma_X u} e^{\left(-\frac{(10log_{10}(u)-\mu_X)^2}{2\sigma_X^2} \right)} \right] du \simeq \left[\frac{\epsilon}{\sqrt{2\pi}\sigma_f v} e^{\left(-\frac{(10log_{10}(v)-\mu_f)^2}{2\sigma_f^2} \right)} \right] \tag{3.53}$$

the distribution of $v = (\sum_{l=1}^{N_T} |\alpha_l|^2) X$ and the probability $Prob(SIR \geq \gamma_{mcs})$ can be expressed as:

$$pdf(v) = \prod_{l=1}^{N_T} \left(\frac{\Omega_{min}}{\Omega_l} \right)^m \sum_{k=0}^{\infty} \delta_k \frac{1}{\Omega_{min}(mN_T + k)} \frac{\epsilon}{\sqrt{2\pi}\sigma_f v} e^{-\frac{(10logv - 10log((mN_T+k)\Omega_{min}) - \mu_f)^2}{2\sigma_f^2}} \tag{3.54}$$

$$Prob(SIR \geq \gamma_{mcs}) = \prod_{l=1}^{N_T} \left(\frac{\Omega_{min}}{\Omega_l} \right)^m \sum_{k=0}^{\infty} \delta_k \frac{1}{\Omega_{min}(mN_T + k)} \Bigg[Q\left(\frac{ln(\frac{\gamma_{mcs}}{A_{mcs} - \gamma_{mcs} B_{mcs}}) - (10log(\Omega_{min}(mN_T + k)) + \mu_f)/\epsilon}{\sigma_f/\epsilon} \right) \Bigg] \tag{3.55}$$

where $\mu_f = -\epsilon(\Psi(mN_T + k) - ln(mN_T + k)) + \mu_X$ and $\sigma_f^2 = \epsilon^2\zeta(2, mN_T + k) + \sigma_X^2$. The Euler psi function $\Psi(mN_T + k)$ and the Riemann-Zeta function $\zeta(2, mN_T + k)$ are given respectively by:

$$\Psi(mN_T + k) = -C + \sum_{r=1}^{mN_T+k-1} \frac{1}{r} \tag{3.56}$$

$$\zeta(2, mN_T + k) = \sum_{r=0}^{\infty} \frac{1}{(mN_T + k + r)^2} \tag{3.57}$$

Correlated Nakagami distribution

In the case of correlated Nakagami fading channel, the distribution of $u = \sum_{l=1}^{N_T} |\alpha_l|^2$ can be determined by extending the Moschopoulos results [18], obtained for uncorrelated variables, to the case of correlated variables. This extension consists simply of finding equivalent decorrelated variables having the same moment generation function MGF of the correlated Nakagami variables. This type of analysis has been used widely in the literature (e.g., [19, 20]). To get the distribution function we proceed as follows:

Let $\rho_{l,l'} = \frac{Cov(\omega_l,\omega_{l'})}{\sqrt{Var(\omega_l)Var(\omega_{l'})}}$ be the correlation parameter between the paths l and l' where $\omega_l = \alpha_l^2$. The Moment Generation Function (MGF) of u ($M_u(s) = E_u[e^{su}]$) can be expressed as:

$$M_u(s) = det(\underline{I} - s\underline{DC})^{-m} = \prod_{l=1}^{N_T}(1 - s\lambda_l)^{-m} \tag{3.58}$$

where λ_l, l = 1,...,N_T are the eigenvalues of the matrix $\underline{DC}$. $\underline{D}$ and $\underline{C}$ are the $N_T \times N_T$ path power and covariance matrices given by:

$$\underline{D} = \begin{pmatrix} \Omega_1 & 0 & ... & 0 \\ 0 & \Omega_2 & ... & 0 \\ . & . & . & . \\ . & . & . & . \\ 0 & 0 & ... & \Omega_{N_T} \end{pmatrix} \tag{3.59}$$

$$\underline{C} = \begin{pmatrix} 1 & \sqrt{\rho_{12}} & ... & \sqrt{\rho_{1N_T}} \\ \sqrt{\rho_{21}} & 1 & ... & \sqrt{\rho_{2N_T}} \\ . & . & . & . \\ . & . & . & . \\ \sqrt{\rho_{N_T1}} & \sqrt{\rho_{N_T2}} & ... & 1 \end{pmatrix} \tag{3.60}$$

The $M_u(s)$ has a similar form as the MGF of independent gamma variates. Hence, by inverting the

MGF $M_u(s)$ (for example using the inversion method described by Moschopoulos in [18]), one can get the distribution function of u:

$$pdf(u) = \prod_{l=1}^{N_T}\left(\frac{\lambda_{min}}{\lambda_l}\right)^m \sum_{k=0}^{\infty}\delta_k \frac{1}{\lambda_{min}^{mN_T+k}\Gamma(mN_T+k)} u^{mN_T+k-1}e^{-u/\lambda_{min}} \tag{3.61}$$

where $\lambda_{min} = min(\lambda_l)$, l = 1,...,N_T and δ_k is a parameter obtained recursively by the following expression:

$$\begin{cases} \delta_0 = 1 \\ \delta_{k+1} = \frac{m}{k+1}\sum_{i=1}^{k+1}\left[\sum_{j=1}^{N}\left(1-\frac{\lambda_{min}}{\lambda_j}\right)^i\right]\delta_{k+1-i} \end{cases} \tag{3.62}$$

Using the same method as in the uncorrelated Nakagami fading channel, the distribution of $v = (\sum_{l=1}^{N_T}|\alpha_l|^2)X$ and the probability $Prob(SIR \geq \gamma_{mcs})$ can be expressed as:

$$pdf(v) = \prod_{l=1}^{N_T}\left(\frac{\lambda_{min}}{\lambda_l}\right)^m \sum_{k=0}^{\infty}\delta_k \frac{1}{\lambda_{min}(mN_T+k)}\frac{\epsilon}{\sqrt{2\pi}\sigma_f v} e^{-\frac{(10logv-10log((mN_T+k)\lambda_{min})-\mu_f)^2}{2\sigma_f^2}} \tag{3.63}$$

$$Prob(SIR \geq \gamma_{mcs}) = \prod_{l=1}^{N_T}\left(\frac{\lambda_{min}}{\lambda_l}\right)^m \sum_{k=0}^{\infty}\delta_k \frac{1}{\lambda_{min}(mN_T+k)}\Bigg[Q\left(\frac{ln(\frac{\gamma_{mcs}}{A_{mcs}-\gamma_{mcs}B_{mcs}}) - (10log(\lambda_{min}(mN_T+k)) + \mu_f)/\epsilon}{\sigma_f/\epsilon}\right)\Bigg] \tag{3.64}$$

where $\mu_f = -\epsilon(\Psi(mN_T+k) - ln(mN_T+k)) + \mu_X$ and $\sigma_f^2 = \epsilon^2\zeta(2, mN_T+k) + \sigma_X^2$. The probability K_{mcs} of use of each modulation and coding scheme mcs is then given by 3.29.

Dense multipath channel with uncorrelated Rayleigh fading

In this section, we consider the case of composite dense multipath/shadowing channel with Wide-sense Stationary Uncorrelated Scattering (WSSUS), frequency selective fading and constant Power Dispersion Profile (PDP).

If γ_i denotes the instantaneous SNR of the detector output samples (i.e. at the output of the matched

filter and before the combiner), the instantaneous SNR of the Rake receiver [21-23] is:

$$\gamma_{Rake} = \sum_{i=1}^{N_T} \gamma(i) \tag{3.65}$$

where $\gamma(i)$ is the ordered γ_i, i.e., $\gamma(1) > \gamma(2) > ... > \gamma(N_T)$. Since the channel is a Wide-sense Stationary Uncorrelated Scattering (WSSUS) channel with dense multipaths (N_r increases with the spreading bandwidth BW) and constant Power Dispersion Profile (PDP), it was shown in [23], using the theory of "order statistics" [24] and the Virtual Branch technique (linear transform), that the joint probability distribution function $pdf(\gamma(1), \gamma(2), ..., \gamma(N_T))$ can be expressed as:

$$pdf(\gamma(1), \gamma(2), ..., \gamma(N_T)) = \begin{cases} N_T!(\frac{1}{\overline{\gamma}})e^{-\frac{1}{\overline{\gamma}}\Sigma_{i=1}^{N_T}\gamma(i)} & \gamma(1) > \gamma(2) > ... > \gamma(N_T) > 0 \\ 0 & \text{otherwise} \end{cases} \tag{3.66}$$

where $\overline{\gamma}$ is the mean SNR of the matched filter output. In [21], it was shown that $\overline{\gamma}$ is related to the mean SNR of the Rake output (combiner output), Γ_{Rake}, by:

$$\overline{\gamma} = \frac{\Gamma_{Rake}}{L} \tag{3.67}$$

Due to the effect of shadowing (slow variation of the mean signal) and mobile position, Γ_{Rake} is not constant. The expression of Γ_{SRake} can be written as follows:

$$\Gamma_{Rake} = \frac{SF}{log2(M)\tau} \frac{\frac{P_j - NP_{sig} - \xi P_j}{N} d_j^{-\mu} 10^{s_j/10}}{\underbrace{\beta\left(P_j - \frac{P_j - NP_{sig} - \xi P_j}{N}\right) d_j^{-\mu} 10^{s_j/10}}_{I_{intra}} + \underbrace{\sum_{l \neq j}\left(P_l d_l^{-\mu} 10^{s_l/10}\right)}_{I_{inter}} + \eta_0} \tag{3.68}$$

P_j is the transmitted power of cell j, P_{sig} is the power of the associated control channel HS-SCCH per one HS-DSCH channel, ξP_j is the power of the other control channels in the cell (CPICH, FACH, SCH amounting to 20% of P_j). SF is the spreading factor of the downlink channel (SF=16 in HSDPA), M is the modulation order, τ is the coding rate, η_0 is the receiver thermal noise power, d_j is the distance between mobile and node B of cell j. Parameter μ is the path loss slope, s_j corresponds to log-normal shadowing with zero mean and standard deviation σ ($\sigma = 8$ to 12dB) and α is the orthogonality loss factor ($\alpha = 0.4$ in macro cell and 0.06 in micro cell environment [1]).

Proposition1:distributions of SNR Using the distribution function $pdf(\gamma(1), \gamma(2), ..., \gamma(N_T))$, the distribution function (pdf) and the cumulative distribution function (cdf) of γ_{Rake} can be deduced using the virtual branch technique. Each $\gamma(i)$ is transformed into a set of virtual path SNR, called V_n, as follows:

$$\gamma(i) = \sum_{n=i}^{N_T} \frac{\overline{\gamma}}{n} V_n \tag{3.69}$$

The SNR, at the output of the receiver, can be then written using the following equation:

$$\begin{aligned} \gamma_{Rake} &= \sum_{i=1}^{N_T} \sum_{n=i}^{N_T} \frac{\overline{\gamma}}{n} V_n \\ &= \overline{\gamma} \sum_{n=1}^{N_T} V_n \end{aligned} \tag{3.70}$$

In [23], it is shown that $V_n s$ are independent and identically distributed (i.i.d.) normalized exponential random variables. Hence,in the case of selective rake receiver, the pdf of γ_{Rake} (for a given $\overline{\gamma}$) is given by the following expressions where $\Gamma(.)$ is the Gamma function:

$$pdf(\gamma_{Rake}/\overline{\gamma}) = \frac{(\gamma)^{N_T-1}}{\Gamma(N_T)\overline{\gamma}^{N_T-1}} e^{-\gamma/\overline{\gamma}} \tag{3.71}$$

Note that in the case of selective rake receiver with L fingers ($L \leq N_T$) the derivation of the distribution function is much more complicated. In this case, the SNR at the output of the receiver can be expressed as:

$$\begin{aligned} \gamma_{Rake} &= \sum_{i=1}^{L} \sum_{n=i}^{N_T} \frac{\overline{\gamma}}{n} V_n \\ &= \sum_{n=L+1}^{N_T} L\frac{\overline{\gamma}}{n} V_n + \overline{\gamma} \sum_{n=1}^{L} V_n \end{aligned} \tag{3.72}$$

The probability distribution function pdf of γ_{Rake} (for a given $\overline{\gamma}$) is given by the following expression:

$$\begin{aligned} pdf(\gamma_{Rake}/\overline{\gamma}) = \frac{N_T!}{L!(L)^{N_T-L}} e^{-\gamma/\overline{\gamma}} \Bigg[\sum_{i=1}^{L} \frac{\gamma^{i-1}}{\overline{\gamma}^i \Gamma(i)} \Bigg(\sum_{j=1}^{N_T-L} \frac{(-1)^{(L-i+j-1)} L^{(L-i+1)}}{(j-1)!(N_T-L-j)!(j)^{(L-i+1)}} \Bigg) \\ + \sum_{i=1}^{N_T-L} \frac{(-1)^{(L+i-1)} L^L}{(N_T-L-i)!i!i^{(L-1)}(N_T-L)} e^{-\frac{i\gamma}{L\overline{\gamma}}} \Bigg] \end{aligned} \tag{3.73}$$

Proposition2:Distribution of $\overline{\gamma}$ As we said before, the mean signal level is affected by slow variation due to the effect of the shadowing. The SNR at the output of the Rake changes instantaneously according

to the multipath fast fading and its mean value changes slowly according to the shadowing. In this section, the distribution function of the mean SNR $\overline{\gamma}$ is deduced.

$\overline{\gamma}$ for a given mobile position in the cell can be written as follows:

$$\overline{\gamma} = \frac{A}{B+X} \tag{3.74}$$

where

$$A_{mcs} = \frac{SF}{log2(M)\tau}\frac{P_j - NP_{sig} - \xi P_j}{N}\frac{1}{N_T} \tag{3.75}$$

$$B_{mcs} = \beta\left(P_j - \frac{P_j - NP_{sig} - \xi P_j}{N}\right) \tag{3.76}$$

$$X = \frac{1}{10^{bs_{sj}/10}}\sum_{l\neq j}\left(P_l\left(\frac{d_l}{d_j}\right)^{-\mu}10^{bs_{sl}/10}\right) \tag{3.77}$$

The distribution function of X is determined above wherein we have shown that it can be approximated by a log-normal variable. Consequently, A/(B+X) is a log-normal variable.

To evaluate the mean value and the variance of $\overline{\gamma}$, ($\mu_{\overline{\gamma}}$ and $\sigma^2_{\overline{\gamma}}$), we proceed as follows:

Let μ_1 and σ_1 be the parameters of the expression $Y = (B_{mcs} + X)/A_{mcs}$. Since Y is a log-normal variable, μ_1 and σ_1 can be evaluated by the following equations:

$$\mu_1 = \ln\left(\frac{E^2(Y)}{\sqrt{V(Y)+E^2(Y)}}\right) \tag{3.78}$$

$$\sigma_1^2 = \ln\left(\frac{V(Y)+E^2(Y)}{E^2(Y)}\right) \tag{3.79}$$

Note that $E(Y) = (B_{mcs} + E(X))/A_{mcs}$ and $V(Y) = V(X)/A^2_{mcs}$. Since $\overline{\gamma} = 1/Y$ and Y is log-normal, the parameters $\mu_{\overline{\gamma}}$ and $\sigma^2_{\overline{\gamma}}$ are given by:

$$\mu_{\overline{\gamma}} = -\mu_1 = \ln\left(\frac{\sqrt{A^2_{mcs}V(X) + A^2_{mcs}(E(X)+B_{mcs})^2}}{(E(X)+B_{mcs})^2}\right) \tag{3.80}$$

$$\sigma^2_{\overline{\gamma}} = \sigma_1^2 = \ln\left(\frac{V(X)+(E(X)+B_{mcs})^2}{(E(X)+B_{mcs})^2}\right) \tag{3.81}$$

where E(X), and V(X) are given respectively by equations 3.34, 3.35 and 3.36.

Consequently, $\overline{\gamma}$ is a log-normal variable with mean value and variance $\mu_{\overline{\gamma}}$ and $\sigma^2_{\overline{\gamma}}$ given by (3.80) and (3.81).

Consequently, the probability and cumulative distribution functions, pdf and cdf, of γ_{Rake} can be

written as:

$$\begin{aligned} pdf(\gamma) &= \int_{\overline{\gamma}} pdf(\gamma_{Rake}/\overline{\gamma}) pdf(\overline{\gamma}) d(\overline{\gamma}) \\ &= \int_0^{\infty} \frac{(\gamma)^{N_T-1}}{\Gamma(N_T)\overline{\gamma}^{N_T-1}} e^{-\gamma/\overline{\gamma}} \frac{1}{\sqrt{2\pi}\sigma_{\overline{\gamma}}\overline{\gamma}} e^{-\frac{(\ln\overline{\gamma}-\mu_{\overline{\gamma}})^2}{2\sigma_{\overline{\gamma}}^2}} d(\overline{\gamma}) \end{aligned} \tag{3.82}$$

$$cdf(\gamma_{Rake}) = F(\gamma) = \int_0^{\infty} \left(1 - e^{-\gamma/\overline{\gamma}} (\sum_{k=0}^{N_T-1} \frac{\gamma^k}{\overline{\gamma}^k k!})\right) \frac{1}{\sqrt{2\pi}\sigma_{\overline{\gamma}}\overline{\gamma}} e^{-\frac{(\ln\overline{\gamma}-\mu_{\overline{\gamma}})^2}{2\sigma_{\overline{\gamma}}^2}} d(\overline{\gamma}) \tag{3.83}$$

In the case of selective rake receiver with L fingers, the pdf and cdf of γ_{Rake} are obtained by:

$$\begin{aligned} pdf(\gamma) &= \int_{\overline{\gamma}} pdf(\gamma_{Rake}/\overline{\gamma}) pdf(\overline{\gamma}) d(\overline{\gamma}) \\ &= \int_0^{\infty} \Big[\sum_{i=1}^{L} \frac{\gamma^{i-1}}{\overline{\gamma}^i \Gamma(i)} \Big(\sum_{j=1}^{N_T-L} \frac{(-1)^{(L-i+j-1)} L^{(L-i+1)}}{(j-1)!(N_T-L-j)!(j)^{(L-i+1)}} \Big) \\ &+ \sum_{i=1}^{N_T-L} \frac{(-1)^{(L+i-1)} L^L}{(N_T-L-i)!i!i^{(L-1)}(N_T-L)} e^{-\frac{i\gamma}{L\overline{\gamma}}} \Big] \frac{N_T!}{L!(L)^{N_T-L}} e^{-\gamma/\overline{\gamma}} \frac{1}{\sqrt{2\pi}\sigma_{\overline{\gamma}}} e^{-\frac{(\ln\overline{\gamma}-\mu_{\overline{\gamma}})^2}{2\sigma_{\overline{\gamma}}^2}} d(\overline{\gamma}) \end{aligned} \tag{3.84}$$

$$\begin{aligned} cdf(\gamma_{Rake}) = F(\gamma) = \int_0^{\infty} \Big[\sum_{i=1}^{L} \Big(1 - e^{-\gamma/\overline{\gamma}} (\sum_{k=0}^{i-1} \frac{\gamma^k}{\overline{\gamma}^k k!})\Big) \Big(\sum_{j=1}^{N_T-L} \frac{(-1)^{(L-i+j-1)} L^{(L-i+1)}}{(j-1)!(N_T-L-j)!(j)^{(L-i+1)}} \Big) \\ + \sum_{i=1}^{N_T-L} \frac{(-1)^{(L+i-1)} L^{L+1}}{(L+i)(N_T-L-i)!i!i^{(L-1)}(N_T-L)} \Big(1 - e^{-\frac{(i+L)\gamma}{L\overline{\gamma}}}\Big) \Big] \frac{N_T!}{L!(L)^{N_T-L}} \frac{1}{\sqrt{2\pi}\sigma_{\overline{\gamma}}\overline{\gamma}} e^{-\frac{(\ln\overline{\gamma}-\mu_{\overline{\gamma}})^2}{2\sigma_{\overline{\gamma}}^2}} d(\overline{\gamma}) \end{aligned} \tag{3.85}$$

Finally, the probability $P(\gamma_{mcs} \leq SIR < \gamma_{mcs+1})$, k_{mcs}, can be evaluated using the following expression:

$$k_{mcs} = \begin{cases} 1 - F(\gamma_{mcs}) & \text{highest order } (M, \tau, N)_m \\ F(\gamma_{mcs+1}) - F(\gamma_{mcs}) & \text{other } (M, \tau, N)_m \end{cases} \tag{3.86}$$

Dense multipath channel with correlated Rayleigh fading

In general, the outputs of the matched filter $\gamma(i)$ are correlated since the channel paths reaching the receiver are correlated. Based on the approach described herein, we derive in this section a tractable and solvable SIR distribution with the assumption of the presence of full rake receiver and composite

dense correlated multipath/shadowing channel.

Let us start by decorrelating the outputs of the detector using the eigenvalues of the outputs covariance matrix. In fact, each output sample $\gamma(i)$ can be written as follows [21-23]:

$$\gamma(i) = |\alpha|^2 \overline{\frac{Es}{N_0}}_i \tag{3.87}$$

where α is the n-by-1 instantaneous complex channel gain vector and $\overline{\frac{Es}{N_0}}$ is the average signal to noise ration. Like in [21-23], we assume that the instantaneous branch SNR $\gamma(i)$ has the same average $\overline{\gamma_i} = \overline{\gamma}$. For Rayleigh fading, the gain vector α follows the complex Gaussian distribution with zero mean value and covariance matrix R (symbolically it is represented by $\alpha \sim CN(0, R)$).

The SNR at the output of the Rake (after the combiner) can be rewritten as:

$$\gamma_{Rake} = \sum_{i=1}^{N_T} \gamma(i) = \left(\sqrt{\overline{\frac{Es}{N_0}}}.\alpha\right)^H \left(\sqrt{\overline{\frac{Es}{N_0}}}.\alpha\right) \tag{3.88}$$

where the superscript H denotes the Hermitian Transposition. The covariance matrix R can be written as $R = U\Lambda U^H$, where $\Lambda = diag(\lambda_1, ..., \lambda_{N_T})$ is the diagonal matrix of the eigenvalues of R, and the columns of U consist of the corresponding eigenvectors. Since α is composed of correlated complex Gaussian variables, it can be decorrelated by proceeding as follows: Let $e = \Lambda^{-1/2} U^H \alpha$ (i.e. $\alpha = U\Lambda^{1/2} e$). According to [20], e is a vector of independent and identically distributed (iid) complex Gaussian variables ($e(i) \sim CN(0, 1)$). By replacing α by its value in (3.88), the SNR expression can be given by:

$$\gamma_{Rake} = \sum_{i=1}^{N_T} \lambda_i \overline{\frac{Es}{N_0}}_i |e(i)|^2 = \sum_{i=1}^{L} \lambda_i \gamma'_i \tag{3.89}$$

$\gamma'(i)$s are ordered and have the same mean value $\overline{\gamma'}$ [20]. By using the virtual branch technique and the theory of order statistics for $\gamma'(i)$ (exactly the same procedure used in [21-23] and described in the previous section), the joint pdf of $\gamma'(i)$ can be given by:

$$pdf(\gamma'(1), \gamma'(2), ..., \gamma'(N_T)) = \begin{cases} N_T! (\frac{1}{\overline{\gamma'}})^{N_T} e^{-\frac{1}{\overline{\gamma'}} \Sigma_{i=1}^{N_T} \gamma'(i)} & \gamma'(1) > \gamma'(2) > ... > \gamma'(N_T) > 0 \\ 0 & \text{otherwise} \end{cases} \tag{3.90}$$

By using the virtual Branch (VB) technique, each $\gamma'(i)$ is transformed into a set of virtual path SNR,

called V_n, as follows:

$$\gamma'(i) = \sum_{n=i}^{N_T} \frac{\overline{\gamma'}}{n} V_n \tag{3.91}$$

Note that $V_n s$ are independent exponential random variables (see [21-23]). The SNR, at the output of the receiver, can then be written using the following equation:

$$\begin{aligned} \gamma_{Rake} &= \sum_{i=1}^{N_T} \lambda_i \sum_{n=i}^{N_T} \frac{\overline{\gamma'}}{n} V_n \\ &= \sum_{n=1}^{N_T} \Gamma_n V_n \end{aligned} \tag{3.92}$$

where $\Gamma_n = \frac{\overline{\gamma'}}{n} \sum_{m=1}^{n} \lambda_m$. Hence, the Moment Generation Function (MGF) of γ'_{Rake} is given by:

$$M_u(s) = \prod_{l=1}^{N_T} (1 - s\Gamma_l)^{-1} \tag{3.93}$$

Consequently, the pdf of γ_{Rake} (for a given $\overline{\gamma'}$)) can be expressed as:

$$pdf(\gamma_{Rake}/\overline{\gamma'}) = \sum_{l=1}^{N_T} \frac{(\Gamma_l)^{N_T-2}}{\prod_{r\neq l}^{N_T}(\Gamma_l - \Gamma_r)} e^{-\gamma/\Gamma_l} \tag{3.94}$$

Consequently, the pdf and cdf of γ_{Rake} are given by:

$$\begin{aligned} pdf(\gamma) &= \int_{\overline{\gamma'}} pdf(\gamma_{Rake}/\overline{\gamma'}) pdf(\overline{\gamma'}) d(\overline{\gamma'}) \\ &= \int_0^\infty \sum_{l=1}^{N_T} \frac{(\Gamma_l)^{N_T-2}}{\prod_{r\neq l}^{N_T}(\Gamma_l - \Gamma_r)} e^{-\gamma/\Gamma_l} \frac{1}{\sqrt{2\pi}\sigma_{\overline{\gamma'}}\overline{\gamma'}} e^{-\frac{(\ln\overline{\gamma'} - \mu_{\overline{\gamma'}})^2}{2\sigma^2_{\overline{\gamma'}}}} d(\overline{\gamma'}) \end{aligned} \tag{3.95}$$

$$cdf(\gamma_{Rake}) = F(\gamma) = \int_0^\infty \sum_{l=1}^{N_T} \frac{(\Gamma_l)^{N_T-2}}{\prod_{r\neq l}^{N_T}(\Gamma_l - \Gamma_r)} \left(1 - e^{-\gamma/\Gamma_l}\right) \frac{1}{\sqrt{2\pi}\sigma_{\overline{\gamma'}}\overline{\gamma'}} e^{-\frac{(\ln\overline{\gamma'} - \mu_{\overline{\gamma'}})^2}{2\sigma^2_{\overline{\gamma'}}}} d(\overline{\gamma'}) \tag{3.96}$$

where $\mu_{\overline{\gamma'}}$ and $\sigma_{\overline{\gamma'}}$ are given respectively by equations (3.80) and (3.81) as in the case of uncorrelated dense multipath channel with the difference that A_{mcs} in this case is not given by equation (3.75) but the following expression:$A_{mcs} = \frac{SF}{log2(M)\tau} \frac{P_j - NP_{sig} - \xi P_j}{N} \frac{1}{\sum_{i=1}^{N_T} \lambda_i}$.

Finally, the probability $P(\gamma_{mcs} \leq SIR < \gamma_{mcs+1})$, k_{mcs}, can be evaluated using the following

expression:

$$k_{mcs} = \begin{cases} 1 - F(\gamma_{mcs}) & \text{highest order } (M, \tau, N)_m \\ F(\gamma_{mcs+1}) - F(\gamma_{mcs}) & \text{other } (M, \tau, N)_m \end{cases} \tag{3.97}$$

3.3.4 Scheduling

Fast scheduling is one of the HSDPA key techniques that have a direct impact on the user bit rate and the cell capacity. To complete the HSDPA analytical models and get the final expressions of the cell throughput and user bit rate, we have conducted in this chapter a mathematical analysis on the effect of schedulers on the HSDPA performance. Five scheduling algorithms are considered: Round Robin (RR), Fair Throughput (FT), Max C/I, Proportional Fair (PF) and Score Based (SB). The cell capacity and the user bit rate are evaluated in each case.

Round Robin (RR)

In the Round Robin (RR) scheduler, the channel is shared equally between users i.e. the same number of TTIs is allocated to each user. If N_u is the number of users in the cell, then the probability that a TTI is allocate to a given user is $1/N_u$. Hence, the mean bit rate of user i is given by:

$$\begin{aligned} R_i &= \frac{1}{N_u} \sum_{mcs} \frac{R_{mcs} k_{mcs,i}}{N_{s,i}} \\ &= \frac{1}{N_u} \sum_{mcs} k_{mcs} \frac{W}{SF} \frac{(N \log 2(M)\tau)_{mcs,i}}{N_{s,i}} \end{aligned} \tag{3.98}$$

where R_{mcs} is the bit rate of transmission scheme mcs during a TTI, $N_{s,i}$ is the number of transmissions of user i due to HARQ, W is the chip rate and SF is the spreading factor. Note that $k_{mcs,i}$ varies with the mobile position. The cell throughput in this case is given by:

$$th = E\Big(\sum_{i=1}^{N_u} R_i\Big) \tag{3.99}$$

Fair Throughput (FT)

The Fair Throughput (FT) scheduler allocates a fixed bit rate to users independently of channel condition and mobile position.

Proposition The cell throughput of HSDPA can be evaluated using the following equation:

$$Th = \frac{1}{T} E(N_u) \sum_{j=1}^{J} perc_j E(S_j) \tag{3.100}$$

where T is a given observation time (observation time of the HS-DSCH channel), J is the number of various services, $perc_j$ is the percentage, in average, of a given service in the cell, S_j is the size of the user j data conveyed on the HS-DSCH channel and N_u is the number of users. N_u is a function of the service type (bit rate, size of the packets) and of the modulation and coding schemes selected for each user data. The probability that N_u is equal to a given number n is given by:

$$P(N_u = n) = \left(Q(-\frac{E}{\sigma}) - Q\left(\frac{\frac{WT}{SF} - (n-1)E}{(n-1)\sigma} \right) \right) \times Q\left(\frac{\frac{WT}{SF} - nE}{n\sigma} \right) \tag{3.101}$$

where E and σ given, by (3.102) and (3.103), are respectively the mean value and the standard deviation of a variable that represents the packet size, the modulation and coding scheme, and the HARQ. Note that N_M is the maximum number of Transmission schemes (30 schemes [25]) and μ_{S_j} is the mean value of the user data size.

$$E = N_s \sum_{j=1}^{J} perc_j \mu_{S_j} \sum_{mcs=1}^{N_M} \left(\frac{1}{(Nlog_2(M)\tau)_{mcs}} \underbrace{\int\int}_{A} k_{mcs} \rho dA \right) \tag{3.102}$$

$$\sigma^2 = N_s^2 \sum_{j=1}^{J} perc_j \int Pdf(S_j) S_j^2 d(S_j) \sum_{mcs=1}^{N_M} \left(\frac{1}{(Nlog_2(M)\tau)_{mcs}} \underbrace{\int\int}_{A} k_{mcs} \rho dA \right)^2 - E^2 \tag{3.103}$$

Proofs

Proof of (3.101) The flow of the channel in symbols/sec is given by $R = \frac{W}{SF}$. Since the HS-DSCH channel is shared by users, in a given time interval T we have:

$$\frac{\sum_{i=1}^{N_u} Rs_i T_i}{T} = \frac{W}{SF} \tag{3.104}$$

where Rs_i is the throughput of each user in symbols/sec and T_i is the connection duration. The modulation and coding scheme change during the transfer of the packet calls. Hence, equation (3.104)

is written as :

$$\frac{\sum_{i=1}^{N_u} R_i T_i \sum_{mcs} \frac{k_{mcs}}{(Nlog2(M)\tau)_{i,mcs}}}{T} = \frac{W}{SF} \tag{3.105}$$

where R_i is the service bit rate. Due to the effect of HARQ, N_s packets are transmitted instead of one packet, having all the same modulation and coding scheme. Hence, the following equation is obtained after introducing the mean number of transmissions N_s and the transmission scheme.

$$\sum_{i=1}^{N_u} R_i N_s T_i \Big(\sum_{mcs=1}^{N_M} \frac{k_{mcs}}{(Nlog_2(M)\tau)_{mcs}} \Big)_i = \frac{W}{SF} T \tag{3.106}$$

Let $S_i = R_i T_i$ be the data packets size of a given service modeled as a Pareto distribution. If we suppose that the packets size of a given user 1 is known, say S_1, equation (3.106) can be rewritten as follows:

$$\sum_{i=2}^{N_u} \underbrace{R_i N_s T_i \Big(\sum_{mcs=1}^{N_M} \frac{k_{mcs}}{(Nlog_2(M)\tau)_{mcs}} \Big)_i}_{x_i} = \frac{W}{SF} T - S_1 N_s \Big(\sum_{mcs=1}^{N_M} \frac{k_{mcs}}{(Nlog_2(M)\tau)_{mcs}} \Big)_1 \tag{3.107}$$

Using (3.107), the conditional probability that $N_u = n$ given S_1 can be evaluated using (3.108) (the reason for introducing a specific user S_1 is explained later in this section).

$$\begin{aligned} P(N_u = n/S_1) = \; & E\Big[Prob\Big(0 < \textstyle\sum_{i=2}^{n} x_i \le \frac{W}{SF} T - S_1 N_s \Big(\sum_{mcs=1}^{N_M} \frac{k_{mcs}}{(Nlog_2(M)\tau)_{mcs}} \Big)_1 ; \\ & \textstyle\sum_{i=2}^{n+1} x_i > \frac{W}{SF} T - S_1 N_s \Big(\sum_{mcs=1}^{N_M} \frac{k_{mcs}}{(Nlog_2(M)\tau)_{mcs}} \Big)_1 \Big) \Big] \end{aligned} \tag{3.108}$$

The transmission scheme is a random variable depending on location, target SIR of each modulation and coding scheme and radio channel conditions (fast fading, shadowing). Hence, x_i are independent variables. For large T, N_u is large and the sum of the N_u independent variables, using the central limit theorem, tends to a gaussian. Hence, $P(N_u = n/S_1)$ can be evaluated using equation (3.109).

$$\begin{aligned} P(N_u = n/S_1) = \; & E\Big[\Big(Q(-\tfrac{E}{\sigma}) - Q\Big(\frac{\frac{WT}{SF} - S_1 N_s (\sum_{mcs=1}^{N_M} \frac{k_{mcs}}{(Nlog_2(M)\tau)_{mcs}})_1 - (n-1)E}{(n-1)\sigma} \Big) \Big) \times \\ & Q\Big(\frac{\frac{WT}{SF} - S_1 N_s (\sum_{mcs=1}^{N_M} \frac{k_{mcs}}{(Nlog_2(M)\tau)_{mcs}})_1 - nE}{n\sigma} \Big) \Big] \end{aligned} \tag{3.109}$$

where E and σ are the mean value and the standard deviation of x_i. Moreover, for large T, $S_1 N_s \Big(\sum_{mcs=1}^{N_M} \frac{k_{mcs}}{(Nlog_2(M)\tau)_{mcs}} \Big)_1 \ll \frac{W}{SF} T$ and in (3.109) the term $S_1 N_s \Big(\sum_{mcs=1}^{N_M} \frac{k_{mcs}}{(Nlog_2(M)\tau)_{mcs}} \Big)_1$ can be neglected. Hence, the probability $P(N_u = n/S_1)$ is independent of S_1 and (3.109) reduces to equation (3.101).

Note that the mean value and the variance of x_i can be simply evaluated as in (3.102) and (3.103).

Proof of (3.100) Since N_u is the number of users on the HS-DSCH channels, the mean value of the HSDPA throughput can be simply computed by $Th = E(\frac{\sum_{i=1}^{N_u} R_i T_i}{T})$. The mean value is according to the data packets size (bit rate and connection time) and N_u. Let us suppose that J various services are active on the HS-DSCH channel. Each service is modeled by a Pareto distribution with specific parameters. Letting n_j represent the number of users of each service transmitted on the HS-DSCH channel, yields the HSDPA throughput expression given in (3.110) and (3.111).

$$Th = \sum_{n=1}^{\infty} P(N_u = n) Th_n \tag{3.110}$$

where Th_n is the possible throughput when the number of packet calls per channel is n.

$$Th_n = \frac{1}{T} \int_{S_{1,1}} .. \int_{S_{n_J,J}} pdf((S_{1,1}..S_{n_1,1}..S_{1,J}..S_{n_J,J})/N_u = n) \Big(\sum_{j=1}^{J} \sum_{i=1}^{n_j} S_{i,j} \Big) d(S_{1,1}..S_{n_1,1}..S_{1,J}..S_{n_J,J}) \tag{3.111}$$

Since the packets sizes of the users are independent, the throughput can be written after several manipulations as:

$$Th = \frac{1}{T} \sum_{n=1}^{\infty} P(N_u = n) \Big(\sum_{j=1}^{J} \sum_{i=1}^{n_j} \int_{S_{i,j}} P(S_{i,j}/N_u = n) S_{i,j} d(S_{i,j}) \Big) \tag{3.112}$$

Using the extension of Bayes law to arbitrary random variables, gives :

$$pdf(S) P(N_u = n/S) = pdf(S/N_u = n) P(N_u = n) \tag{3.113}$$

For large T, the probability $P(N_u = n/S_{i,j})$, evaluated using (3.101), is independent of $S_{i,j}$. The packet size probability distribution is identical for all the users in each service. This yields, after several manipulation, the following throughput equation:

$$Th = \frac{1}{T} \sum_{n=1}^{\infty} \sum_{j=1}^{J} n_j \int_{S_j} P(N_u = n) pdf(S_j) S_j d(S_j) \tag{3.114}$$

$pdf(S_j)$ is the Pareto distribution function of service j. The number of users for a given service is expressed by $n_j \simeq perc_j N_u$. The approximation can be explained by the fact that n_j must be an integer and $perc_j$ is the percentage in average of a given service. For large T, N_j and N_u are large and the approximation is closer to equality ($\simeq$ is replaced by $=$). Substituting the expression of n_j by $perc_j N_u$

leads to the throughput given in (3.100).

Max C/I

In Max C/I scheduling, the channel is allocated in each TTI to the user having the best SIR, in other words the best channel quality. This scheduler maximizes the cell capacity but does not guarantee any QoS to the user. Users at the border of the cell have always poor channel conditions (due to attenuation, interference, and absence of fast power control) and experience low bit rate.

The cell throughput and user bit rate achieved by this scheduler depends upon the wireless channel model. In this section, we estimate the cell throughput and user bit rate in the case of Rayleigh, Nakagami, or dense Rayleigh multipath channels.

Uncorrelated Rayleigh fading In order to estimate the cell capacity and user bit rate, the probability that the HS-DSCH channel is allocated to a given user (e.g., user i), denoted by pr(i), should be evaluated. pr(i) can be written as:

$$pr(i) = Prob\Big(SIR_i > SIR_j \text{ for j=1..}N_u \text{ and } j \neq i\Big) = \prod_{j \neq i}^{N_u} Prob(SIR_i > SIR_j) \tag{3.115}$$

The expression $SIR_i > SIR_j$ can be expressed as:

$$\Big(\sum_{l_i=1}^{N_T} |\alpha_{l_i,i}|^2\Big) X_i > \Big(\sum_{l_j=1}^{N_T} |\alpha_{l_j,j}|^2\Big) X_j \tag{3.116}$$

where X_i is given by equation 3.30 for user i. The distribution function of the expression $\Big(\sum_{l=1}^{N_T} |\alpha_l|^2\Big) X_i$ is determined by 3.42.

The probability $Prob(SIR_i > SIR_j)$ is then given by:

$$Prob(SIR_i > SIR_j) = \sum_{l_i=1}^{N_T} \sum_{l_j=1}^{N_T} \frac{(\Omega_{l_i,i})^{N_T-2}}{\prod_{r_i \neq l_i}^{N_T} (\Omega_{l_i,i} - \Omega_{r_i,i})} \frac{(\Omega_{l_j,j})^{N_T-2}}{\prod_{r_j \neq l_j}^{N_T} (\Omega_{l_j,j} - \Omega_{r_j,j})} \times \Bigg[Q\Big(-\frac{(10log\Omega_{l_i,i} + \mu_{f,i} - 10log\Omega_{l_j,j} - \mu_{f,j})}{\sqrt{\sigma_{f,i}^2 + \sigma_{f,j}^2}}\Big)\Bigg] \tag{3.117}$$

Consequently, the bit rate of user i is given by:

$$R_i \quad = \quad pr(i) \sum_{mcs} \frac{R_{mcs} k_{mcs,i}}{N_s}$$

$$= pr(i)\sum_{mcs} k_{mcs}\frac{W}{SF}\frac{(N\log 2(M)\tau)_{mcs,i}}{N_s} \quad (3.118)$$

The cell throughput in this case is:

$$th = E\Big(\sum_{i=1}^{N_u} R_i\Big) \quad (3.119)$$

Correlated Rayleigh fading In the case of correlated Rayleigh fading, the user bit rate and cell throughput can be estimated using the same method described above (i.e. in the case of uncorrelated Rayleigh fading). Consequently, the probability that the channel is allocated to user i is given by:

$$\begin{aligned} pr(i) &= Prob\Big(SIR_i > SIR_j \text{ for j=1..}N_u \text{ and } j \neq i\Big) = \prod_{j\neq i}^{N_u} Prob(SIR_i > SIR_j) \\ &= \prod_{j\neq i}^{N_u} \frac{1}{\prod_{l_i=1}^{N_T}\lambda_{l_i,i}}\frac{1}{\prod_{l_j=1}^{N_T}\lambda_{l_j,j}}\sum_{l_i=1}^{N_T}\sum_{l_j=1}^{N_T}\frac{1}{\prod_{r_i\neq l_i}^{N_T}(\frac{1}{\lambda_{r_i,i}}-\frac{1}{\lambda_{l_i,i}})}\frac{1}{\prod_{r_j\neq l_j}^{N_T}(\frac{1}{\lambda_{r_j,j}}-\frac{1}{\lambda_{l_j,j}})}\times\Bigg[\\ &\quad Q\Big(-\frac{(10log\lambda_{l_i,i}+\mu_{f,i}-10log\lambda_{l_j,j}-\mu_{f,j})}{\sqrt{\sigma_{f,i}^2+\sigma_{f,j}^2}}\Big)\Bigg] \end{aligned} \quad (3.120)$$

Consequently, the bit rate of user i is given by:

$$\begin{aligned} R_i &= pr(i)\sum_{mcs}\frac{R_{mcs}k_{mcs,i}}{N_s} \\ &= pr(i)\sum_{mcs} k_{mcs}\frac{W}{SF}\frac{(N\log 2(M)\tau)_{mcs,i}}{N_s} \end{aligned} \quad (3.121)$$

The cell throughput in this case is:

$$th = E\Big(\sum_{i=1}^{N_u} R_i\Big) \quad (3.122)$$

Uncorrelated Nakagami fading In this case, the probability pr(i) is given by:

$$pr(i) = \prod_{j\neq i}^{N_u}\prod_{l_i=1}^{N_T}\Big(\frac{\Omega_{min}}{\Omega_{l_i,i}}\Big)^m \prod_{l_j=1}^{N_T}\Big(\frac{\Omega_{min}}{\Omega_{l_j,j}}\Big)^m \sum_{k_i=0}^{\infty}\sum_{k_j=0}^{\infty}\Bigg[\delta_{k_i}\frac{1}{\Omega_{min}(mN_T+k_i)\Gamma(mN_T+k_i)}\times$$
$$\frac{1}{\Omega_{min}(mN_T+k_j)\Gamma(mN_T+k_j)}Q\Big(-\frac{(10log(\Omega_{min,i}(mN_T+k_i))+\mu_{f,i}-10log(\Omega_{min,j}(mN_T+k_j))-\mu_{f,j})}{\sqrt{\sigma_{f,i}^2+\sigma_{f,j}^2}}\Big)\Bigg] \quad (3.1$$

The bit rate of user i is given by:

$$R_i = pr(i)\sum_{mcs}\frac{R_{mcs}k_{mcs,i}}{N_s}$$

$$= \quad pr(i) \sum_{mcs} k_{mcs} \frac{W}{SF} \frac{(N \log 2(M)\tau)_{mcs,i}}{N_s} \tag{3.124}$$

The cell throughput in this case is:

$$th = E\Big(\sum_{i=1}^{N_u} R_i\Big) \tag{3.125}$$

Correlated Nakagami fading In this case, the probability pr(i) is given by:

$$pr(i) = \prod_{j \neq i}^{N_u} \prod_{l_i=1}^{N_T} \Big(\frac{\lambda_{min}}{\lambda_{l_i,i}}\Big)^m \prod_{l_j=1}^{N_T} \Big(\frac{\lambda_{min}}{\lambda_{l_j,j}}\Big)^m \sum_{k_i=0}^{\infty} \sum_{k_j=0}^{\infty} \Big[\delta_{k_i} \frac{1}{\lambda_{min}(mN_T + k_i)\Gamma(mN_T + k_i)} \times$$
$$\frac{1}{\lambda_{min}(mN_T + k_j)\Gamma(mN_T + k_j)} Q\Big(-\frac{(10log(\lambda_{min,i}(mN_T + k_i)) + \mu_{f,i} - 10log(\lambda_{min,j}(mN_T + k_j)) - \mu_{f,j})}{\sqrt{\sigma_{f,i}^2 + \sigma_{f,j}^2}}\Big)\Big] \tag{3.1}$$

The bit rate of user i is given by:

$$\begin{aligned} R_i &= pr(i) \sum_{mcs} \frac{R_{mcs} k_{mcs,i}}{N_s} \\ &= pr(i) \sum_{mcs} k_{mcs} \frac{W}{SF} \frac{(N \log 2(M)\tau)_{mcs,i}}{N_s} \end{aligned} \tag{3.127}$$

The cell throughput in this case is:

$$th = E\Big(\sum_{i=1}^{N_u} R_i\Big) \tag{3.128}$$

Uncorrelated and correlated dense multipath channel The probability that a TTI is allocated to user i can be written as follows:

$$\begin{aligned} pr(i) &= Prob\Big(SIR_i > SIR_j \text{ for j=1..}N_u \text{ and } j \neq i\Big) = \prod_{j \neq i}^{N_u} Prob(SIR_i > SIR_j) \\ &= \prod_{j \neq i}^{N_u} \Big(1 - \int_0^{+\infty} F_i(SIR_j) pdf(SIR_j) d(SIR_j)\Big) \end{aligned} \tag{3.129}$$

where F_i is the cdf of SIR_i evaluated at SIR_j. F_i is given by (3.83) for uncorrelated Rayleigh and by (3.96) for correlated Rayleigh. pdf(SIR_j) is the pdf of SIR_j given by (3.95) for uncorrelated Rayleigh and by (3.82) for correlated Rayleigh. Hence, the bit rate of user i is given by:

$$R_i \quad = \quad pr(i) \sum_{m} \frac{R_m k_{m,i}}{N_{s,i}}$$

$$= \quad pr(i) \sum_m k_m \frac{W}{SF} \frac{(N \log 2(M)\tau)_{m,i}}{N_{s,i}} \tag{3.130}$$

The cell throughput in this case is:

$$th = E\Big(\sum_{i=1}^{N_u} R_i\Big) \tag{3.131}$$

Proportional Fair (PF)

The Proportional Fair (PF) scheduler is a compromise between Max C/I and Fair Throughput schedulers [26]. In each TTI, the channel is allocated to the user having max(r/S) where r is the transmission rate in this TTI (according to the transmission scheme selected) and S is the mean bit rate transmitted in previous TTIs.

In the literature, there are several versions of Proportional fair [26-29]. Some versions propose to evaluate the mean bit rate R through an exponentially smoothed average when others increase the influence of the instantaneously transmission rate by using the user selection condition : max(r^c/S) where c is a parameter depending on channel conditions.

This section provides an analytical study of the basic Proportional Fair scheduler. It was shown in [30] that the performance in this case can be considered as the asymptotic performance of the other PF schedulers. The mean bit rate S in the basic PF is a linear function of the mean bit rate when S is evaluated through an exponentially smoothed average (for details see [30]).

The mean bit rate S_i achieved by user i, when the TTIs are allocated to this user, is:

$$S_i = \sum_{mcs} k_{mcs} \frac{W}{SF} \frac{(N \log 2(M)\tau)_{mcs,i}}{N_s} \tag{3.132}$$

Note that the condition max(r/S) is equivalent to max(SIR/S) due to the fact that according to each SIR value, there is a given possible transmission rate r in a given TTI (in fact, r values correspond to a range of SIRs. Since the number of transmission schemes is high, approximately 30 [25], this hypothesis is still a good approximation and it can be seen as an asymptotic study of the PF scheduler). Hence, if N_u is the number of users in the cell, the probability that a TTI is allocated to a given user i can be evaluated using the following equation:

$$pr(i) \quad = \quad Prob\Big(\frac{SIR_i}{S_i} > \frac{SIR_j}{S_j} \text{ for j=1..}N_u \text{ and } j \neq i\Big) = \prod_{j \neq i}^{N_u} Prob\Big(SIR_i > \frac{S_i}{S_j} SIR_j\Big)$$

$$= \prod_{j\neq i}^{N_u} Prob\Big[\frac{1}{\Big(\sum_{l_i=1}^{N_T}|\alpha_{l_i,i}|^2\Big)X_i} < \frac{S_j}{S_i}\frac{1}{\Big(\sum_{l_j=1}^{N_T}|\alpha_{l_j,j}|^2\Big)X_j} + (\frac{S_j}{S_i}-1)B_{mcs}\Big] \tag{3.133}$$

where X_i is given by equation (3.30) for user i. The distribution function of the expression $\Big(\sum_{l=1}^{N_T}|\alpha_l|^2\Big)X_i$ is determined by 3.42.

Consequently, the bit rate achieved by user i is:

$$R_i = pr(i)\sum_{mcs} k_{mcs}\frac{W}{SF}\frac{(N\log 2(M)\tau)_{mcs,i}}{N_s} \tag{3.134}$$

The cell throughput in this case is given by:

$$th = E\Big(\sum_{i=1}^{N_u} R_i\Big) \tag{3.135}$$

In the rest of this section, we evaluate the probability pr(i) in the case of Rayleigh, Nakagami, and dense uncorrelated and correlated multipath channels.

Uncorrelated Rayleigh fading In this case, the probability pr(i) is given by:

$$pr(i) = \prod_{j\neq i}^{N_u}\sum_{l_i=1}^{N_T}\sum_{l_j=1}^{N_T}\frac{(\Omega_{l_i,i})^{N_T-2}}{\prod_{r_i\neq l_i}^{N_T}(\Omega_{l_i,i}-\Omega_{r_i,i})}\frac{(\Omega_{l_j,j})^{N_T-2}}{\prod_{r_j\neq l_j}^{N_T}(\Omega_{l_j,j}-\Omega_{r_j,j})}\times\Big[Q\Big(-\frac{(10log\Omega_{l_i,i}+\mu_{f,i}-m_{f,j})}{\sqrt{\sigma_{f,i}^2+\sigma_{f,j}^2}}\Big)\Big] \tag{3.136}$$

where

$$m_{f,j} = -\epsilon ln\Big(\frac{\sqrt{e^{2(-10log(\frac{S_j}{S_i})-10log\Omega_{l_j,j}-\mu_{f,j})+\sigma_{f,j}^2}(e^{\sigma^2}-1)+(E)^2}}{(E)^2}\Big) \tag{3.137}$$

$$E = e^{2(-10log(\frac{S_j}{S_i})-10log\Omega_{l_j,j}-\mu_{f,j})+\sigma_{f,j}^2} + (\frac{S_j}{S_i}-1)B_{mcs}\frac{\prod_{r_j\neq l_j}^{N_T}(\Omega_{l_j,j}-\Omega_{r_j,j})}{N_T(\Omega_{l_j,j})^{N_T-2}} \tag{3.138}$$

Consequently, the user bit rate and the cell throughput are determined by (3.134) and (3.135).

Correlated Rayleigh fading In the case of correlated Rayleigh fading, the probability that the channel is allocated to user i is given by:

$$pr(i) = \prod_{j\neq i}^{N_u}\frac{1}{\prod_{l_i=1}^{N_T}\lambda_{l_i,i}}\frac{1}{\prod_{l_j=1}^{N_T}\lambda_{l_j,j}}\sum_{l_i=1}^{N_T}\sum_{l_j=1}^{N_T}\frac{1}{\prod_{r_i\neq l_i}^{N_T}(\frac{1}{\lambda_{r_i,i}}-\frac{1}{\lambda_{l_i,i}})}\frac{1}{\prod_{r_j\neq l_j}^{N_T}(\frac{1}{\lambda_{r_j,j}}-\frac{1}{\lambda_{l_j,j}})}\Big[$$

$$Q\Big(-\frac{(10log\lambda_{l_i,i}+\mu_{f,i}-m_{f,j})}{\sqrt{\sigma_{f,i}^2+\sigma_{f,j}^2}}\Big)\Big] \tag{3.139}$$

where

$$m_{f,j}=-\epsilon ln\Big(\frac{\sqrt{e^{2(-10log(\frac{S_j}{S_i})-10log\lambda_{l_j,j}-\mu_{f,j})+\sigma_{f,j}^2}(e^{\sigma^2}-1)+(E)^2}}{(E)^2}\Big) \tag{3.140}$$

$$E=e^{2(-10log(\frac{S_j}{S_i})-10log\lambda_{l_j,j}-\mu_{f,j})+\sigma_{f,j}^2}+(\frac{S_j}{S_i}-1)B_{mcs}\frac{\prod_{r_j\neq l_j}^{N_T}(\lambda_{l_j,j}-\lambda_{r_j,j})}{N_T(\lambda_{l_j,j})^{N_T-2}}\prod_{l_j=1}^{N_T}\lambda_{l_j,j} \tag{3.141}$$

Consequently, the user bit rate and the cell throughput are determined by (3.134) and (3.135).

Uncorrelated Nakagami fading In this case, the probability pr(i) is given by:

$$\begin{aligned} pr(i) &= \prod_{j\neq i}^{N_u}\prod_{l_i=1}^{N_T}\Big(\frac{\Omega_{min}}{\Omega_{l_i,i}}\Big)^m\prod_{l_j=1}^{N_T}\Big(\frac{\Omega_{min}}{\Omega_{l_j,j}}\Big)^m\sum_{k_i=0}^{\infty}\sum_{k_j=0}^{\infty}\Big[\delta_{k_i}\frac{1}{\Omega_{min}(mN_T+k_i)\Gamma(mN_T+k_i)}\times \\ &\delta_{k_j}\frac{1}{\Omega_{min}(mN_T+k_j)\Gamma(mN_T+k_j)}\times \\ &Q\Big(-\frac{(10log(\Omega_{min,i}(mN_T+k_i))+\mu_{f,i}-m_{f,j})}{\sqrt{\sigma_{f,i}^2+\sigma_{f,j}^2}}\Big)\Big] \end{aligned} \tag{3.142}$$

where

$$m_{f,j}=-\epsilon ln\Big(\frac{\sqrt{e^{2(-10log(\frac{S_j}{S_i})-10log(\Omega_{min,j}(mN_T+k_j))-\mu_{f,j})+\sigma_{f,j}^2}(e^{\sigma^2}-1)+(E)^2}}{(E)^2}\Big) \tag{3.143}$$

$$E=\begin{cases} e^{2(-10log(\frac{S_j}{S_i})-10log(\Omega_{min,j}(mN_T+k_j))-\mu_{f,j})+\sigma_{f,j}^2}+(\frac{S_j}{S_i}-1)B_{mcs}(mN_T!)\prod_{l_j=1}^{N_T}\Big(\frac{\Omega_{l_j,j}}{\Omega_{min}}\Big)^m & k_j=0 \\ e^{2(-10log(\frac{S_j}{S_i})-10log(\Omega_{min,j}(mN_T+k_j))-\mu_{f,j})+\sigma_{f,j}^2} & \text{Elsewhere} \end{cases} \tag{3.144}$$

Consequently, the user bit rate and the cell throughput are determined by (3.134) and (3.135).

Correlated Nakagami fading In this case, the probability pr(i) is given by:

$$\begin{aligned} pr(i) &= \prod_{j\neq i}^{N_u}\prod_{l_i=1}^{N_T}\Big(\frac{\lambda_{min}}{\lambda_{l_i,i}}\Big)^m\prod_{l_j=1}^{N_T}\Big(\frac{\lambda_{min}}{\lambda_{l_j,j}}\Big)^m\sum_{k_i=0}^{\infty}\sum_{k_j=0}^{\infty}\Big[\delta_{k_i}\frac{1}{\lambda_{min}(mN_T+k_i)\Gamma(mN_T+k_i)}\times \\ &\delta_{k_j}\frac{1}{\lambda_{min}(mN_T+k_j)\Gamma(mN_T+k_j)}\times \end{aligned}$$

$$Q\Big(-\frac{(10log(\lambda_{min,i}(mN_T+k_i))+\mu_{f,i}-m_{f,j})}{\sqrt{\sigma_{f,i}^2+\sigma_{f,j}^2}}\Big)\Big] \tag{3.145}$$

where

$$m_{f,j}=-\epsilon ln\Big(\frac{\sqrt{e^{2(-10log(\frac{S_j}{S_i})-10log(\lambda_{min,j}(mN_T+k_j))-\mu_{f,j})+\sigma_{f,j}^2}(e^{\sigma^2}-1)+(E)^2}}{(E)^2}\Big) \tag{3.146}$$

$$E=\begin{cases} e^{2(-10log(\frac{S_j}{S_i})-10log(\lambda_{min,j}(mN_T+k_j))-\mu_{f,j})+\sigma_{f,j}^2}+(\frac{S_j}{S_i}-1)B_{mcs}(mN_T!)\prod_{l_j=1}^{N_T}\Big(\frac{\lambda_{l_j,j}}{\lambda_{min}}\Big)^m & k_j=0 \\ e^{2(-10log(\frac{S_j}{S_i})-10log(\lambda_{min,j}(mN_T+k_j))-\mu_{f,j})+\sigma_{f,j}^2} & \text{Elsewhere} \end{cases} \tag{3.147}$$

Consequently, the user bit rate and the cell throughput are determined by (3.134) and (3.135).

Uncorrelated and correlated dense multipath channel The probability that a TTI is allocated to user i can be written as follows:

$$\begin{aligned} pr(i) &= Prob\Big(\frac{SIR_i}{S_i}>\frac{SIR_j}{S_j} \text{ for j=1..}N_u \text{ and } j\neq i\Big)=\prod_{j\neq i}^{N_u}Prob\Big(SIR_i>\frac{S_i}{S_j}SIR_j\Big) \\ &= \prod_{j\neq i}^{N_u}\Big(1-\int_0^{+\infty}F_i(\frac{S_i}{S_j}SIR_j)pdf(SIR_j)d(SIR_j)\Big) \end{aligned} \tag{3.148}$$

where F_i is the cdf of SIR_i evaluated at SIR_j. F_i is given by (3.83) for uncorrelated Rayleigh and by (3.96) for correlated Rayleigh. pdf(SIR_j) is the pdf of SIR_j given by (3.82) for uncorrelated Rayleigh and by (3.95) for correlated Rayleigh. The user bit rate and the cell throughput are determined by (3.134) and (3.135).

Score Based(SB)

In this section, we evaluate the cell capacity and the user bit rate when SB is used. For that, we proceed as follows:

Let $p_{mcs,i}$, mcs=1..M, the probability that a transmission scheme mcs is selected and that the channel is attributed to the user "i" where M is the total number of transmission schemes (30 in HSDPA). Note that the transmission schemes are classified by decreased order. When SB is used, an mcs is selected for user i when it is high relative to its own statistics. For example, the second mcs is selected for user

i if the first mcs does not occur for all other users. Hence, $p_{mcs,i}$ can be expressed by the following equation:

$$p_{mcs,i} = k_{mcs,i} \prod_{j \neq i}^{N_u} \Big(1 - \sum_{t=1}^{mcs} k_{t,j}\Big) + k_{mcs,i} \sum_{n=2}^{N_u} \frac{1}{n} \Big[\sum_{j_1 \neq i}^{N_u} \ldots \sum_{j_n \neq i, j_1, \ldots, j_{n-1}}^{N_u} k_{mcs,j_1} \ldots k_{mcs,j_n} \prod_{h \neq i, j_1, \ldots, j_n}^{N_u} \Big(1 - \sum_{t=1}^{mcs} k_{t,h}\Big) \Big] \tag{3.149}$$

Consequently, the bit rate achieved by user i is:

$$\begin{aligned} R_i &= \sum_{mcs}^{M} \frac{R_m p_{mcs,i}}{N_{s,i}} \\ &= \sum_{mcs}^{M} p_{mcs,i} \frac{W}{SF} \frac{(N \log 2(M)\tau)_{m,i}}{N_{s,i}} \end{aligned} \tag{3.150}$$

The cell throughput in this case is given by:

$$th = E\Big(\sum_{i=1}^{N_u} R_i\Big) \tag{3.151}$$

3.4 Network Simulation

In this section, we describe the simulation model adopted in our simulations to evaluate the HSDPA performance and to assess the accuracy of the analytical models proposed in this chapter. The simulation is conducted for the scheduling algorithms described above and for various uncorrelated and correlated fading channels (Rayleigh, Nakagami and dense multipath).

The topology used in our simulation consists of both link level and network level simulation. The link-level simulator implements all physical layer aspects of HSDPA as specified by 3GPP (release 5). The network level simulator implements end to end sessions between applications on UE and the core network side. The simulator focuses on MAC (Medium Access Control) and RLC (Radio Link Control), where high-speed versions of these protocols are implemented for HSDPA according to the 3GPP W-CDMA standard, release 5.

The users are supposed to be uniformly distributed in the cell. Since the network simulator is static, several scenarios are simulated to cover all the possible cases or scenarios (10000 scenarios simulated). Each simulation was run for 500 s giving us 500 s long traces.

Note that the correlation distance of the shadowing is set to 40m and that the users are assumed to move around their geographical position within a short range and the environment is assumed to be

variable, which is modeled by a fast fading with independently fading Rayleigh processes, whose power delay profile is described by the ITU Pedestrian A model. A speed dependent Doppler spectrum as given by Clarke and Jakes [4-8] is included in every tap of the power delay profile, and the user default speed is 3 km/h.

The link-level simulator estimates the performance of each single TBS (Transport Block Size). The simulator considers radio communication between the Node-B and the UE using the HS-DSCH, and follows the 3GPP specifications. The simulations assume a full Rake receiver.

The node B transmission power is 42dBm and its antenna gain is 17dBi. The SNR/BLER Matrix file is also an important input file for our simulations. The values in this file correspond to the BLER values 0.0005:0.001:0.9995 and 30 columns, corresponding to CQI values 1 to 30. The values are the SNR values as a function of BLER and CQI. The input file is then fed into the network level simulation (NS2) where the RLC and the MAC-hs are implemented.

The source uses FTP traffic for the simulation. The L2 PDU Header/Payload size is 40 Bytes. The wired core links between GGSN and node B are 20 Mb/s in bandwidth and 10ms in propagation delay. The switching and the processing delays in the SGSN and GGSN are around 5ms. Since in this chapter we do not consider the interaction with the TCP protocol, the TCP parameter are selected in such a way to not trigger timeouts at the TCP level. In other words, the TCP layer is completely transparent and it merely transfers the packets from/to the lower and upper layers (congestion rate p=0 and timeout retransmission timer selected to be high enough to not trigger any timeout). In chapter 5, this configuration of the transport layer will be changed allowing to assess the interaction between the MAC-hs and TCP layers.

3.5 Results

In this section, results obtained from the analytical models and network simulations are reported. 8 HSDPA users are active in the cell and selected using a uniform distribution. To assess the degree of fairness of the schedulers used, we are focusing on two users from the 8 users: one situated at 800m from the node B and the other at 200m from the node B. The Cumulative Distribution Function (CDF) of these two users bit rate for several schedulers and various wireless fading channels are reported in figures 1 to 20. Several wireless fading models and parameters are considered: uncorrelated and correlated multipaths (with correlation equal to 0.3, 0.5 or 0.7), Rayleigh fading, Nakagami fading (with m=2 or 4). In addition, the case of dense multipath channel with constant PDP is also considered. In figures

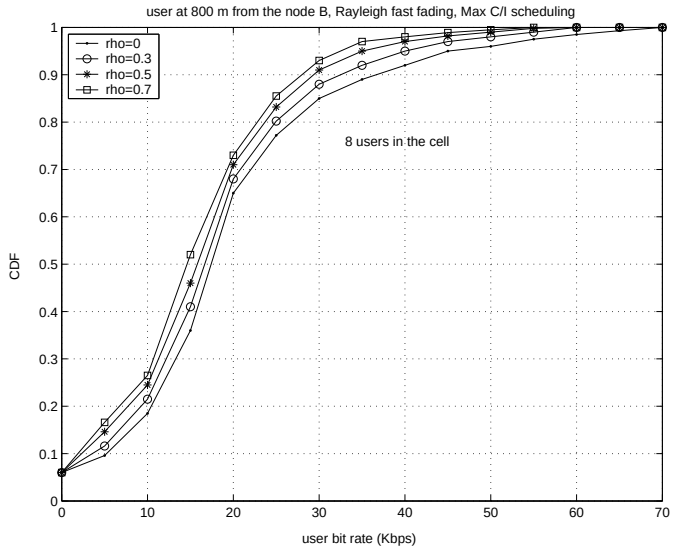

Figure 3.1: CDF of the bit rate of a user situated at 800m from the node B in the case of Max C/I scheduler and Rayleigh fast fading

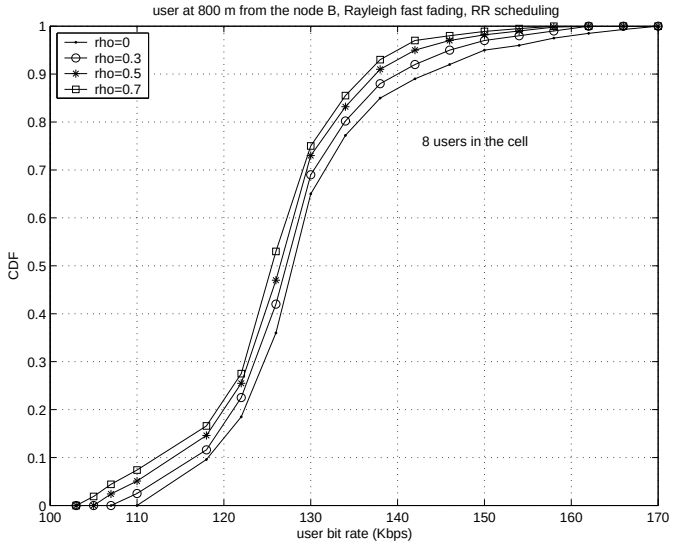

Figure 3.2: CDF of the bit rate of a user situated at 800m from the node B in the case of RR scheduler and Rayleigh fast fading

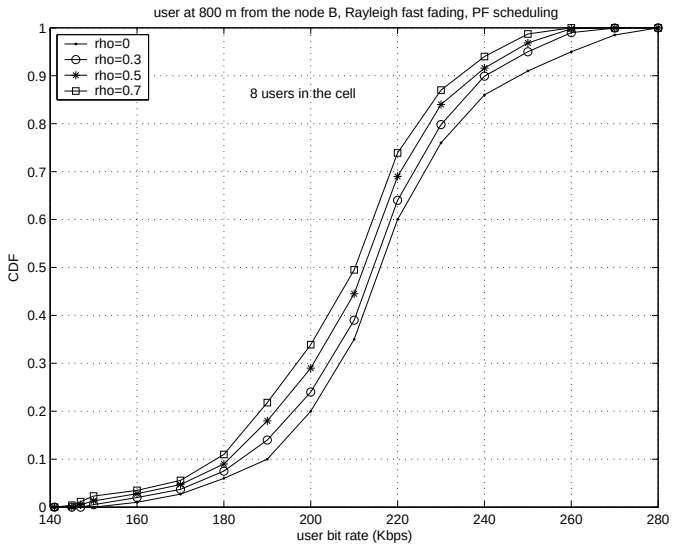

Figure 3.3: CDF of the bit rate of a user situated at 800m from the node B in the case of PF scheduler and Rayleigh fast fading

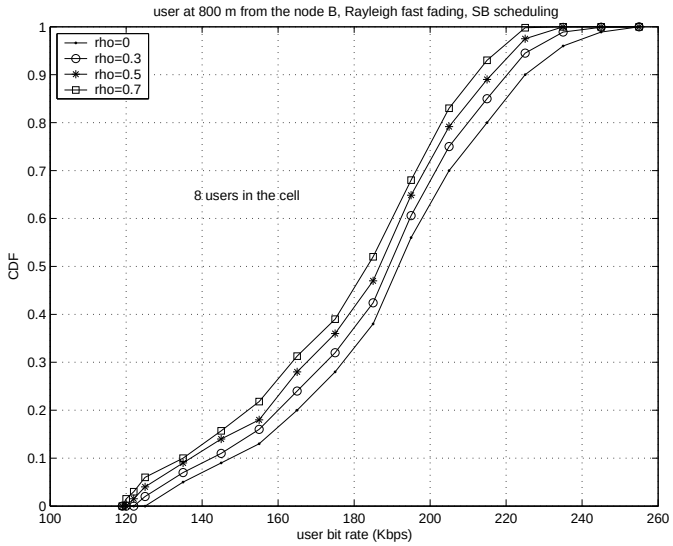

Figure 3.4: CDF of the bit rate of a user situated at 800m from the node B in the case of SB scheduler and Rayleigh fast fading

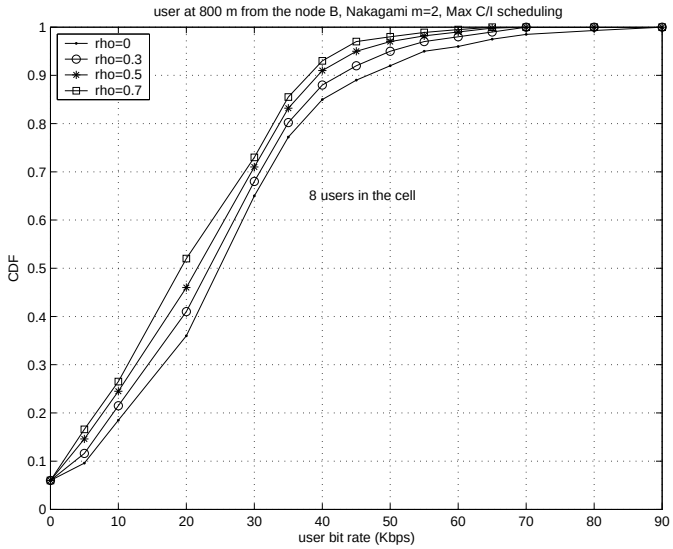

Figure 3.5: CDF of the bit rate of a user situated at 800m from the node B in the case of Max C/I scheduler and Nakagami fast fading

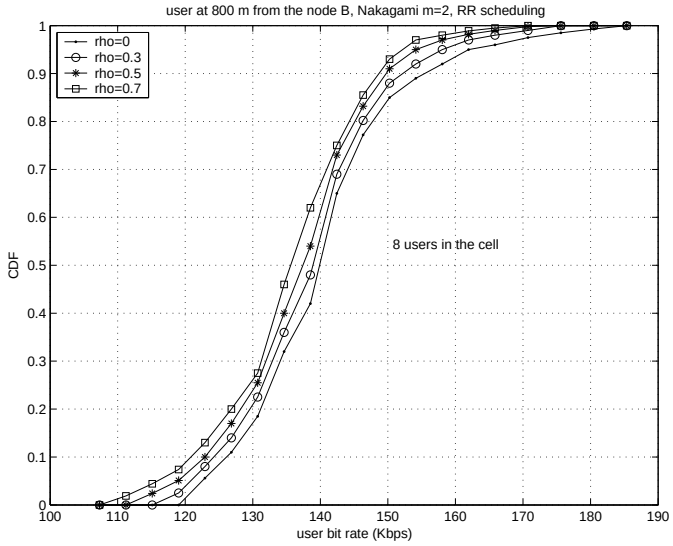

Figure 3.6: CDF of the bit rate of a user situated at 800m from the node B in the case of RR scheduler and Nakagami fast fading

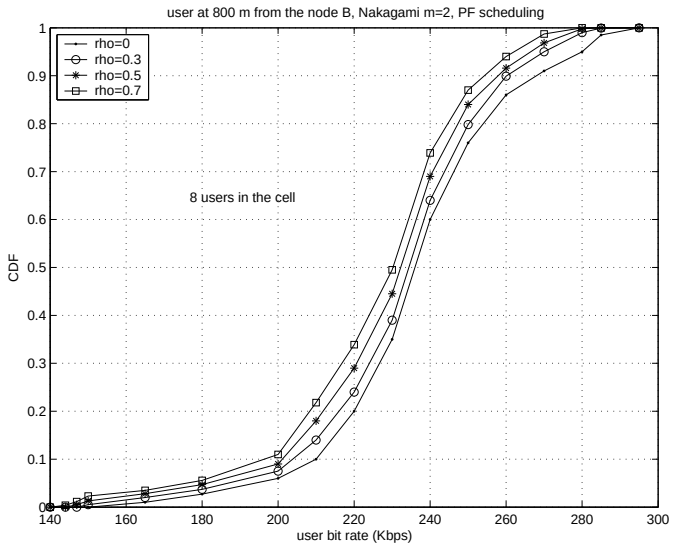

Figure 3.7: CDF of the bit rate of a user situated at 800m from the node B in the case of PF scheduler and Nakagami fast fading

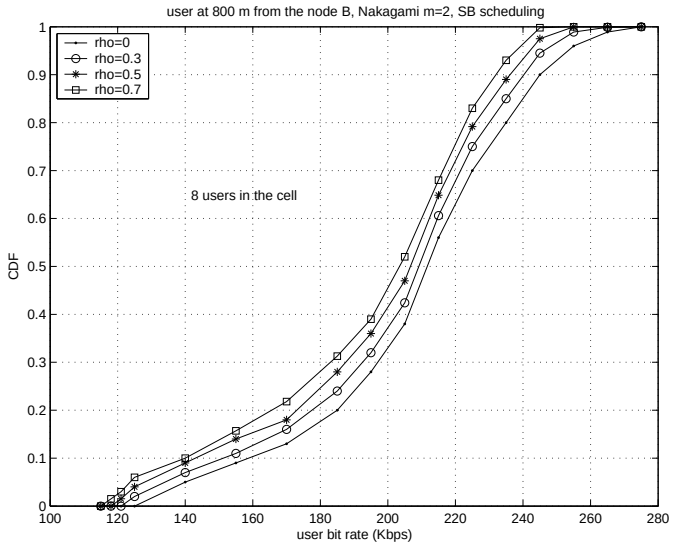

Figure 3.8: CDF of the bit rate of a user situated at 800m from the node B in the case of SB scheduler and Nakagami fast fading

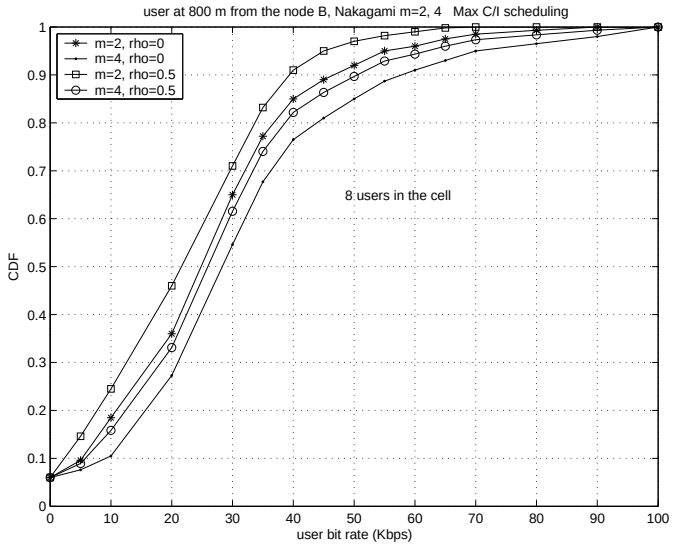

Figure 3.9: CDF of the bit rate of a user situated at 800m from the node B in the case of Max C/I scheduler and Nakagami (m=2 or 4) fast fading

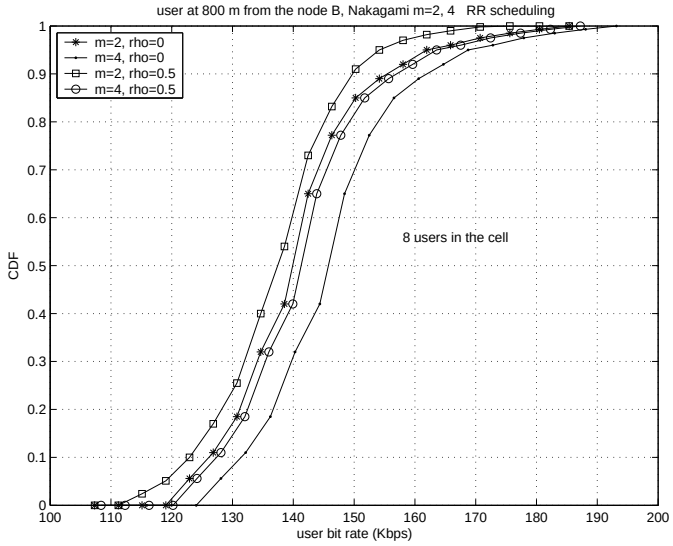

Figure 3.10: CDF of the bit rate of a user situated at 800m from the node B in the case of RR scheduler and Nakagami (m=2 or 4) fast fading

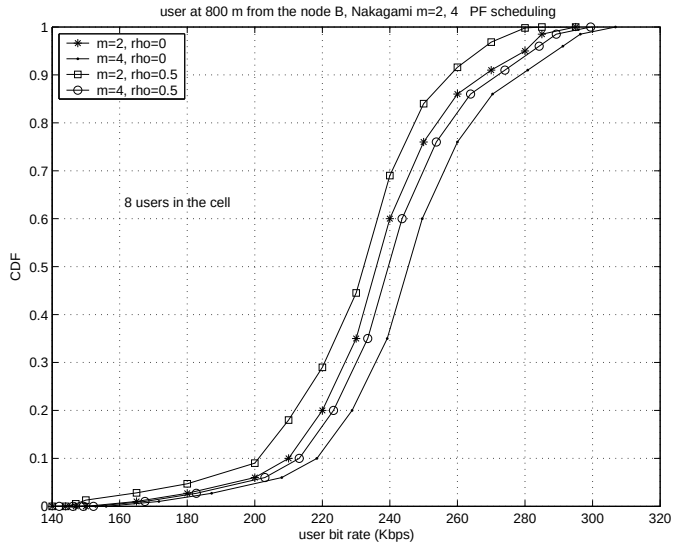

Figure 3.11: CDF of the bit rate of a user situated at 800m from the node B in the case of PF scheduler and Nakagami (m=2 or 4) fast fading

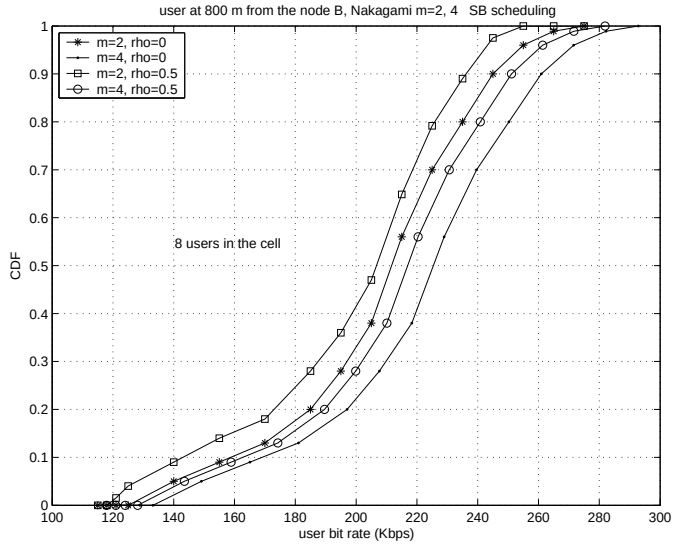

Figure 3.12: CDF of the bit rate of a user situated at 800m from the node B in the case of SB scheduler and Nakagami (m=2 or 4) fast fading

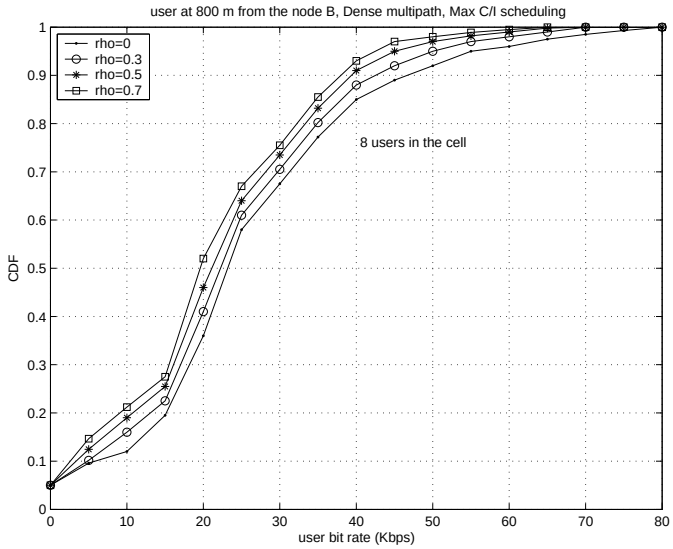

Figure 3.13: CDF of the bit rate of a user situated at 800m from the node B in the case of Max C/I scheduler and dense multipath channel

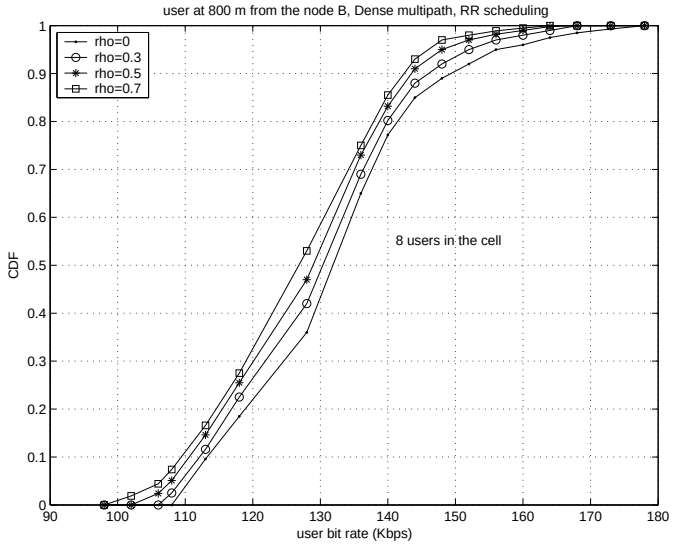

Figure 3.14: CDF of the bit rate of a user situated at 800m from the node B in the case of RR scheduler and dense multipath channel

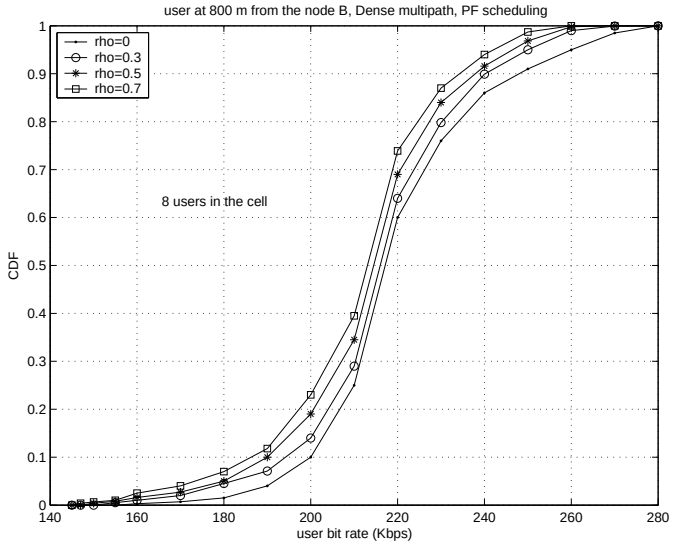

Figure 3.15: CDF of the bit rate of a user situated at 800m from the node B in the case of PF scheduler and dense multipath channel

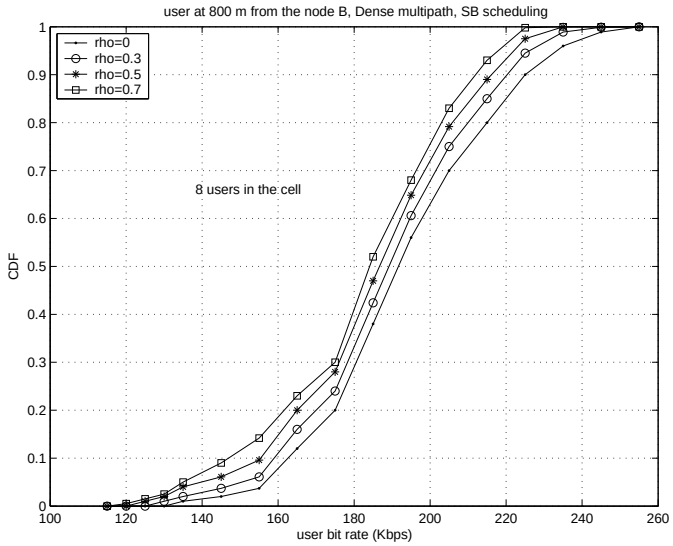

Figure 3.16: CDF of the bit rate of a user situated at 800m from the node B in the case of SB scheduler and dense multipath channel

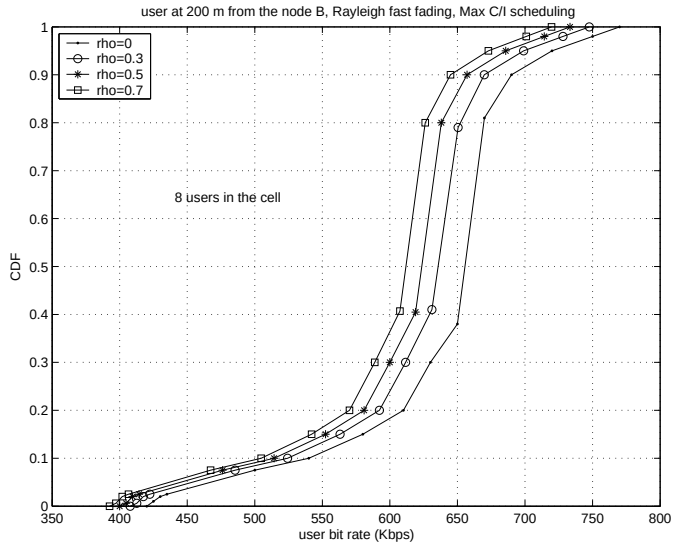

Figure 3.17: CDF of the bit rate of a user situated at 200m from the node B in the case of Max C/I scheduler and Rayleigh fast fading

21 to 23, the CDFs of user bit rate are compared to those obtained by simulation. The mean user bit rates obtained by analytical models and simulation are reported in tables 1 to 4. In these tables (plus table 5), the average cell throughput is also depicted to present the system performance achieved for each scheduler. These simulation results assess the accuracy of the analyses conducted in this chapter. A deviation of 5 to 8% between analytical and simulation results are observed. Besides, the obtained results indicate that the correlation and the fading model affects the user bit rate and cell throughput (increase or decrease) without affecting the degree of fairness of the scheduling algorithms. When the correlation increases from 0 to 0.7, the user bit rate decreases for all users with approximately the same amount (4.5 to 5%). In addition, when the Nakagami parameter m increases from 2 to 4, the system performance increases by approximately 6%. Consequently, efficiency and fairness study of the schedulers in HSDPA can be conducted uniquely for a given fading model. The comparison between the schedulers efficiency is still valid in other wireless conditions and fading models.

Finally, the analysis of these results shows that the proportional fair algorithm seems to be an acceptable trade-off between fairness and cell throughput (compared to the other schedulers) in all wireless conditions. In the following chapters, it is more important to focus on the study of scheduling algorithm and its interaction with upper layers and to compare its performance to other new opportunistic schedulers proposed along in this thesis.

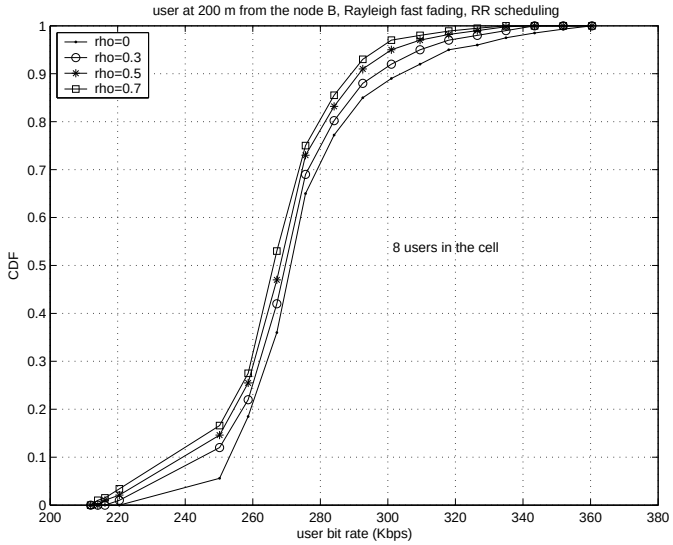

Figure 3.18: CDF of the bit rate of a user situated at 200m from the node B in the case of RR scheduler and Rayleigh fast fading

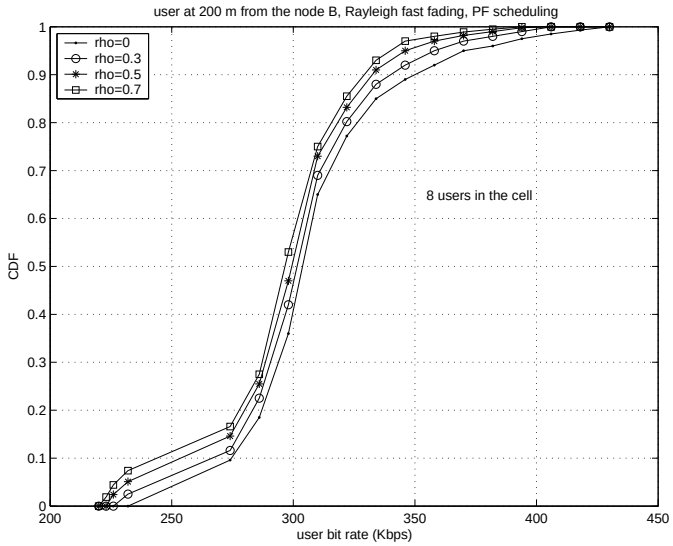

Figure 3.19: CDF of the bit rate of a user situated at 200m from the node B in the case of PF scheduler and Rayleigh fast fading

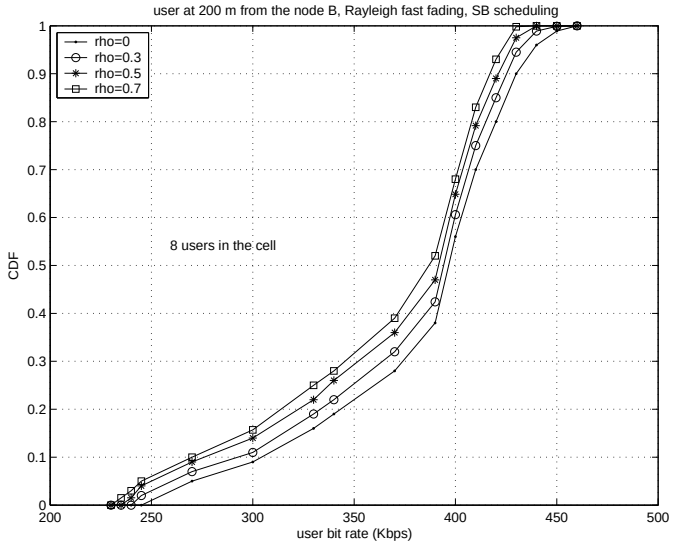

Figure 3.20: CDF of the bit rate of a user situated at 200m from the node B in the case of SB scheduler and Rayleigh fast fading

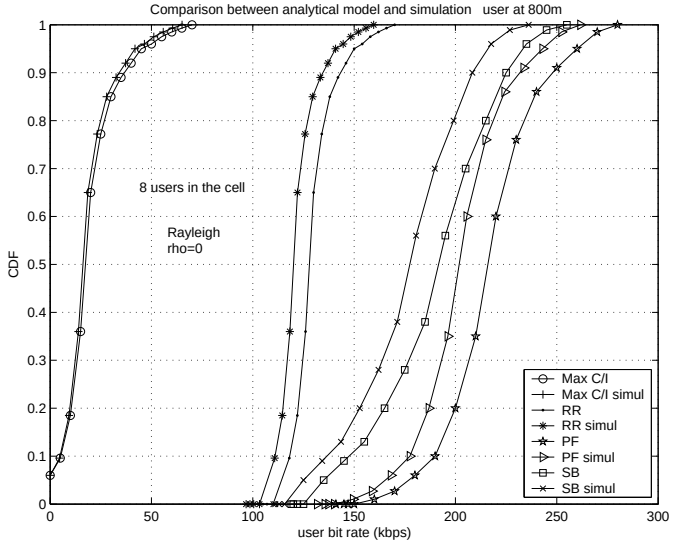

Figure 3.21: Comparison between user the bit rates obtained by analytical model and simulation for various schedulers and Rayleigh fast fading

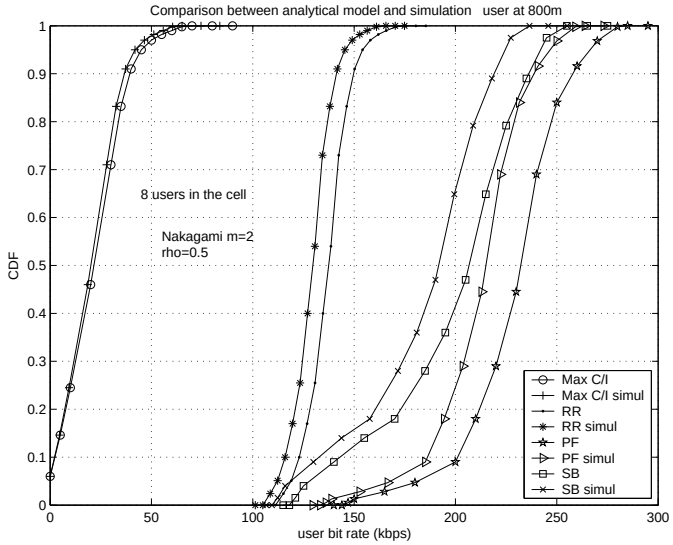

Figure 3.22: Comparison between user bit rates obtained by analytical model and simulation for various schedulers and Nakagami fast fading

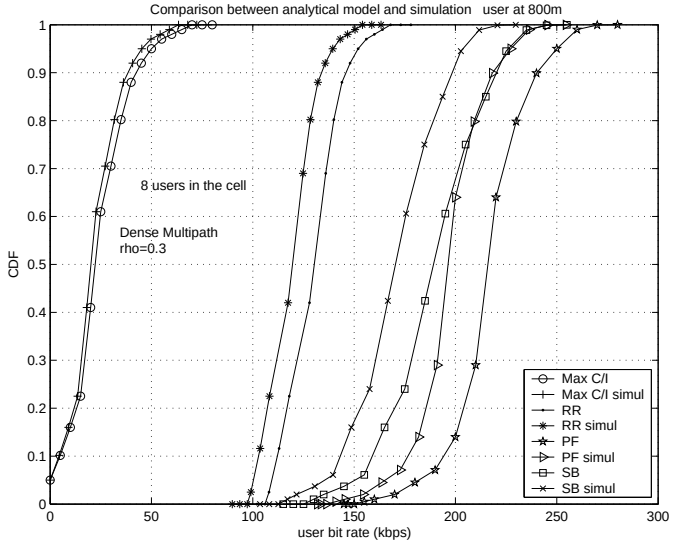

Figure 3.23: Comparison between user bit rates obtained by analytical model and simulation for various schedulers and dense multipath channel

Table 3.1: Mean Max C/I performance obtained by analytical model and simulation

Channel	ρ	**Cell throughput model/simulation (Kbps)**	**user bit rate (800m) model/simulation (Kbps)**	**user bit rate (200m) model/simulation (Kbps)**
Rayleigh	0	2710/2506	21.77/18.6	647.825/600.3
	0.3	2640/2480	20.135/16.5	628.78/575.87
	0.5	2600/2430	18.735/15	616.71/547.3
	0.7	2550/2350	17.7/14.3	605.144/535.78
Dense multipath	0	2790/2550	28.145/20.67	663.175/615.45
	0.3	2736/2500	26.232/18.6	650/582
	0.5	2698/2460	24.567/17	637.43/567
	0.7	2655/2400	23.262/15.78	628/552
Nakagami m=2	0	2916.15/2735	29.155/27.2	700.2/650.45
	0.3	2838.3/2650	27.01/25.7	688.3/632
	0.5	2789.22/2580	25.21/23.87	673.9/613.89
	0.7	2750/2545.34	23.775/21	665.35/604
Nakagami m=4	0	3020.5/2800	34.715/30.45	724.35/670
	0.3	2960/2730	32.48/28.34	710.7/660
	0.5	2908.56/2706.56	31/27.46	698.76/645.67
	0.7	2861.17/2665	28.262/25	685.65/638.12

Table 3.2: Mean Round Robin performance obtained by analytical model and simulation

Channel	ρ	**Cell throughput model/simulation (Kbps)**	**user bit rate (800m) model/simulation (Kbps)**	**user bit rate (200m) model/simulation (Kbps)**
Rayleigh	0	1560/1485	131.656/125.67	279.45/263.12
	0.3	1535/1460	130.028/123.87	275.595/258
	0.5	1520/1440	128.588/122	272.9585/254.38
	0.7	1502/1425	127.478/120.23	270.775/251.87
Dense multipath	0	1600/1490	135.032/126.96	287.7/265
	0.3	1580/1470	132.957/125	283/260
	0.5	1565/1447.56	131.21/123.5	280/255.97
	0.7	1540/1430	128.77/121	277.8/254
Nakagami m=2	0	1670/1570	142.7873/133	300/280
	0.3	1648/1540.76	140/130.9	295.2/271.32
	0.5	1628/1523	138.4023/128.88	292/268.76
	0.7	1605/1510	136.46/126.945	288/266
Nakagami m=4	0	1720/1615	145.943/137	308/288.64
	0.3	1700/1598.56	144.062/135.21	303/283.45
	0.5	1675/1570	142.4/133.65	298/278
	0.7	1658/1546.78	140.8417/131.53	295/274.57

Table 3.3: Mean Proportional Fair performance obtained by analytical model and simulation

Channel	ρ	**Cell throughput model/simulation (Kbps)**	**user bit rate (800m) model/simulation (Kbps)**	**user bit rate (200m) model/simulation (Kbps)**
Rayleigh	0	2220/2075	221.88/207.45	314.968/295
	0.3	2187/2034.87	218.164/204	309.634/287.2
	0.5	2154/2010.29	214.93/199.47	304.918/281.56
	0.7	2120/1986	211.84/197.2	301.2912/278
Dense multipath	0	2255/2085	225.2/210	319.7//297.1
	0.3	2230/2040.34	221.4495/205.3	314.2/288
	0.5	2192.7/2019.5	218.535/201	311/283.43
	0.7	2160/1991.59	215.7655/198.48	307/280
Nakagami m=2	0	2397.6/2239	241.31/225.74	340.2/316.76
	0.3	2362/2207.8	237.6185/221.8	330.8/309
	0.5	2324/2160	234.245/218.6	326/303.82
	0.7	2288/2130.3	230.989/214.2	320.3/297.5
Nakagami m=4	0	2460/2292.3	250.9624/233.45	351.2/325.2
	0.3	2422/2257	247/228.2	343/316.24
	0.5	2384.2/2215	244.93/226.32	338.45/306.49
	0.7	2341/2175.2	240/221.9	333.78/300.53

Table 3.4: Mean Score Based performance obtained by analytical model and simulation

Channel	ρ	**Cell throughput model/simulation (Kbps)**	**user bit rate (800m) model/simulation (Kbps)**	**user bit rate (200m) model/simulation (Kbps)**
Rayleigh	0	2440/2278.2	194.61/181.39	390/362.46
	0.3	2410/2246	190.17/178.5	383.57/356.32
	0.5	2362/2207.47	186.3014/175.6	377.071/350
	0.7	2320/2168.22	182.922/170.1	372.535/346.54
Dense multipath	0	2495/2282.23	198.24/183	398.6/366.7
	0.3	2460/2250	194.14/180.24	391/360.2
	0.5	2400/2219.34	190.327/176.93	384.2/352.48
	0.7	2370/2185.21	187.077/172.76	378.7/347.41
Nakagami m=2	0	2600/2421.4	213.26/198.1	420.4/390.69
	0.3	2560/2375.2	208.37/194.35	407/378
	0.5	2510/2334.87	204.0362/188.9	400.6/369.2
	0.7	2470/2288.1	200.202/185.97	395/363.72
Nakagami m=4	0	2760/2557.34	227.122/211	440/405.9
	0.3	2700/2507.7	221/205.68	430/398.14
	0.5	2660/2462.96	218.591/202	420.4/387.66
	0.7	2600/2403.2	213/196.31	412.24/382

Table 3.5: Mean Fair Throughput performance obtained by analytical model and simulation

Channel	ρ	**Cell throughput model/simulation (Kbps)**
Rayleigh	0	1580/1483.48
	0.3	1550/1456
	0.5	1525/1422.57
	0.7	1495/1384.25
Dense multipath	0	1607/1486
	0.3	1578.4/1463.57
	0.5	1558.5/1430.7
	0.7	1540.37/1385.98
Nakagami m=2	0	1690/1580
	0.3	1666/1554.1
	0.5	1642/1522.37
	0.7	1613/1496.52
Nakagami m=4	0	1756/1640.12
	0.3	1725.23/1609.64
	0.5	1695/1585.11
	0.7	1670.3/1540.97

3.6 Conclusion

This chapter studied analytically the effect of wireless fading on the performance of various schedulers in HSDPA system. This study has been conducted using statistical models of wireless channel fading. The proposed analytical models estimate cell throughput and user bit rate and enable performance comparisons between schedulers.

The user bit rate and cell capacity estimation requires the introduction into the model of the techniques used in HSDPA, in particular AMC, HARQ and scheduling. In addition, derivation of the analytical expressions requires the description of the channel model, the receiver type and an approximate expression of SIR (Signal to Interference Ratio). Several statistical channel models are considered in the study. The cases of composite uncorrelated and correlated (correlation equal to 0.3, 0.5 and 0.7) multipath/shadowing channels with path amplitude following Rayleigh and Nakagami (m=2 and 4) distributions are investigated. The case of composite dense uncorrelated and correlated multipath/shadowing channel is also studied. This last case considers the presence of Wide-sense Stationary channel, constant Power Dispersion Profile (PDP) and frequency selective fading following a Rayleigh distribution.

Results obtained of the Cumulative Distribution Function (CDF) of user bit rate and average cell throughput indicate a decrease of system performance of 5% when the correlation increases from 0

to 0.7 without affecting much the degree of fairness of the studied schedulers. In addition, when the Nakagami parameter m increases from 2 to 4, the system performance increases by approximately 6%. Consequently, the comparison between the schedulers in HSDPA, conducted for a given fading model, can still be valid in other wireless conditions and fading models even if the user bit rate and cell throughput change in these new conditions. Besides, the obtained results show that the proportional fair algorithm is the best trade-off between fairness and cell throughput compared to the other schedulers studied in this chapter. finally, the results obtained by the analytical models are compared to those obtained via simulation. A deviation of 5 to 8% between these results allow to assess the accuracy of the analyses conducted in this chapter.

Bibliography

[1] 3GPP TR 25.942 V5.1.0 (2002-06), "RF System Scenario", (Rel. 5).

[2] John G. Proakis, Digital Communications, Fourth edition, McGraw-Hill Edition, 2001, ISBN 0072321113.

[3] W. C. Jakes, Ed., Microwave Mobile Communications, John Wiley and Sons, New York, 1974.

[4] Theodore S. Rappaport, Wireless Communications: Principles and Practice, Prentice Hall, 2002, ISBN 0-13-042232-0.

[5] J. D. Parsons, Radio Wave Propagation, in Land Mobile Radio Systems, R. J. Holbeche, ed. London: Peter Peregrinus, Ltd., 1985.

[6] J. D. Parsons, The Mobile Radio Propagation Channel, John Wiley and Sons, 1992.

[7] ITU Recommandation, Guidelines for Evaluation of Radio Transmission Technologies for IMT-2000 ITU-R M.1225, 2450,1997.

[8] K.S. Gilhousen, I.M. Jacobs, R. Padovani, A.J. Viterbi, L.A. Weaver, and C.E. Wheatley, "On the capacity of a cellular CDMA system", Vehicular Technology, IEEE Transactions on , Volume: 40 Issue: 2 , May 1991.

[9] N.B. Mehta, L.J. Greenstein, T.M. Willis, III, and Z. Kostic, Analysis and Results for the orthogonality factor in WCDMA downlinks, IEEE Trans. Wireless Commun., 2002.

[10] M.-H. Fong, V. K. Bhargava, and Q. Wang, "Concatenated orthogonal / PN spreading sequences and their application to cellular DS-CDMA systems with integrated traffic," IEEE J. Select. Areas Commun., vol. 14, pp. 547-558, Apr. 1996.

[11] D. Chase, "Code Combining–A Maximum-Likelihood Decoding Approach for Combining an Arbitrary Number of Noisy Packets", Communications, IEEE Transactions on [legacy, pre - 1988] , Volume: 33 Issue: 5 , May 1985.

[12] P. Sindhu, "Retransmission Error Control with Memory", Communications, IEEE Transactions on [legacy, pre - 1988] , Volume: 25 Issue: 5 , May 1977.

[13] Finalising TFRC reference list and uplink signalling definition, 3GPP input paper TSGR1 24(02) 2002.

[14] L.F. Fenton, "The Sum of Log-Normal Probability Distributions in Scatter Transmission Systems", IRE Trans. Commun. Syst. CS-8, No 1 (March 1960), pp. 57-67.

[15] P. Pirinen, "Statistical Power Sum Analysis for Nonidentically Distributed Correlated Lognormal Signals," In the 2003 Finnish Signal Processing Symposium (FINSIG'03), Tampere, Finland, May 19, 2003, pp. 254-258.

[16] G. L. Stuber, "Principles of Mobile Communication", Kluwer Academic publisher, 1996, ISBN 0792397320.

[17] W. A. Janos, "Tail of the Distribution of Sums of Log-Normal Variates," IEEE Transactions on Information Theory, vol. IT-16, no. 3, May 1970, pp. 299-302.

[18] P. G. Moschopoulos, The distribution of the sum of independent gamma random variables, Ann. Inst. Statist. Math. (Part A), vol. 37, pp. 541-544, 1985.

[19] M. K. Simon and M.-S. Alouini, Digital Communication over Fading Channels: A Unified Approach to Performance Analysis, John Wiley and Sons, Inc., 2000, ISBN 0471317799.

[20] Q. T. Zhang, "A simple Capacity Formula for Correlated Diversity Rician Fading Channels," IEEE Communications Letters, vol. 6, no. 11, Nov. 2002, pp. 481-483.

[21] M.Z. Win and Z.A. Kostic, "Impact of Spreading Bandwidthon Rake Reception in dense multipath channels", IEEE J. Select. Areas Commun., vol 17, no.10, pp.1794-1806, Oct. 1999.

[22] M.Z. Win and J.H. Winters, "Analysis of Hybrid Selection/Maximun Ratio Combining in Rayleigh Fading", IEEE Tran. Commun., vol 47, no.12, pp.1773-1776, Dec. 1999.

[23] M.Z. Win and J.H. Winters, "Virtual Branch Analysis of Symbol Error Probability for Hybrid Selection/Maximun Ratio Combining in Rayleigh Fading", IEEE Tran. Commun., vol 49, no.11, pp.1926-1934, Nov. 2001.

[24] P.J. Bickel and K. Docksum, "Mathematical Statistics: Basic Ideas and Selected Topics", 1st edition Oakland, CA:Holden-Day, 1977.

[25] 3GPP TS 25.308 V5.2.0 (2002-03), "HSDPA Overall Description", (Rel. 5).

[26] A. Jalali, R. Padovani, and R. Pankaj, "Data Throughput of CDMA-HDR a high efficiency-high data Wireless personal communication system", in Proc. 50th annual Int. VTC, vol. 3, Tokyo, May 2000, pp. 1854-1858.

[27] J.M. Holtzman, "CDMA forward link waterfilling power control". Proc. of IEEE VTC Spring, 2000.

[28] J.M. Holtzman, "Asymptotic analysis of Proportional Fair algorithm". Proc. of 12th IEEE PIMRC, 2001.

[29] G. Aniba and S. Aissa, "Adaptive proportional fairness for packet scheduling in HSDPA," IEEE Global Telecommunications Conference (GLOBECOM 2004), Vol. 6, Nov./Dec. 2004, pp. 4033-4037.

[30] S. Borst, "User-Level Performance of Channel-Aware Scheduling Algorithms in Wireless Data Networks", Proc. to IEEE INFOCOM 2003.

Chapter 4

Interaction of HSDPA with Circuit Switched (CS) Services

This chapter focuses on the effect of circuit switched (CS) services on High Speed Downlink Packet Access (HSDPA) packet services with the objective of providing guidelines for the UMTS planning process when resources are dynamically shared between circuit and packet services.

Since HS-DSCH is reserved only for non real time data services [1-7], CS services will be transmitted on the downlink DPCH channel (Dedicated Physical Channel). This channel, normalized by the 3GGP in Release 99, supports fast power control and soft handover. AMC and HARQ are not used on this channel. Note that in this chapter, a perfect power control is assumed for CS services.

The scenario of interest in this chapter corresponds to the simultaneous presence of circuit switched (CS) services on the DPCH channel and of HSDPA packet services on the HS-DSCH channel. To assess interaction between CS and HSDPA packets services, we propose an analytical model to estimate the capacity of HSDPA in the presence of CS users on the DPCH channels. A network level simulation, implemented in NS-2 and using the same assumptions as the analytical model, is used to evaluate the accuracy of the proposed model.

CS services consume part of the code tree resources and the node B power and exert interference on the HSDPA packet services. We assume that the entire left over node B power is used to serve HSDPA packet services. Estimating, approximating or lower bounding the capacity of the HSDPA system requires prior analysis of CS services. The basic analytical expression for HSDPA capacity includes terms related to HARQ, fast scheduling, and the selected AMC combination according to radio link conditions. Consequently, the derivation of the analytical model requires prior assessment of CS

services behavior in terms of total power consumption (including soft handover aspects), the relationship that exists between codes used by CS services and those left for HSDPA users, the scheduling and the ensuing AMC combination for HSDPA users. The derivation of the analytical model proposed in the contribution to estimate the capacity of HSDPA considers as in the analyses presented in chapter 3 several scheduling algorithms under various wireless channel model (cases of composite uncorrelated and correlated multipath/shadowing channels with path amplitude following Rayleigh and Nakagami distributions, case of composite dense uncorrelated and correlated multipath/shadowing channel with Wide-sense Stationary channel, constant Power Dispersion Profile (PDP) and frequency selective fading following a Rayleigh distribution).

The chapter has been consequently organized according to these compulsory steps in deriving the analytical model. The steps are provided, in the order needed to derive the overall HSDPA capacity expression, below:

- Evaluation of the power consumed by CS users.
- Estimation of the code tree resources consumed by CS users.
- Estimation of the probability of selecting a given AMC combination under various radio channel models.
- Estimation of HS-DSCH channel capacity for several schedulers.

Note that the selected scheduling algorithms in this chapter are the same as in the previous chapter.

4.1 Part I: Circuit Switched services analysis

The scenario of interest in this chapter corresponds to the simultaneous presence of circuit switched (CS) services with the HSDPA packet services. While CS services use fast power control to maintain a given Quality of Service, in HSDPA the QoS is achieved by using AMC and fast link adaptation. If P is the transmitted power of the admitted CS users (according to the fast power control), all the remaining (left over) Node B power is allocated to HSDPA. Hence, all the available Node B power of 43dBm (as specified in the 3GPP standard) is used.

CS services support fast power control with their associated powers changing in each slot (equivalent to 1/3 TTI). Changes in modulation and coding schemes in HSDPA, using link adaptation, occur only over each TTI. Since the coherence time of the radio channel is approximately equal to 2ms (TTI) [8],

the radio channel does not change during a TTI. Hence, we can assume that the powers of CS users do not change significantly during each TTI, and that the Block Error Rate (BLER) and the target SIR for HSDPA are maintained.

In this section, we evaluate the CS services required powers $\sum_{i=1}^{N_{cs}} P_{cs}(i)$ needed to derive the induced interference by these services on the HS-DSCH channels and the available power for HSDPA.

Note that the considered CS services in this study are : speech at 12.2Kbps, LCD (Low Constraint Data services) at 32Kbps, 64Kbps and 128Kbps.

4.1.1 Distribution of the sum of CS services required powers

proposition

Let N_{cs} be the number of CS users in the cell. If $N_{cs} \geq 10$, the sum of CS users powers can be approximated by a gaussian variable with mean value $\sum_{i=1}^{N_{cs}} E(P_{cs}(i))$ and variance $\sum_{i=1}^{N_{cs}} \sigma^2(P_{cs}(i))$. In the case when the number of CS users is less than 10, the result still provides an approximation. Besides, analyzing the effect of CS services on HSDPA when the number of CS users is less than 10 is not of great interest. Interference will typically be acceptable and the impact on HSDPA services weak.

proof

Let $P_{cs}(i)$ be the required power of CS user i. The SIR expression at the receiver for this user can be given by:

$$SIR = \frac{W}{\lambda R_i} \frac{P_{cs}(i) G_{ij} \sum_{l=1}^{N_T} |\alpha_l|^2}{\beta (P_{cell} - P_{cs}(i)) G_{ij} \sum_{l=1}^{N_T} |\alpha_l|^2 + I_{inter}} \tag{4.1}$$

where W is the chip rate, λ is the service activity factor of user i, R_i is the user bit rate, G_{ij} is the path loss including shadowing, P_{cell} is the total cell transmitted power, and I_{inter} is the other cell interference. Since the total cell power is constant (as we explained above), the SIR expression of each CS user is independent of other users (this is one of the effect of HSDPA on CS services). Note that if HSDPA is not applied, the SIR expression of each CS user depends on the power of other users. Hence, in the case of HSDPA+CS, the required power of each user is independent of other users. For more than 10 to 15 users in the cell, we can consider that $\sum_{i=1}^{N_{cs}} P_{cs}(i)$ can be approximated by a gaussian variable (central limit theorem) with mean value $\sum_{i=1}^{N_{cs}} E(P_{cs}(i))$ and variance $\sum_{i=1}^{N_{cs}} \sigma^2(P_{cs}(i))$. To validate this Gaussian approach, 10 CS users in the cell are considered. According to the mobile location in the cell, the shadowing, the transmitted power and the interference, the empirical distribution $f = \sum_{i=1}^{N_{cs}} P_{cs}(i)$ is

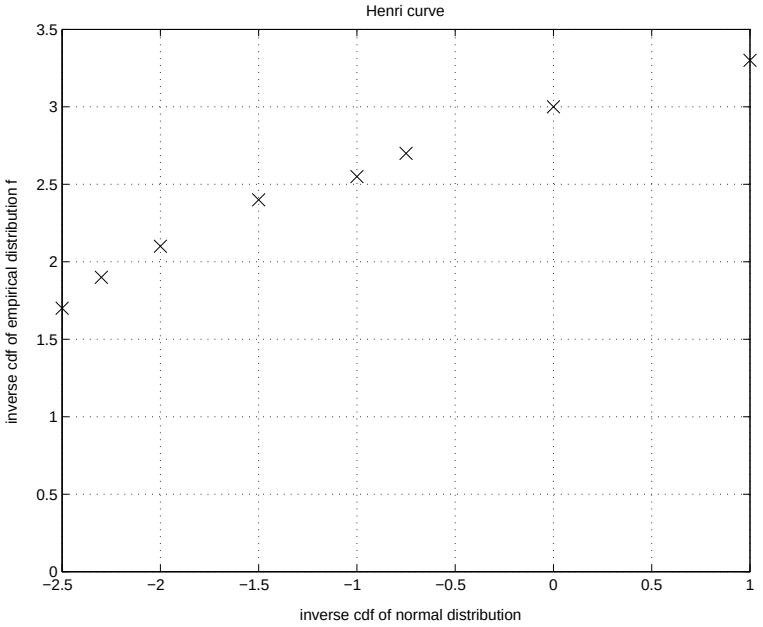

Figure 4.1: HENRI straight line of $cdf^{-1}(f)$ according to normal cdf^{-1} when the CS users number is 10

evaluated by Monte carlo simulations. The cumulative distribution function (cdf) of f and of the normal distribution function according to equidistant values of f are then deduced. The points corresponding to (cdf^{-1} of f; cdf^{-1} of normal) are gathered to get the "*HENRI curve*". The more the "*Henri*" curve approaches a straight line the more f approaches the Gaussian law [9]. The result depicted in figure 1 proves that f could be approximated by a Gaussian variable. If the number of CS users is 15, the HENRI curve is a perfect straight line and $f = \sum_{i=1}^{N_{cs}} P_{cs}(i)$ is gaussian essentially.

4.1.2 Evaluation of $E(P_{cs})$ and $\sigma^2(P_{cs})$

To complete our study, the expression of $E(P_{cs})$ and $\sigma^2(P_{cs})$ must be derived.

CS services use soft handover with users in soft handover state receiving power from two node Bs (only macro diversity of order two is considered in this chapter). The power needed by a mobile to achieve its target QoS is not the same in the case of soft handover compared to the no soft handover case. Let MSH (Margin of Soft Handover) be the soft handover margin of the CS services. The condition that a CS user is connected to a node B j and is not in soft handover is $Pr_j \geq Pr_l + MSH$ for all $l \neq l', j$, where Pr_j and Pr_l are the received powers at the terminal from base stations j and l. The condition of soft handover is : $Pr_{l'} - MSH < Pr_j < Pr_{l'} + MSH$, $Pr_j > Pr_l$ and $Pr_{l'} > Pr_l$ for all $l \neq l', j$.

Consequently, we must distinguish between two cases: mobile in soft handover and mobile connected

to one node B (not in soft handover). Let $P_{cs,sh}$ ($P_{cs,nsh}$) and $prob_{sh}$ ($prob_{nsh}$) be the transmitted power from a node B to a mobile in soft handover (not in handover) and the probability that a mobile is in soft handover (not in handover). The probabilities $prob_{sh}$ and $prob_{nsh}$ are functions of the mobile location and shadowing. The mean value and the variance of a CS service power can be evaluated using (3) and (4).

$$E(P_{cs}) = \underbrace{\int\int}_{A}\Big[prob_{sh}E(P_{cs,sh}) + prob_{nsh}E(P_{cs,nsh})\Big]\rho dA \tag{4.2}$$

$$\sigma^2(P_{cs}) = \underbrace{\int\int}_{A}\Big[prob_{sh}E(P^2_{cs,sh}) + prob_{nsh}E(P^2_{cs,nsh})\Big]\rho dA - E^2(P_{cs}) \tag{4.3}$$

where A is the cell area and ρ is the user density per unit area. To obtain the mean value and the variance of P_{cs}, the mean values (according to shadowing) of the powers $P_{cs,sh}$ and $P_{cs,nsh}$ for a given mobile location have to be evaluated first. These mean values are determined in the next two paragraphs.

User not in soft handover

For a CS user in the cell, the power needed to guarantee a given QoS taking into account the inter-cell and intra-cell interference is given by:

$$P_{cs,nsh}(i) = \frac{\lambda\beta R_i SIR_i}{W + \beta\lambda R_i SIR_i}P_j + \frac{\lambda R_i SIR_i}{W + \beta\lambda R_i SIR_i}g(i) \tag{4.4}$$

where $g(i) = (\frac{1}{\sum_{n=1}^{N_T}|\alpha_n|^2})\sum_{l\neq j}P_l(\frac{d_j}{d_l})^{\mu}[10^{b(s_{sl}-s_{sj})/10}, Pr_j > Pr_l + MSH]$, λ is the activity factor of the CS service allocated to the user i. Due the fact that the node B power is constant, the power of each user depends on the position of the mobile, shadowing and the allocated service. This power changes according to an unknown law, but its mean value and standard deviation can be evaluated in the cases of uncorrelated and correlated Rayleigh and Nakagami fading channel.

Uncorrelated Rayleigh distribution The mean power of user i $E(P_{cs,nsh}(i))$ can be evaluated as follows:

$$E(P_{cs,nsh}(i)) = \frac{\lambda R_i SIR_i}{W + \beta\lambda R_i SIR_i}\left[\beta P_j + \sum_{l=1}^{N_T}\frac{(\Omega_l)^{N_T-2}}{\prod_{r\neq l}^{N_T}(\Omega_l - \Omega_r)}\left(e^{C+\zeta(2)/2}\frac{E1}{\Omega_l}\right)\right] \tag{4.5}$$

where

$$E1 = e^{(b\theta\sigma)^2} \times \sum_{l\neq j}P_l(\frac{d_j}{d_l})^{\mu}Q(\sqrt{2}b\theta\sigma + \frac{10\mu log10(\frac{d_j}{d_l}) - MSH}{\sqrt{2}b\sigma}) \tag{4.6}$$

$\theta = ln10/10$ and Q(.) is the one dimensional Gaussian Q-function. The evaluation of $P^2_{cs,nsh}$ mean value is much more complicated and to our knowledge is not available in the literature. In this section, it is provided by the following equations:

$$E(P^2_{cs,nsh}) = \Big(\frac{\lambda R_i SIR_i}{W+\beta\lambda R_i SIR_i}\Big)^2\Big[(\beta P_j)^2+\sum_{l=1}^{N_T}\frac{(\Omega_l)^{N_T-2}}{\prod_{r\neq l}^{N_T}(\Omega_l-\Omega_r)}\Big(2\beta P_j e^{C+\zeta(2)/2}\frac{E1}{\Omega_l}+e^{2C+2\zeta(2)}\frac{V+E1^2}{(\Omega_l)^2}\Big)\Big] \tag{4.7}$$

$$\begin{aligned} V1 &= e^{(b\theta\sigma)^2}\Big[\sum_{l\neq j}\sum_{l'\neq l,j}P_l P_{l'}(\frac{d_j}{d_l})^{\mu}(\frac{d_j}{d_{l'}})^{\mu}E(d_j,d_l,d_{l'},MSH) \\ &\quad +e^{3(b\theta\sigma)^2}\sum_{l\neq j}(P_l)^2(\frac{d_j}{d_l})^{2\mu}Q(2\sqrt{2}b\theta\sigma+\frac{10\mu log10(\frac{d_j}{d_l})-MSH}{\sqrt{2}b\sigma})\Big] \end{aligned} \tag{4.8}$$

$$\begin{aligned} E(d_j,d_l,d_{l'},MSH) = \frac{1}{\sqrt{2\pi}\sigma}\int_{-\infty}^{+\infty}\Big[e^{-2\theta b s_{sj}}e^{-\frac{s^2_{sj}}{2\sigma^2}}Q(b\theta\sigma+\frac{10\mu log10(\frac{d_j}{d_l})-MSH-bs_{sj}}{b\sigma}) \\ Q(b\theta\sigma+\frac{10\mu log10(\frac{d_j}{d_{l'}})-MSH-bs_{sj}}{b\sigma})\Big]ds_{sj} \end{aligned} \tag{4.9}$$

Correlated Rayleigh distribution The mean value $E(P_{cs,nsh}(i))$ and $E(P^2_{cs,nsh})$ can be evaluated as follows:

$$E(P_{cs,nsh}(i)) = \frac{\lambda R_i SIR_i}{W+\beta\lambda R_i SIR_i}\Big[\beta P_j+\frac{1}{\prod_{l=1}^{N_T}\lambda_l}\sum_{l=1}^{N_T}\frac{1}{\prod_{r\neq l}^{N_T}(\frac{1}{\lambda_r}-\frac{1}{\lambda_l})}\Big(e^{C+\zeta(2)/2}\frac{E1}{\lambda_l}\Big)\Big] \tag{4.10}$$

$$\begin{aligned} E(P^2_{cs,nsh}) &= \Big(\frac{\lambda R_i SIR_i}{W+\beta\lambda R_i SIR_i}\Big)^2\Big[(\beta P_j)^2+\frac{1}{\prod_{l=1}^{N_T}\lambda_l}\sum_{l=1}^{N_T}\frac{1}{\prod_{r\neq l}^{N_T}(\frac{1}{\lambda_r}-\frac{1}{\lambda_l})}\Big(2\beta P_j e^{C+\zeta(2)/2}\frac{E1}{\lambda_l}+ \\ &\quad e^{2C+2\zeta(2)}\frac{V+E1^2}{(\lambda_l)^2}\Big)\Big] \end{aligned} \tag{4.11}$$

Uncorrelated Nakagami distribution The mean value $E(P_{cs,nsh}(i))$ and $E(P^2_{cs,nsh})$ can be evaluated as follows:

$$\begin{aligned} E(P_{cs,nsh}(i)) &= \frac{\lambda R_i SIR_i}{W+\beta\lambda R_i SIR_i}\Big[\beta P_j+\prod_{l=1}^{N_T}\Big(\frac{\Omega_{min}}{\Omega_l}\Big)^m\sum_{k=0}^{\infty}\delta_k\frac{1}{\Omega_{min}(mN_T+k)}\Big(\\ &\quad e^{(\Psi(mN_T+k)-ln(mN_T+k))+\zeta(2,mN_T+k)/2}\frac{E1}{\Omega_{min}(mN_T+k)}\Big)\Big] \end{aligned} \tag{4.12}$$

$$E(P_{cs,nsh}^2) = \left(\frac{\lambda R_i SIR_i}{W+\beta\lambda R_i SIR_i}\right)^2\left[(\beta P_j)^2+\prod_{l=1}^{N_T}\left(\frac{\Omega_{min}}{\Omega_l}\right)^m\sum_{k=0}^{\infty}\delta_k\frac{1}{\Omega_{min}(mN_T+k)}\right.\left(2\beta P_j e^{(\Psi(mN_T+k)-ln(mN_T+k))+\zeta(2,mN_T+k)/2}\frac{E1}{\Omega_{min}(mN_T+k)}\right.$$
$$\left.\left.+e^{2(\Psi(mN_T+k)-ln(mN_T+k))+2\zeta(2,mN_T+k)}\frac{V+E1^2}{(\Omega_{min}(mN_T+k))^2}\right)\right] \quad (4.13)$$

Correlated Nakagami distribution The mean value expressions for $E(P_{cs,nsh}(i))$ and $E(P_{cs,nsh}^2)$ are:

$$E(P_{cs,nsh}(i)) = \frac{\lambda R_i SIR_i}{W+\beta\lambda R_i SIR_i}\left[\beta P_j+\prod_{l=1}^{N_T}\left(\frac{\lambda_{min}}{\lambda_l}\right)^m\sum_{k=0}^{\infty}\delta_k\frac{1}{\lambda_{min}(mN_T+k)}\right.\left(e^{(\Psi(mN_T+k)-ln(mN_T+k))+\zeta(2,mN_T+k)/2}\frac{E1}{\lambda_{min}(mN_T+k)}\right)\Big] \quad (4.14)$$

$$E(P_{cs,nsh}^2) = \left(\frac{\lambda R_i SIR_i}{W+\beta\lambda R_i SIR_i}\right)^2\left[(\beta P_j)^2+\prod_{l=1}^{N_T}\left(\frac{\lambda_{min}}{\lambda_l}\right)^m\sum_{k=0}^{\infty}\delta_k\frac{1}{\lambda_{min}(mN_T+k)}\right.\left(2\beta P_j e^{(\Psi(mN_T+k)-ln(mN_T+k))+\zeta(2,mN_T+k)/2}\frac{E1}{\lambda_{min}(mN_T+k)}\right.$$
$$\left.\left.+e^{2(\Psi(mN_T+k)-ln(mN_T+k))+2\zeta(2,mN_T+k)}\frac{V+E1^2}{(\lambda_{min}(mN_T+k))^2}\right)\right] \quad (4.15)$$

Evaluation of the probability $prob_{nsh}$ Finally, the probability $prob_{nsh}$, that a mobile is not in soft handover, is calculated for each mobile location using (4.16).

$$prob_{nsh} = prob(Pr_j > Pr_l + MSH;\ for\ all\ l \neq j) = prob(s_{sl} \leq s_{sj} - \frac{10\mu log10(d_j/d_l)+MSH}{b})$$
$$= \frac{1}{\sqrt{2\pi}\sigma}\int_{-\infty}^{\infty} e^{\frac{-s_{sj}^2}{2\sigma^2}}\prod_{l\neq j}\left(1-Q\left(s_{sj}-\frac{10\mu log10(d_j/(d_l))+MSH}{\sqrt{2}b\sigma}\right)\right)ds_{sj} \quad (4.16)$$

Mobile user in soft handover

For a mobile user in soft handover between two cells j and l, the power transmitted is the same for the two node Bs [10-11]. In the case of perfect power control, this power can be evaluated by the following equation where the conditions to be satisfied condI, condII and condIII are respectively $Pr_{l'} - MSH < Pr_j < Pr_{l'} + MSH$, $Pr_j > Pr_l$ and $Pr_{l'} > Pr_l$.

$$P_{cs,sh}(i) = \left(\frac{\frac{W}{\lambda R_i SIR_i}}{\beta P_j+\left(\frac{1}{\sum_{n=1}^{N_T}|\alpha_n|^2}\right)\left(Pl'(\frac{d_j}{d_{l'}})^{\mu}[10^{b(s_{sl'}-s_{sj})/10};condI]+\sum_{l\neq j,l'}Pl(\frac{d_j}{d_l})^{\mu}[10^{b(s_{sl}-s_{sj})/10};condII]\right)}\right.$$

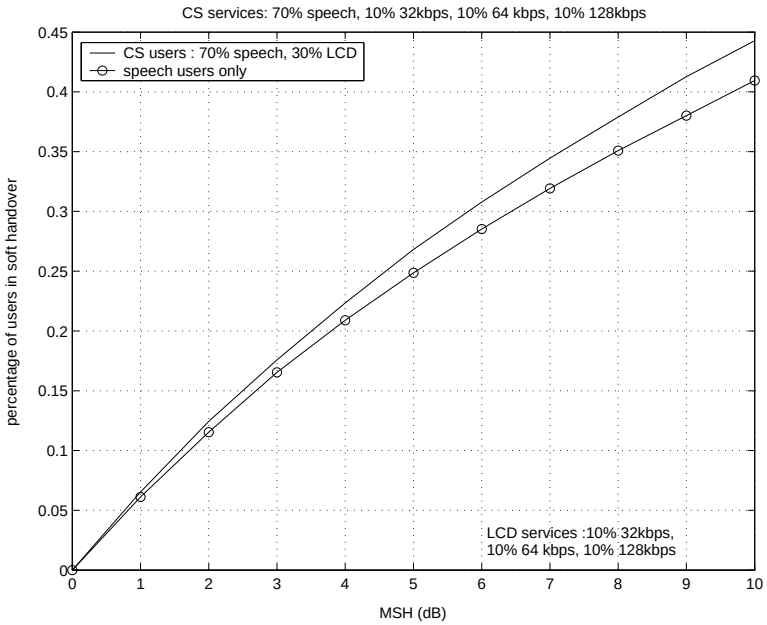

Figure 4.2: percentage of speech and speech and LCD (Low Constraint Data) users (70% speech, 10% 32kbps, 10% 64kbps, 10% 128kbps) in soft handover according to the soft handover margin (MSH)

$$+\frac{\frac{W}{\lambda R_i SIR_i}}{\beta P_{l'}+\left(\frac{1}{\sum_{n'=1}^{N_T}|\alpha_{n'}|^2}\right)\left(P_j(\frac{d_{l'}}{d_j})^{\mu}[10^{b(s_{sj}-s_{sl'})/10};condI]+\sum_{l\neq j,l'}P_l(\frac{d_{l'}}{d_l})^{\mu}[10^{b(s_{sl}-s_{sl'})/10};condIII]\right)}\Bigg)^{-1} \tag{4.1}$$

The evaluation of the mean value of $P_{cs,sh}$ and $P_{cs,sh}^2$ does not lead to any simple analytical equation due to the fraction in the expression of $P_{cs,sh}$. To circumvent this difficulty, the mean value is obtained via MonteCarlo simulation. The probability to be in soft handover can be calculated using:

$$\begin{aligned}
prob_{sh} &= prob(Pr_j > Pr_l; Pr_{l'} > Pr_l; Pr_{l'} - MSH < Pr_j < Pr_{l'} + MSH \qquad for\ \ all\ \ l \neq j, l') \\
&= prob\Bigg(s_{sl} \leq s_{sj} - \frac{10\mu log10(d_j/d_l)}{b}; s_{sl} \leq s_{sl'} - \frac{10\mu log10(d_{l'}/d_l)}{b}; \\
&\quad s_{sl'} + \frac{10\mu log10(d_j/d_l) - MSH}{b} \leq s_{sj} \leq s_{sl'} + \frac{10\mu log10(d_j/d_l) + MSH}{b}\Bigg) \\
&= \frac{1}{2\pi\sigma^2}\int_{-\infty}^{\infty} e^{\frac{-s_{sj}^2}{2\sigma^2}} \prod_{l\neq j,l'}\left(1 - Q\left(s_{sj} - \frac{10\mu log10(d_j/(d_l))}{\sqrt{2}b\sigma}\right)\right)\left[\int_{s_{sj}+\frac{10\mu log10(d_j/d_l)-MSH}{b}}^{s_{sj}+\frac{10\mu log10(d_j/d_l)-MSH}{b}} e^{\frac{-s_{sl'}^2}{2\sigma^2}}\right. \\
&\quad \left.\prod_{l\neq j,l'}\left(1 - Q\left(s_{sl'} - \frac{10\mu log10(d_{l'}/(d_l))}{\sqrt{2}b\sigma}\right)\right) ds_{sl'}\right] ds_{sj}
\end{aligned} \tag{4.18}$$

In figure 2, we present the percentage of users in soft handover as an example of the results obtained from the analysis conducted in this section.

Finally, by replacing $P_{cs,sh}$, $P_{cs,nsh}$, $prob_{sh}$, and $prob_{nsh}$ by their values in (4.2) and (4.3) the mean

value and the variance $E(P_{cs})$ and $\sigma^2(P_{cs})$ of the required CS service power are evaluated.

4.1.3 Relation between the maximum number of HS-DSCH codes N and N_{cs}

The use of a given modulation and coding scheme is conditioned by an upper bound on the number of HS-DSCH codes N. The CS services and the HS-DSCH use the same code tree with a fraction (1-δ) of the code tree reserved for HSDPA signaling channels. If N_{csi} is the number of users having a CS service i, the number of available HS-DSCH codes has an upper bound given by the following equation (when we have one service i):

$$N_{DSCH} = \lfloor \delta SF_{DSCH} \rfloor - \lceil \frac{SF_{DSCH}}{SF_{csi}} N_{csi} \rceil \tag{4.19}$$

where $\lceil x \rceil$ represent the first integer greater or equal to x and $\lfloor x \rfloor$ the first integer smaller or equal to x.

Actually, there are multiple CS services and not just one service in each cell. Each CS service has a spreading factor SF different from the others (128 for speech, 64 for LCD 32Kbps, 32 for LCD 64Kbps and 16 for LCD 128Kbps). Consequently, the number of available codes for the HS-DSCH channels is given by:

$$N_{DSCH} = \lfloor \delta SF_{DSCH} \rfloor - \lceil \sum_{csi=1}^{CS} \frac{SF_{DSCH}}{SF_{csi}} N_{csi} \rceil \tag{4.20}$$

where N_{csi} and SF_{csi} are the number of users and the spreading factor of the CS service csi. The use of $\lceil \sum \frac{SF_{DSCH}}{SF} N_{csi} \rceil$ instead of $\sum \lceil \frac{SF_{DSCH}}{SF} N_{csi} \rceil$ can be interpreted by the following example: one branch at SF=16 could have 1 user with SF=32, 1 user with SF=64, and 2 users with SF=128. Hence, if there are for instance 3 speech users (SF=128), they would consume less than one branch at SF=16 ($\sum \lceil \frac{SF_{DSCH}}{SF} N_{csi} \rceil$ gives a consumption of one branch) and one must sum $\frac{SF_{DSCH}}{SF_{csi}} N_{csi}$ before applying $\lceil\ \rceil$.

4.2 Part II: HSDPA Analysis

After evaluating the CS services required powers and the remaining codes for HSDPA, we can study in this section the effect of CS services on the capacity of HSDPA system. The same derivation method of HSDPA performance, described in the previous chapter, is used in this section with the difference that the total number of available HS-DSCH codes will depend upon the part of the channelization code tree reserved for CS users and that an additional interference, generated by CS users power, will affect the expression of SIR on the HS-DSCH channel. Consequently, the expression of SIR on HS-DSCH channel

is given by:

$$SIR_i = \frac{SF}{log_2(M)\tau} \frac{\frac{\delta P_j - \sum_{q=1}^{N_{cs}} P_{cs}(q) - N_{c,i}P_{sig}}{N_{c,i}} G_{ij} \left(|\sum_{n=1}^{N_F} \alpha_n \omega_n^*|^2 \right)}{\left[\beta \left(P_j - \frac{\delta P_j - \sum_{q=1}^{N_{cs}} P_{cs}(q) - N_{c,i}P_{sig}}{N_{c,i}} \right) G_{ij} \left(\sum_{l=1}^{N_T} |\alpha_l|^2 \right) + I_{inter} + \eta_0 \right] \left(\sum_{n=1}^{N_F} |\omega_n^*|^2 \right)} \tag{4.21}$$

4.2.1 Adaptive Modulation and Coding (AMC)

To track the variation of the channel conditions, AMC is used in HSDPA where a transmission scheme (a modulation order M, a coding rate τ, and a number of HS-DSCH codes N) is selected on a dynamic basis according to the value of SIR (Signal to Interference Ratio). Since CS users consumes part of the code tree, the upper bound of N is evaluated by (4.12). Consequently, the highest order of used CQI is limited by the number of available codes N and by the available power and interference effect. Let k_{mcs} be the probability of selection of transmission scheme mcs. By using the same analysis provided in the previous chapter, k_{mcs} can be written as follows:

$$k_{mcs} = \begin{cases} Prob(SIR \geq \gamma_{mcs})) & \text{highest order } (M, \tau, N)_m \\ Prob(SIR \geq \gamma_{mcs}) - Prob(SIR > \gamma_{mcs+1}) & \text{other } (M, \tau, N)_m \end{cases} \tag{4.22}$$

To get the probability $Prob(SIR \geq \gamma_{mcs})$, we proceed similarly to the derivation described in the previous chapter. Consequently, the expression $SIR \geq \gamma_{mcs}$ can be written as follows:

$$\left(\sum_{l=1}^{N_T} |\alpha_l|^2 \right) X \geq \frac{\gamma_{mcs}}{A_{mcs} - \gamma_{mcs} B_{mcs}} \tag{4.23}$$

where:

$$A_{mcs} = \frac{SF}{log_2(M)\tau} \frac{\delta P_j - \sum_{q=1}^{N_{cs}} P_{cs}(q) - N_{c,i}P_{sig}}{N_{c,i}} \tag{4.24}$$

$$B_{mcs} = \beta \left(P_j - \frac{\delta P_j - \sum_{q=1}^{N_{cs}} P_{cs}(q) - N_{c,i}P_{sig}}{N_{c,i}} \right) \tag{4.25}$$

$$X = \frac{10^{bs_{sj}/10}}{\sum_{l \neq j} \left(P_l \left(\frac{d_l}{d_j} \right)^{-\mu} 10^{bs_{sl}/10} \right)} \tag{4.26}$$

Since the expression $\sum_{q=1}^{N_{cs}} P_{cs}(q)$ can be approximated by a gaussian variable, the expression $A_{mcs} - \gamma_{mcs} B_{mcs}$ is then approximated by a gaussian variable with mean value and variance given respectively

by:

$$m_g = \frac{SF}{log_2(M)\tau}\frac{\delta P_j - N_{c,i}P_{sig}}{N_{c,i}} - \gamma_{mcs}\beta\Big(P_j - \frac{\delta P_j - N_{c,i}P_{sig}}{N_{c,i}}\Big) + (\gamma_{mcs}\beta - \frac{SF}{log_2(M)\tau})\sum_{q=1}^{N_{cs}} E(P_{cs}(q)) \tag{4.27}$$

$$\sigma_g^2 = (\gamma_{mcs}\beta - \frac{SF}{log_2(M)\tau})^2\sum_{q=1}^{N_{cs}} \sigma^2(P_{cs}(q)) \tag{4.28}$$

where $E(P_{cs})$ and $\sigma^2(P_{cs})$ are given respectively by equations (4.2) and (4.3). Consequently, the probability $Prob(SIR \geq \gamma_{mcs})$ are derived using the same method described in the previous chapter at the difference that $A_{mcs} - \gamma_{mcs}B_{mcs}$ is gaussian in this case instead to be constant. Consequently, the probability $Prob(SIR \geq \gamma_{mcs})$ for various wireless channel models can be written as follows:

Uncorrelated Rayleigh distribution

$$Prob(SIR \geq \gamma_{mcs}) = \sum_{l=1}^{N_T}\frac{(\Omega_l)^{N_T-2}}{\prod_{r\neq l}^{N_T}(\Omega_l - \Omega_r)}\int_0^{\infty} Q\Big[\frac{ln\Big(\frac{\gamma_{mcs}}{x}\Big) - (10log\Omega_l + \mu_f)/\epsilon}{\sigma_f/\epsilon}\Big]\frac{1}{\sqrt{2\pi}\sigma_g}e^{-\frac{(x-m_g)^2}{2\sigma_g^2}}dx \tag{4.29}$$

Correlated Rayleigh distribution

$$Prob(SIR \geq \gamma_{mcs}) = \frac{1}{\prod_{l=1}^{N_T}\lambda_l}\sum_{l=1}^{N_T}\frac{1}{\prod_{r\neq l}^{N_T}(\frac{1}{\lambda_r} - \frac{1}{\lambda_l})}\int_0^{\infty} Q\Big[\frac{ln\Big(\frac{\gamma_{mcs}}{x}\Big) - (10log\lambda_l + \mu_f)/\epsilon}{\sigma_f/\epsilon}\Big]\frac{1}{\sqrt{2\pi}\sigma_g}e^{-\frac{(x-m_g)^2}{2\sigma_g^2}}dx \tag{4.30}$$

Uncorrelated Nakagami distribution

$$Prob(SIR \geq \gamma_{mcs}) = \prod_{l=1}^{N_T}\Big(\frac{\Omega_{min}}{\Omega_l}\Big)^m\sum_{k=0}^{\infty}\delta_k\frac{1}{\Omega_{min}(mN_T+k)\Gamma(mN_T+k)}\Big[$$
$$\int_0^{\infty} Q\Big(\frac{ln(\frac{\gamma_{mcs}}{x}) - (10log(\Omega_{min}(mN_T+k)) + \mu_f)/\epsilon}{\sigma_f/\epsilon}\Big)\frac{1}{\sqrt{2\pi}\sigma_g}e^{-\frac{(x-m_g)^2}{2\sigma_g^2}}dx\Big] \tag{4.31}$$

where $\mu_f = -\epsilon(\Psi(mN_T+k) - ln(mN_T+k)) + \mu_X$ and $\sigma_f^2 = \epsilon^2\zeta(2, mN_T+k) + \sigma_X^2$. The Euler psi function $\Psi(mN_T+k)$ and the Riemann-Zeta function $\zeta(2, mN_T+k)$ are given respectively by:

$$\Psi(mN_T+k) = -C + \sum_{r=1}^{mN_T+k-1} \frac{1}{r} \tag{4.32}$$

$$\zeta(2, mN_T+k) = \sum_{r=0}^{\infty} \frac{1}{(mN_T+k+r)^2} \tag{4.33}$$

Correlated Nakagami distribution

$$Prob(SIR \geq \gamma_{mcs}) = \prod_{l=1}^{N_T}\Big(\frac{\lambda_{min}}{\lambda_l}\Big)^m \sum_{k=0}^{\infty}\delta_k \frac{1}{\lambda_{min}(mN_T+k)\Gamma(mN_T+k)}\Big[\int_0^{\infty} Q\Big(\frac{ln(\frac{\gamma_{mcs}}{x}) - (10log(\lambda_{min}(mN_T+k)) + \mu_f)/\epsilon}{\sigma_f/\epsilon}\Big)\frac{1}{\sqrt{2\pi}\sigma_g}e^{-\frac{(x-m_g)^2}{2\sigma_g^2}}dx\Big] \tag{4.34}$$

where $\mu_f = -\epsilon(\Psi(mN_T+k) - ln(mN_T+k)) + \mu_X$ and $\sigma_f^2 = \epsilon^2\zeta(2, mN_T+k) + \sigma_X^2$.

Dense multipath channel with uncorrelated Rayleigh fading

In this case, the gaussian distribution of the CS users powers can be included in the estimation of k_{mcs} as follows:

$$\begin{aligned} Prob(SIR \geq \gamma_{mcs}) = 1 - F(\gamma) &= 1 - \int_0^{\infty}\int_0^{\infty}\Big(1 - e^{-\gamma/\overline{\gamma}}(\sum_{k=0}^{N_T-1}\frac{\gamma^k}{\overline{\gamma}^k k!})\Big)\frac{1}{\sqrt{2\pi}\sigma_{\overline{\gamma}}\overline{\gamma}}e^{-\frac{(\ln\overline{\gamma}-\mu_{\overline{\gamma}})^2}{2\sigma_{\overline{\gamma}}^2}} \\ &\quad \frac{1}{\sqrt{2\pi}\sigma_{P_{cs}}}e^{-\frac{(x-E(P_{cs}))^2}{2\sigma_{P_{cs}}^2}}d(\overline{\gamma})dx \end{aligned} \tag{4.35}$$

where

$$\mu_{\overline{\gamma}} = \ln\Big(\frac{\sqrt{A_{mcs}^2V(X) + A_{mcs}^2(E(X)+B_{mcs,x})^2}}{(E(X)+B_{mcs,x})^2}\Big) \tag{4.36}$$

$$\sigma_{\overline{\gamma}}^2 = \ln\Big(\frac{V(X) + (E(X)+B_{mcs,x})^2}{(E(X)+B_{mcs,x})^2}\Big) \tag{4.37}$$

E(X), and V(X) are given respectively by equations 3.34, 3.35 and 3.36 and $B_{mcs,x}$ is given by:

$$B_{mcs,x} = \beta\Big(P_j - \frac{\delta P_j - x - N_{c,i}P_{sig}}{N_{c,i}}\Big) \tag{4.38}$$

Dense multipath channel with correlated Rayleigh fading

$$Prob(SIR \geq \gamma_{mcs}) = 1 - F(\gamma) = 1 - \int_0^\infty \int_0^\infty \sum_{l=1}^{N_T} \frac{(\Gamma_l)^{N_T-2}}{\prod_{r\neq l}^{N_T}(\Gamma_l - \Gamma_r)} \left(1 - e^{-\gamma/\Gamma_l}\right) \frac{1}{\sqrt{2\pi}\sigma_{\overline{\gamma}}\overline{\gamma}} e^{-\frac{(\ln\overline{\gamma} - \mu_{\overline{\gamma}})^2}{2\sigma_{\overline{\gamma}}^2}} \frac{1}{\sqrt{2\pi}\sigma_{P_{cs}}} e^{-\frac{(x-E(P_{cs}))^2}{2\sigma_{P_{cs}}^2}} d(\overline{\gamma})dx \quad (4.39)$$

4.2.2 Scheduling

To deduce the user bit rate and cell throughput, the scheduling effect should be included in the analysis. In the previous chapter, several schedulers have been modeled when HSDPA uses all the cell resources. The introduction of CS users does not affect the expression derived in the previous chapter for Round Robin, Fair Throughput, Max C/I and Score Based. This does not mean that the performance of these schedulers does not change. This performance depends on the number of CS users via k_{mcs} (as presented in the scheduling models in chapter 3).

The fact that the introduction CS users does not affect the modeling expressions of Round Robin, Fair Throughput or Score Based can be verified trivially. In the case of Max C/I, this can be proved as follows: The probability that the channel is allocated to user i is $prob(SIR_i > SIR_j)\ \forall\ j \neq i$. After simplification, the expression $SIR_i > SIR_j$ can be written as:

$$\left(\sum_{l_i=1}^{N_T} |\alpha_{l_i,i}|^2\right) X_i > \left(\sum_{l_j=1}^{N_T} |\alpha_{l_j,j}|^2\right) X_j \quad (4.40)$$

where X_i is given by equation (3.30) for user i. This expression has the same form of that found in the previous chapter (i.e. it is explicitly independent of P_{cs}) and therefore the probability $prob(SIR_i > SIR_j)$ has the same expression as in the case when CS users are not used.

Proportional Fair (PF)

If N_u is the number of users in the cell, the probability that a TTI is allocated to a given user i can be evaluated using the following equation:

$$pr(i) = Prob\left(\frac{SIR_i}{S_i} > \frac{SIR_j}{S_j} \text{ for j=1..}N_u \text{ and } j \neq i\right) = \prod_{j\neq i}^{N_u} Prob\left(SIR_i > \frac{S_i}{S_j} SIR_j\right)$$

$$= \prod_{j\neq i}^{N_u} Prob\Big[\frac{1}{\Big(\sum_{l_i=1}^{N_T}|\alpha_{l_i,i}|^2\Big)X_i} < \frac{S_j}{S_i}\frac{1}{\Big(\sum_{l_j=1}^{N_T}|\alpha_{l_j,j}|^2\Big)X_j} + (\frac{S_j}{S_i}-1)B_{mcs}\Big] \tag{4.41}$$

where X_i is given by equation (3.33) for user i.

Uncorrelated Rayleigh fading In this case, the probability pr(i) is given by:

$$pr(i) = \prod_{j\neq i}^{N_u}\sum_{l_i=1}^{N_T}\sum_{l_j=1}^{N_T}\frac{(\Omega_{l_i,i})^{N_T-2}}{\prod_{r_i\neq l_i}^{N_T}(\Omega_{l_i,i}-\Omega_{r_i,i})}\frac{(\Omega_{l_j,j})^{N_T-2}}{\prod_{r_j\neq l_j}^{N_T}(\Omega_{l_j,j}-\Omega_{r_j,j})}\times\Big[$$
$$\int_0^\infty Q\Big(-\frac{(10log\Omega_{l_i,i}+\mu_{f,i}-m_{f,j})}{\sqrt{\sigma_{f,i}^2+\sigma_{f,j}^2}}\Big)\frac{1}{\sqrt{2\pi}\sigma(P_{cs})}e^{-\frac{(x-E(P_{cs}))^2}{2\sigma^2(P_{cs})}}dx\Big] \tag{4.42}$$

where

$$m_{f,j} = -\epsilon ln\Big(\frac{\sqrt{e^{2(-10log(\frac{S_j}{S_i})-10log\Omega_{l_j,j}-\mu_{f,j})+\sigma_{f,j}^2}(e^{\sigma^2}-1)+(E)^2}}{(E)^2}\Big) \tag{4.43}$$

$$E = e^{2(-10log(\frac{S_j}{S_i})-10log\Omega_{l_j,j}-\mu_{f,j})+\sigma_{f,j}^2} + (\frac{S_j}{S_i}-1)B_{mcs,x}\frac{\prod_{r_j\neq l_j}^{N_T}(\Omega_{l_j,j}-\Omega_{r_j,j})}{N_T(\Omega_{l_j,j})^{N_T-2}} \tag{4.44}$$

$$B_{mcs,x} = \beta\Big(P_j - \frac{\delta P_j - x - N_{c,i}P_{sig}}{N_{c,i}}\Big) \tag{4.45}$$

Consequently, the user bit rate and the cell throughput are determined by (3.134) and (3.135).

Correlated Rayleigh fading In the case of correlated Rayleigh fading, the probability that the channel is allocated to user i is given by:

$$pr(i) = \prod_{j\neq i}^{N_u}\frac{1}{\prod_{l_i=1}^{N_T}\lambda_{l_i,i}}\frac{1}{\prod_{l_j=1}^{N_T}\lambda_{l_j,j}}\sum_{l_i=1}^{N_T}\sum_{l_j=1}^{N_T}\frac{1}{\prod_{r_i\neq l_i}^{N_T}(\frac{1}{\lambda_{r_i,i}}-\frac{1}{\lambda_{l_i,i}})}\frac{1}{\prod_{r_j\neq l_j}^{N_T}(\frac{1}{\lambda_{r_j,j}}-\frac{1}{\lambda_{l_j,j}})}\Big[$$
$$\int_0^\infty Q\Big(-\frac{(10log\lambda_{l_i,i}+\mu_{f,i}-m_{f,j})}{\sqrt{\sigma_{f,i}^2+\sigma_{f,j}^2}}\Big)\frac{1}{\sqrt{2\pi}\sigma(P_{cs})}e^{-\frac{(x-E(P_{cs}))^2}{2\sigma^2(P_{cs})}}dx\Big] \tag{4.46}$$

where

$$m_{f,j} = -\epsilon ln\Big(\frac{\sqrt{e^{2(-10log(\frac{S_j}{S_i})-10log\lambda_{l_j,j}-\mu_{f,j})+\sigma_{f,j}^2}(e^{\sigma^2}-1)+(E)^2}}{(E)^2}\Big) \tag{4.47}$$

$$E = e^{2(-10log(\frac{S_j}{S_i})-10log\lambda_{l_j,j}-\mu_{f,j})+\sigma_{f,j}^2} + (\frac{S_j}{S_i}-1)B_{mcs,x}\frac{\prod_{r_j\neq l_j}^{N_T}(\lambda_{l_j,j}-\lambda_{r_j,j})}{N_T(\lambda_{l_j,j})^{N_T-2}}\prod_{l_j=1}^{N_T}\lambda_{l_j,j} \tag{4.48}$$

$$B_{mcs,x} = \beta\Big(P_j - \frac{\delta P_j - x - N_{c,i}P_{sig}}{N_{c,i}}\Big) \tag{4.49}$$

Consequently, the user bit rate and the cell throughput are determined by (3.134) and (3.135).

Uncorrelated Nakagami fading In this case, the probability pr(i) is given by:

$$\begin{aligned} pr(i) &= \prod_{j\neq i}^{N_u}\prod_{l_i=1}^{N_T}\left(\frac{\Omega_{min}}{\Omega_{l_i,i}}\right)^m \prod_{l_j=1}^{N_T}\left(\frac{\Omega_{min}}{\Omega_{l_j,j}}\right)^m \sum_{k_i=0}^{\infty}\sum_{k_j=0}^{\infty}\Bigg[\delta_{k_i}\frac{1}{\Omega_{min}(mN_T+k_i)\Gamma(mN_T+k_i)}\times \\ &\delta_{k_j}\frac{1}{\Omega_{min}(mN_T+k_j)\Gamma(mN_T+k_j)}\times \\ &\int_0^{\infty} Q\Big(-\frac{(10log(\Omega_{min,i}(mN_T+k_i))+\mu_{f,i}-m_{f,j})}{\sqrt{\sigma_{f,i}^2+\sigma_{f,j}^2}}\Big)\frac{1}{\sqrt{2\pi}\sigma(P_{cs})}e^{-\frac{(x-E(P_{cs}))^2}{2\sigma^2(P_{cs})}}dx\Bigg] \end{aligned} \tag{4.50}$$

where

$$m_{f,j} = -\epsilon ln\Big(\frac{\sqrt{e^{2(-10log(\frac{S_j}{S_i})-10log(\Omega_{min,j}(mN_T+k_j))-\mu_{f,j})+\sigma_{f,j}^2}(e^{\sigma^2}-1)+(E)^2}}{(E)^2}\Big) \tag{4.51}$$

$$E = \begin{cases} e^{2(-10log(\frac{S_j}{S_i})-10log(\Omega_{min,j}(mN_T+k_j))-\mu_{f,j})+\sigma_{f,j}^2}+(\frac{S_j}{S_i}-1)B_{mcs,x}(mN_T!)\prod_{l_j=1}^{N_T}\left(\frac{\Omega_{l_j,j}}{\Omega_{min}}\right)^m & k_j=0 \\ e^{2(-10log(\frac{S_j}{S_i})-10log(\Omega_{min,j}(mN_T+k_j))-\mu_{f,j})+\sigma_{f,j}^2} & \text{Elsewhere} \end{cases} \tag{4.52}$$

$$B_{mcs,x} = \beta\Big(P_j - \frac{\delta P_j - x - N_{c,i}P_{sig}}{N_{c,i}}\Big) \tag{4.53}$$

Consequently, the user bit rate and the cell throughput are determined by (3.134) and (3.135).

Correlated Nakagami fading In this case, the probability pr(i) is given by:

$$\begin{aligned} pr(i) &= \prod_{j\neq i}^{N_u}\prod_{l_i=1}^{N_T}\left(\frac{\lambda_{min}}{\lambda_{l_i,i}}\right)^m \prod_{l_j=1}^{N_T}\left(\frac{\lambda_{min}}{\lambda_{l_j,j}}\right)^m \sum_{k_i=0}^{\infty}\sum_{k_j=0}^{\infty}\Bigg[\delta_{k_i}\frac{1}{\lambda_{min}(mN_T+k_i)\Gamma(mN_T+k_i)}\times \\ &\delta_{k_j}\frac{1}{\lambda_{min}(mN_T+k_j)\Gamma(mN_T+k_j)}\times \\ &\int_0^{\infty} Q\Big(-\frac{(10log(\lambda_{min,i}(mN_T+k_i))+\mu_{f,i}-m_{f,j})}{\sqrt{\sigma_{f,i}^2+\sigma_{f,j}^2}}\Big)\frac{1}{\sqrt{2\pi}\sigma(P_{cs})}e^{-\frac{(x-E(P_{cs}))^2}{2\sigma^2(P_{cs})}}dx\Bigg] \end{aligned} \tag{4.54}$$

where

$$m_{f,j} = -\epsilon ln\Big(\frac{\sqrt{e^{2(-10log(\frac{S_j}{S_i})-10log(\lambda_{min,j}(mN_T+k_j))-\mu_{f,j})+\sigma_{f,j}^2}(e^{\sigma^2}-1)+(E)^2}}{(E)^2}\Big) \tag{4.55}$$

$$E = \begin{cases} e^{2(-10log(\frac{S_j}{S_i})-10log(\lambda_{min,j}(mN_T+k_j))-\mu_{f,j})+\sigma^2_{f,j}} + (\frac{S_j}{S_i}-1)B_{mcs,x}(mN_T!)\prod_{l_j=1}^{N_T}\left(\frac{\lambda_{l_j,j}}{\lambda_{min}}\right)^m & k_j = 0 \\ e^{2(-10log(\frac{S_j}{S_i})-10log(\lambda_{min,j}(mN_T+k_j))-\mu_{f,j})+\sigma^2_{f,j}} & \text{Elsewhere} \end{cases} \quad (4.56$$

$$B_{mcs,x} = \beta\left(P_j - \frac{\delta P_j - x - N_{c,i}P_{sig}}{N_{c,i}}\right) \quad (4.57)$$

Consequently, the user bit rate and the cell throughput are determined by (3.134) and (3.135).

Dense multipath channel with uncorrelated Rayleigh fading The probability that a TTI is allocated to user i can be written as follows:

$$\begin{aligned} pr(i) &= Prob\left(\frac{SIR_i}{S_i} > \frac{SIR_j}{S_j} \text{ for j=1..}N_u \text{ and } j \neq i\right) = \prod_{j\neq i}^{N_u} Prob\left(SIR_i > \frac{S_i}{S_j}SIR_j\right) \\ &= \prod_{j\neq i}^{N_u}\left(1 - \int_0^{+\infty} F_i(\frac{S_i}{S_j}SIR_j)pdf(SIR_j)d(SIR_j)\right) \end{aligned} \quad (4.58)$$

where F_i is the cdf of SIR_i evaluated at SIR_j. F_i is given by:

$$cdf(\gamma_{Rake}) = F(\gamma) = \int_0^{\infty}\int_0^{\infty}\left(1 - e^{-\gamma/\overline{\gamma}}(\sum_{k=0}^{N_T-1}\frac{\gamma^k}{\overline{\gamma}^k k!})\right)\frac{1}{\sqrt{2\pi}\sigma_{\overline{\gamma}}\overline{\gamma}}e^{-\frac{(\ln\overline{\gamma}-\mu_{\overline{\gamma}})^2}{2\sigma^2_{\overline{\gamma}}}}\frac{1}{\sqrt{2\pi}\sigma_{P_{cs}}}e^{-\frac{(x-E(P_{cs}))^2}{2\sigma^2_{P_{cs}}}}d(\overline{\gamma})dx \quad (4.59)$$

pdf(SIR_j) is the pdf of SIR_j given by:

$$\begin{aligned} pdf(\gamma) &= \int_{\overline{\gamma}} pdf(\gamma_{Rake}/\overline{\gamma})pdf(\overline{\gamma})d(\overline{\gamma}) \\ &= \int_0^{\infty}\int_0^{\infty}\frac{(\gamma)^{N_T-1}}{\Gamma(N_T)\overline{\gamma}^{N_T-1}}e^{-\gamma/\overline{\gamma}}\frac{1}{\sqrt{2\pi}\sigma_{\overline{\gamma}}\overline{\gamma}}e^{-\frac{(\ln\overline{\gamma}-\mu_{\overline{\gamma}})^2}{2\sigma^2_{\overline{\gamma}}}}\frac{1}{\sqrt{2\pi}\sigma_{P_{cs}}}e^{-\frac{(x-E(P_{cs}))^2}{2\sigma^2_{P_{cs}}}}d(\overline{\gamma})dx \end{aligned} \quad (4.60)$$

$$\mu_{\overline{\gamma}} = \ln\left(\frac{\sqrt{A^2_{mcs}V(X) + A^2_{mcs}(E(X)+B_{mcs,x})^2}}{(E(X)+B_{mcs,x})^2}\right) \quad (4.61)$$

$$\sigma^2_{\overline{\gamma}} = \ln\left(\frac{V(X)+(E(X)+B_{mcs,x})^2}{(E(X)+B_{mcs,x})^2}\right) \quad (4.62)$$

E(X), and V(X) are given respectively by equations 3.34, 3.35 and 3.36 and $B_{mcs,x}$ is given by:

$$B_{mcs,x} = \beta\left(P_j - \frac{\delta P_j - x - N_{c,i}P_{sig}}{N_{c,i}}\right) \quad (4.63)$$

The user bit rate and the cell throughput are then determined by (3.134) and (3.135).

Dense multipath channel with correlated Rayleigh fading The probability that a TTI is allocated to user i can be written as follows:

$$\begin{aligned} pr(i) &= Prob\Big(\frac{SIR_i}{S_i} > \frac{SIR_j}{S_j} \text{ for j=1..}N_u \text{ and } j \neq i\Big) = \prod_{j\neq i}^{N_u} Prob\Big(SIR_i > \frac{S_i}{S_j} SIR_j\Big) \\ &= \prod_{j\neq i}^{N_u}\Big(1 - \int_0^{+\infty} F_i(\frac{S_i}{S_j} SIR_j) pdf(SIR_j) d(SIR_j)\Big) \end{aligned} \tag{4.64}$$

where pdf(SIR_j) and F_i are respectively given by:

$$\begin{aligned} pdf(\gamma) &= \int_{\overline{\gamma}} pdf(\gamma_{Rake}/\overline{\gamma}) pdf(\overline{\gamma}) d(\overline{\gamma}) \\ &= \int_0^{\infty}\int_0^{\infty} \sum_{l=1}^{N_T} \frac{(\Gamma_l)^{N_T-2}}{\prod_{r\neq l}^{N_T}(\Gamma_l - \Gamma_r)} e^{-\gamma/\Gamma_l} \frac{1}{\sqrt{2\pi}\sigma_{\overline{\gamma}}\overline{\gamma}} e^{-\frac{(\ln\overline{\gamma}-\mu_{\overline{\gamma}})^2}{2\sigma_{\overline{\gamma}}^2}} \frac{1}{\sqrt{2\pi}\sigma_{P_{cs}}} e^{-\frac{(x-E(P_{cs}))^2}{2\sigma_{P_{cs}}^2}} d(\overline{\gamma}) dx \end{aligned} \tag{4.65}$$

$$cdf(\gamma_{Rake}) = F(\gamma) = \int_0^{\infty}\int_0^{\infty} \sum_{l=1}^{N_T} \frac{(\Gamma_l)^{N_T-2}}{\prod_{r\neq l}^{N_T}(\Gamma_l - \Gamma_r)} \Big(1 - e^{-\gamma/\Gamma_l}\Big) \frac{1}{\sqrt{2\pi}\sigma_{\overline{\gamma}}\overline{\gamma}} e^{-\frac{(\ln\overline{\gamma}-\mu_{\overline{\gamma}})^2}{2\sigma_{\overline{\gamma}}^2}} \frac{1}{\sqrt{2\pi}\sigma_{P_{cs}}} e^{-\frac{(x-E(P_{cs}))^2}{2\sigma_{P_{cs}}^2}} d(\overline{\gamma}) d$$

4.3 Simulation and Results

The analytical model is resolved via a Monte Carlo simulation. Moreover, a network level simulation, implemented in NS-2, is conducted to validate the accuracy of the analytical model.

4.3.1 Monte Carlo Simulation

The simulation area is a regular hexagonal cell, of radius equal to 2km, surrounded by 18 other cells. The simulation consists of Monte Carlo simulations allowing determination of $\underbrace{\int\int}_{A} ...\rho dA$ for the key functions in this study according to the distribution of the users in the cell area. The target SIRs used in this chapter for various transmission schemes (for HSDPA services and various CS services) are extracted from [8] and [12]. Let N_{cs} be the number of such CS users on the DPCH channel. The distribution of the mobiles in the cell is supposed to be uniform. For each HSDPA user, N_{cs} CS users

can be chosen. The terms $E(P_{cs})$, and $\sigma^2(P_{cs})$ (given by (4.2) and (4.3)) are computed. This was repeated 1000000 times by changing the HSDPA users location. The user bit rate and cell throughput are then determined using the models described in this chapter.

4.3.2 NS Simulation

The network simulator implements communications between UE and core network applications. It focuses on MAC (Medium Access Control) and RLC (Radio Link Control) protocols implemented according to the 3GPP standard (release 5 for HSDPA and release 99 for CS services). Traffic generation and associated protocols are implemented according to the 3GPP standard [2], [5] and [6]. To include link adaptation in the simulator, an algorithm selects the CQI (Channel Quality Indicator), based on the Eb/No results from the link level simulations and determines the BLER (Bloc Error Rate) at the receiver. Several types of HSDPA terminals can be tested according to the number of CQIs that the mobile can decode.

Concerning CS services, the power control implemented in the simulator is that used in the analytical model (i.e. perfect power control) to conduct a fair comparison between the analytical model and the simulation and verify the accuracy of the analytical model if one accepts the assumptions.

4.3.3 Results

In order to assess the effect of CS users on HSDPA performance, we present in this section the variation of the average HSDPA cell throughput (in kbps) according to the number of CS users N_{cs} (speech, LCD) in the cell. Two cases are considered: only speech services are transmitted on the DPCH channels or multi-services are conveyed on these channels ((70% speech, 10% 32kbps, 10% 64kbps, 10% 128kbps)). The obtained results, depicted in figures 3 to 5, consider the presence of composite multipath/shadowing channel with uncorrelated or correlated Rayleigh (or Nakagami) fast fading. The soft handoff margin (MSH) is assumed to have a value of 3dB (which is the value used in general in the UMTS). Even though the analytical models described in this chapter are developed for Max C/I, RR, FT, PF and SB schedulers, all the results presented in this section assume the use of the PF algorithm since it is the most popular scheduler that achieve a reasonable trade-off between fairness and capacity. The results are close to those obtained by simulation. A deviation between 7 to 9 % are observed between simulation and analytical model. In addition, figures 3 to 5 show that the HSDPA cell throughput decreases more quickly when a mixture of CS connections are active in the cell. This is due to the fact that the power

of a CS user has a stronger influence on the interference and on the capacity of HSDPA than the power of speech users.

In figures 6 and 7, the variation of the average HSDPA cell throughput according to MSH for a given N_{cs} is reported for Rayleigh and Nakagami fading channel. The macro diversity in soft handover reduces the Node B transmitted power requirement for the users [11]. However, the number of users connected to the node B increases [11]. In figure 6, 30 speech users are considered at MSH=0 i.e. when no soft handover is applied; whereas in figure 7 20 CS users (70% speech, 10% 32kbps, 10% 64kbps, 10% 128kbps) are considered at MSH=0. When MSH increases from 1 to 10, the number of users can be calculated as follows : let N_{cs} be the number of CS users at MSH=0 and N'_{cs} the new number of users at MSH. As the power transmitted by all the node Bs is the same and the users distribution in each cell is uniform, the number of users in soft handover in each cell can be considered by symmetry as the same. Hence, N'_{cs} can be simply evaluated using:

$$N'_{cs} = N_{cs} + \frac{prob_{sh} N_{cs}}{2 - prob_{sh}} \tag{4.67}$$

Once the number of users is obtained, the cell throughput of HSDPA is evaluated using the analytical model described in this chapter. In figure 6, the capacity of HSDPA decreases slowly with MSH (the cell throughput decreases of approximately 11%), whereas in figure 7 it decreases more quickly or abruptly (the cell throughput decreases of 42%). When MSH increases from 0 to 10dB, the number of speech users increases from 30 to 39 whereas the number of CS (speech+LCD) in figure 7 increases from 20 to 27. Since LCD (Low Constraint Data) users consume more resources than speech users in terms of power and codes, the cell throughput of HSDPA decreases more quickly in the case of CS users than in the case of speech users.

In addition, figures 8 to 10 depict the Cumulative Distribution Function (CDF) of the bit rate of a user situated at 800m from the node B. 8 HSDPA users and 40 speech users are active in the cell. The soft handoff margin (MSH) is assumed to be equal to 3dB. Compared to the results obtained in the previous chapter, One can remark a HSDPA user bit rate degradation of around 25%. These results are close to those obtained via simulation. A deviation varying from 8 to 10% is observed in these figures.

Using the analytical models proposed in this chapter, more results can be obtained (e.g., CDF of user bit rate of all HSDPA users in the cell for several number of simultaneous active CS (speech or LCD) users in the cell, cell throughput and CDF of user bit rate when the others schedulers are used,...).

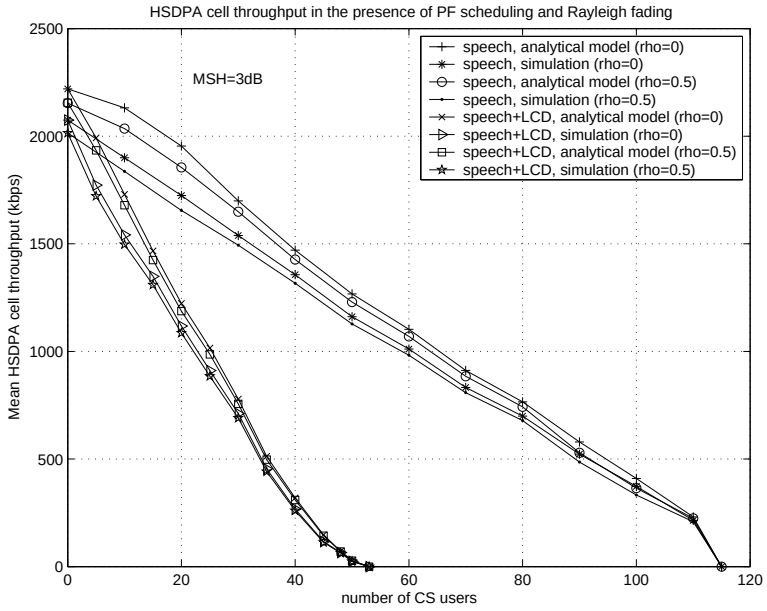

Figure 4.3: Average cell throughput of HSDPA according to the number of speech and LCD (Low Constraint Data) users (70% speech, 10% 32kbps, 10% 64kbps, 10% 128kbps) in the cell in the presence of PF scheduling and Rayleigh fading channel

The results presented in this chapter are only representative results of the possible results that one can obtain using the proposed models.

Finally, it is important to note that all the results depicted in this chapter assume the use of perfect power control on CS services. The use of a real power control (as described in the 3GPP specifications) increases the effect of CS services on HSDPA.

4.3.4 Remark

This study determines the effect of a fixed number of CS service users on the capacity of HSDPA packet data. In the case when a variable number of CS users is used, network providers can still use this fixed number of CS users as the maximum allowable number of CS connections. The provider would reserve a portion of the code tree for these CS services and use the remaining resource in terms of code tree and remaining base station power for the HSDPA packet data. Thereby guaranteeing a minimum capacity for HSDPA services. The number of CS users can still vary as long as the maximum limit is respected. Any unused power or resource would then be used for HSDPA services over the HS-DSCHs.

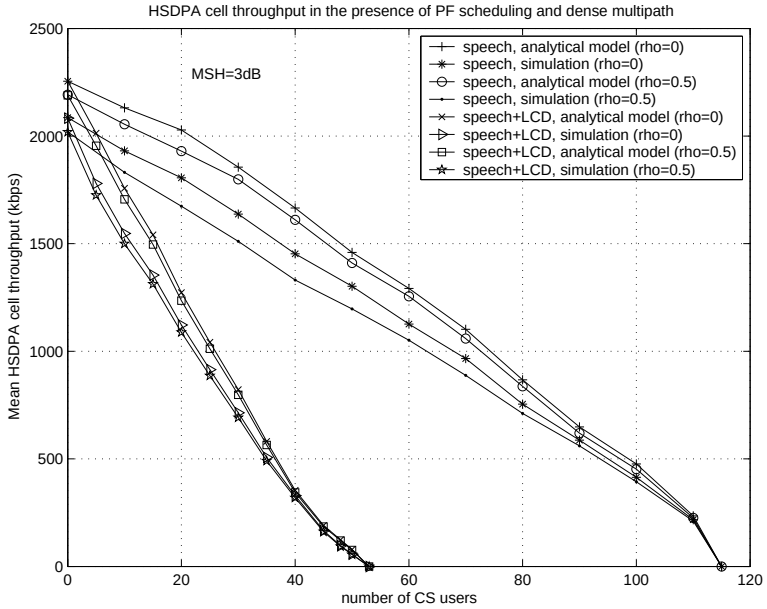

Figure 4.4: Average cell throughput of HSDPA according to the number of speech and LCD (Low Constraint Data) users (70% speech, 10% 32kbps, 10% 64kbps, 10% 128kbps) in the cell in the presence of PF scheduling and dense multipath channel

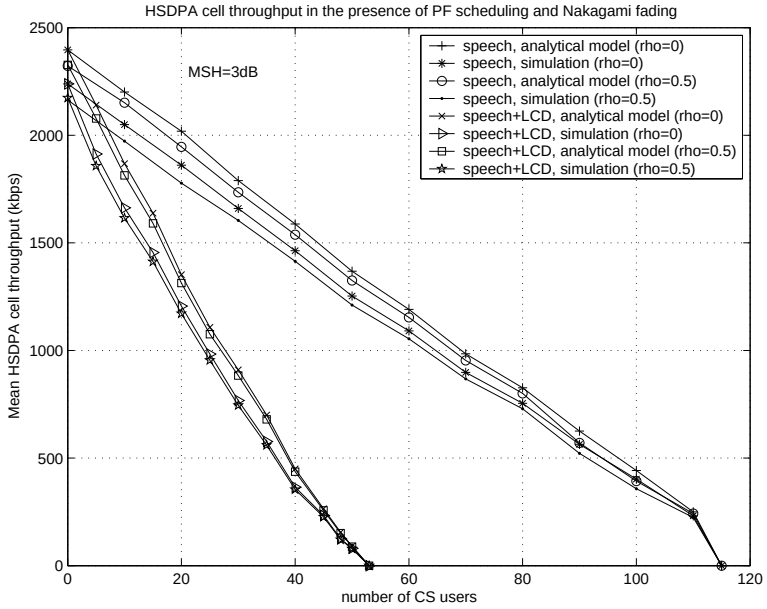

Figure 4.5: Average cell throughput of HSDPA according to the number of speech and LCD (Low Constraint Data) users (70% speech, 10% 32kbps, 10% 64kbps, 10% 128kbps) in the cell in the presence of PF scheduling and Nakagami (m=2) fading channel

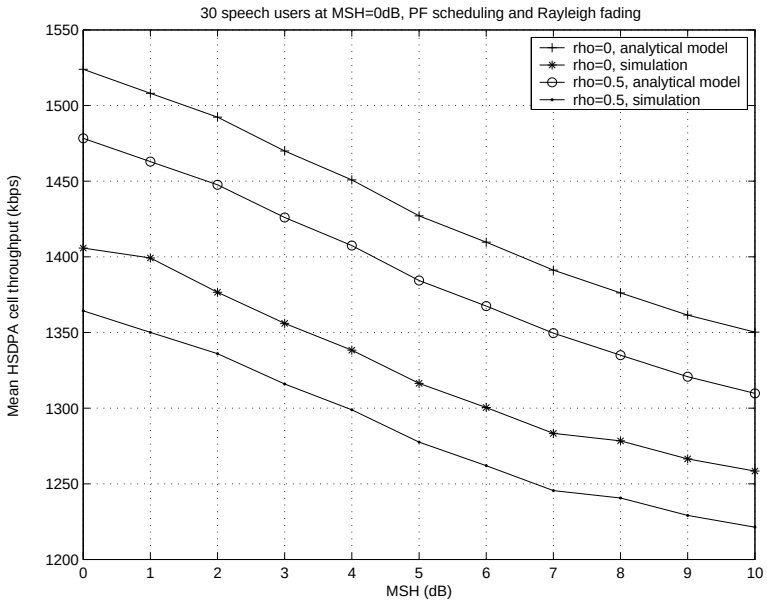

Figure 4.6: Average cell throughput of HSDPA according to the soft handover margin (MSH) of speech users in the cell in the presence of PF scheduling and Rayleigh fading channel

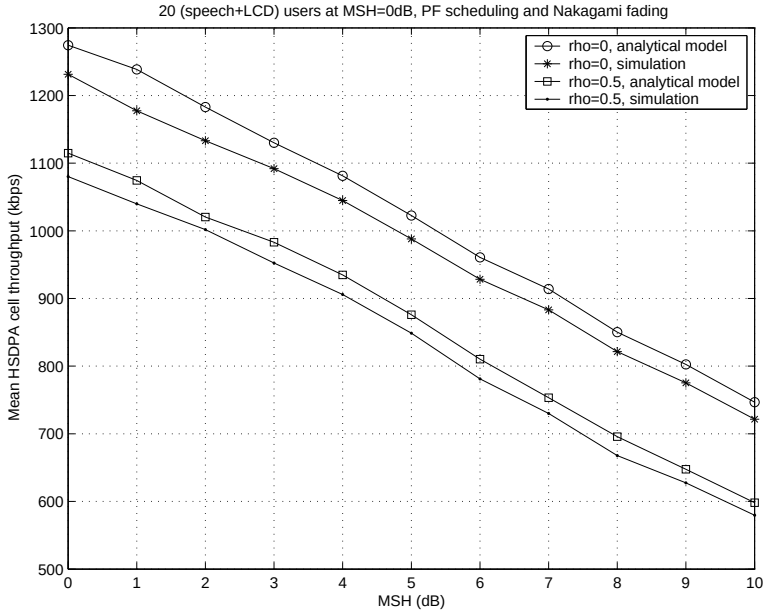

Figure 4.7: Average cell throughput of HSDPA according to the soft handover margin (MSH) of CS (70% speech, 10% 32kbps, 10% 64kbps, 10% 128kbps) users in the cell in the presence of PF scheduling and Nakagami fading channel

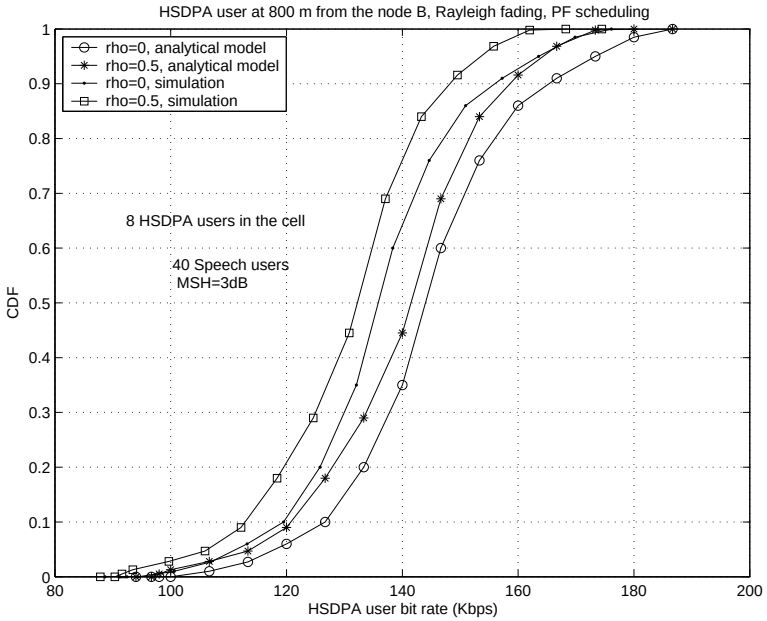

Figure 4.8: CDF of the bit rate of a user situated at 800m from the node B in the case of PF scheduling, Rayleigh fading channel, 40 speech users in the cell and MSH=3dB

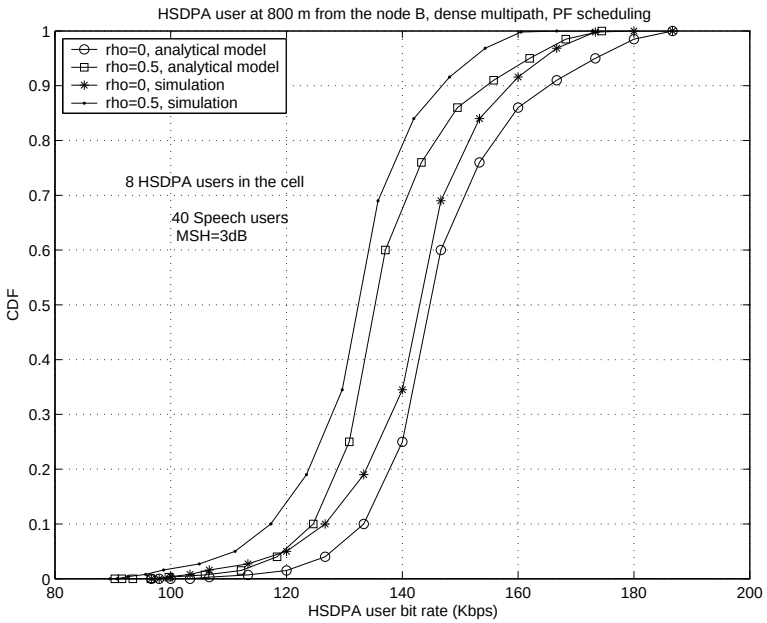

Figure 4.9: CDF of the bit rate of a user situated at 800m from the node B in the case of PF scheduling, dense multipath channel, 40 speech users in the cell and MSH=3dB

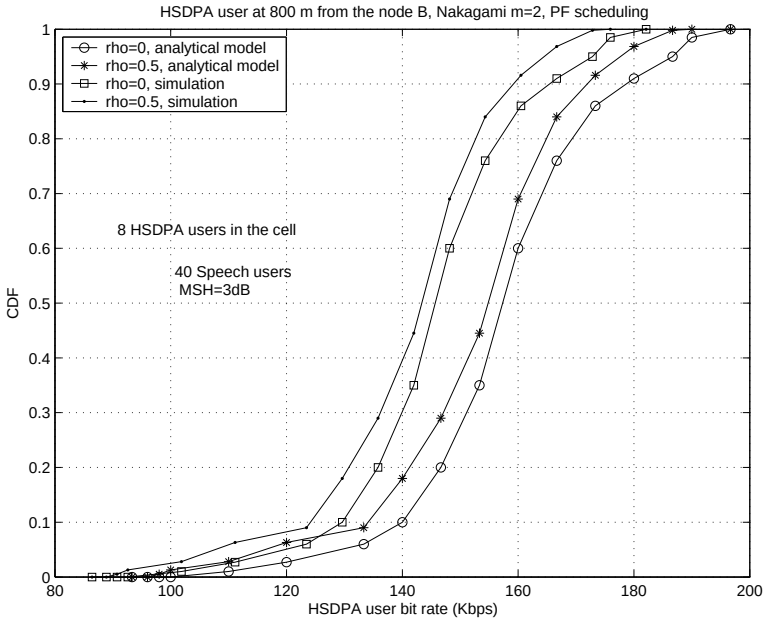

Figure 4.10: CDF of the bit rate of a user situated at 800m from the node B in the case of PF scheduling, Nakagami fading channel, 40 speech users in the cell and MSH=3dB

4.4 Conclusion

The 3GPP specifications allow the use of CS services on DPCH channels in parallel to HSDPA users. The analysis conducted in this chapter allows to assess the effect that CS services have on the capacity of HSDPA. This chapter characterizes analytically the interaction of CS services conveyed on the dedicated DPCH channels of the release 99 on the HSDPA performance. A network level simulation, implemented in NS-2, is used to evaluate the accuracy of the analytical models. HSDPA throughput variations according to the number of CS users and soft handover margins (MSH) are reported. In addition, the CDF of user bit rate in the presence of simultaneous CS users and for various radio fading channel models are depicted. The results of the analytical model are close to those obtained via simulation. A deviation varying from 8 to 10% is observed. Research conducted in this chapter should be pursued by introducing real power control for circuit switched services instead of the assumed perfect power control. In this chapter, the power allocated to HSDPA changes dynamically according to the power allocated to the CS services. The case when a fixed portion of the node B power is allocated to HSDPA independently of the CS power can be investigated. Call Admission Control for both CS and HSDPA users can also be addressed and introduced in the analytical expressions of the CS/HSDPA system performance.

Bibliography

[1] M. Frodigh, S. Parkvall, C. Roobol, P. Johansson, and P. Larsson, "Future-generation wireless networks", IEEE Personal Communications, Volume: 8 Issue: 5 , Oct 2001.

[2] 3GPP TS 25.308 V5.2.0 (2002-03), "HSDPA Overall Description", (Rel. 5).

[3] 3GPP TR 25.848 V4.0.0 (2001-03), "Physical layer aspects of UTRA HSDPA", (Rel. 4).

[4] 3GPP TR 25.858 V5.0.0 (2002-03), "High Speed Downlink Packet Access, Physical layer aspects", (Rel. 5).

[5] 3GPP TR 25.892, "Feasibility Study for OFDM for UTRAN enhancement", (Rel. 6).

[6] Harri Holma and Antti Toskala, "WCDMA for UMTS. Radio Access for Third Generation Mobile Communications", Second Edition, John Wiley and Sons, England, 2002.

[7] M. Assaad and D. Zeghlache, "On the Capacity of HSDPA System", proceedings to Globecom Dec 2003.

[8] 3GPP TR 25.942 V4.0.0 (2001-09), "RF System Scenarios", (Rel. 4).

[9] W. Ladermann and E. Lloyd, "Handbook of Applicable Mathematics-Probability", Volume II, John Wiley and Sons, 1980.

[10] A.J. Viterbi, A.M. Viterbi, K.S. Gilhousen, and E. Zehavi, "Soft handoff extends CDMA cell coverage and increases reverse link capacity", Selected Areas in Communications, IEEE Journal on , Volume: 12 Issue: 8 , Oct 1994.

[11] C. Lee and R. Steele, "Effect of Soft and Softer Handoffs on CDMA System Capacity", IEEE Transactions on Vehicular Technology, Aug. 1998, pp. 830-841.

[12] Finalising TFRC reference list and uplink signalling definition, 3GPP input paper TSGR1 24(02) 2002.

Chapter 5

Interaction of HSDPA with Transport Control Protocol (TCP)

Third generation and beyond Cellular systems such as UMTS and enhancements like HSDPA are conceived to offer users, in addition to speech, new multimedia services with high quality image and video and with access to private and public data networks such as the Internet. Since services built over a TCP/IP are expected to make a large share of the overall traffic volume, particular attention must be paid to the performance of TCP traffic over HSDPA.

The main source of packet loss in wireless systems are the link errors generated by unperfect transmission adaptation to the short term channel variations. Static or fixed link protection techniques (such as channel coding, interleaving, etc.) are not effective in providing link protection and in correcting all errors experienced over the radio link. The use of ARQ to retransmit erroneous packets is mandatory to achieve error free radio transmission. Introducing ARQ incurs however additional delays in packet delivery due to retransmissions. These delays conflict with TCP control mechanisms that interpret delays in packet delivery over the wireless link as congestion in the fixed and Internet segments. Useless retransmissions are experienced and much time is wasted during the slow start and the congestion avoidance phases.

TCP Over wireless networks (especially TCP/ARQ) has been studied widely in the literature when a dedicated channel is allocated to each user. When a shared channel is used on the radio interface, particular attention should be paid to the interactions between TCP, ARQ and the scheduler and not only between TCP and ARQ. The performance of TCP in this case changes and we show in this chapter that the effect of TCP on wireless networks can be reduced according to the scheduler used.

Ideally, changes to TCP should also be avoided since it has already been widely deployed over the past decades. TCP Reno is the most implemented version and is extensively used by Internet applications and services. Section 5.1, providing the state of the art on wireless TCP, shed some light already on expected interactions between radio link control and TCP. Most approaches either mask adaptation in the radio link to TCP or modify TCP to reduce interactions.

This chapter explores the possibility of relying exclusively on scheduling to reduce the interactions for the UMTS HSDPA system.

As indicated previously, interaction between RLC (MAC-hs) and the TCP protocol must be analyzed to evaluate the actual performance improvements achievable by HSDPA.

A comprehensive study of the effect of TCP on both achieved application bit rate performance and system capacity is provided. A simplified analytical model to evaluate the end to end TCP performance is derived. Network simulation results used to extract the TCP performance in HSDPA are also presented. Even though, the PF scheduler represent an acceptable compromise between fairness and capacity, it shows inefficiency and instability at the TCP layer which results in TCP performance degradation. More efficient schedulers are then required to reduce the interaction of TCP with the MAC-hs layer and improve the user throughput and system performance. Consequently, at the end of this chapter, a new scheduler is proposed to reduce the interaction of TCP with wireless link and thereby improve the performance of TCP over UMTS-HSDPA system.

5.1 Related Work

TCP (Transmission Control Protocol) is the most widely used transport protocol for packet data services in wireless networks. TCP was initially designed for wired networks where packet losses and delays are mainly caused by congestion [1]. TCP includes a drastic recovery mechanism that reacts to congestion situations with abrupt throughput reductions. It then takes a long time to reach again its normal operating level.

Over wireless networks, TCP misinterprets delays, caused by ARQ, as congestion indications. Useless retransmissions are experienced and much time is wasted during the slow start and the congestion avoidance phases. To alleviate these problems over wireless links, several approaches have been proposed for TCP enhancement [1-7]. Some solutions introduce changes in the TCP paradigm while others deal with popular TCP versions (Reno and its variants). Eifel and Westwood TCP try to improve the classic TCP behavior to keep it applicable over both wireless and wired networks [8]. TCP SACK (selective

acknowledgments) [9] is proposed to alleviate TCP's inefficiency in handling multiple drops in a single data window. However, TCP SACK does not improve the performance when the sender window size is not sufficiently large [9-11]. TCP FACK (forward acknowledgment) makes more intelligent decisions about the data that should be retransmitted. However, it is more or less targeted towards improving TCP's performance when losses are due to congestion rather than random losses [12]. In Split TCP [13], the end-to-end path is divided into two segments (typically one wireless segment and one wired segment) on which different connections are established and locally optimized. Split TCP violates TCP semantics [12] and is incompatible with security requirements. The use of VPNs and IPSec make impossible for a third party to interpret packet headers or to cut TCP connections. Moreover, with Split TCP, handoffs may take several hundreds of milliseconds to be completed, thus leading to degraded TCP performance [14][15]. In [16] and [17], a snoop agent is introduced at the link layer. The agent monitors the TCP connection, suppresses the duplicate acknowledgments, and retransmits the lost segments. The main advantage is the suppression of the duplicate acknowledgments for lost TCP segments that are locally retransmitted. However, the snoop agent must be located right before the TCP receiver. Thus, when a mobile node has to transmit data to a remote receiver, TCP acknowledgments are returned too late for an efficient recovery of the lost segments.

In [18-27], Automatic Repeat Request (ARQ) and Forward Error Correction (FEC) schemes are used at the link layer and TCP Reno (and its variants) are used at the Transport layer. References [16-21,28,29] consider the 3G system (UMTS) in all its aspects and try to evaluate the effect of the overall system parameters and layers (e.g., MAC, RLC,...) on the TCP throughput degradation. For example, the effect of the TCP slow start (initial congestion window size) on the TCP performance over a Dedicated Channel (DCH) in UMTS can be found in [28]. The effect of RLC buffer size, RLC MaxDAT (which is the maximal number of RLC packet retransmissions), receiver buffer size, congestion rate, Round Trip Time (RTT) in the Internet, RLC transmission window and the CDMA code tree utilization (i.e. the percentage of code tree allocated to TCP services, in other words the fraction of cell capacity assigned to TCP services) on the TCP throughput in UMTS system are provided in [16-19,28,29]. When a shared channel (HSDPA) is used on the radio interface, the interactions are not the same and fewer studies are available in the literature [28-31]. Recently, researchers started investigating the impact of the variable delay introduced by the schedulers in HSDPA on the TCP system performance. References [30-31] propose an interesting approach that improves the long-lived TCP performance while reducing at the same time the latency of short TCP flows. These methods

achieve better wireless channel utilization by using simultaneously two algorithms: a network based solution called Window Regulator and a Proportional Fair scheduler with Rate Priority (PF-RP). The Window Regulator algorithm "*uses the receiver window field in the acknowledgment packets to convey the instantaneous wireless channel conditions to the TCP source and an ack buffer to absorb the channel variations*" as stated in [30]. This approach is found to increase TCP performance for any given buffer size. The PF-RP scheduler part of the proposal, based on the simultaneous use of two schedulers PF and PF with Strict Priority (PF-SP), tries to differentiate short flows from long flows by assigning different priorities to the flows. This scheduler achieves a trade-off between fairness among users and system throughput maximization and minimizes also short flow latency. Results in [30, 31] indicate that combining the Window Regulator and the PF-RP scheduler "*improves the performance of TCP Sack by up to 100% over a simple drop-tail algorithm for small buffer sizes at the congested router*". In addition, the effect of TCP on HSDPA has been studied by [28] and [29] through simulation only.

These studies on the impact of variable delays, caused by schedulers over time shared channels using ARQ for reliable transmission, on TCP performance appear as a promising approach to effectively reduce the TCP throughput degradation in wireless systems. This motivates the modeling and the study in this chapter.

5.2 Modeling of TCP over UMTS/HSDPA

In this section, we present a simple model to evaluate the performance of TCP over HSDPA. This model is an extension of the packet loss model proposed in [32, 33, 34].

The data rate at the TCP layer is computed by dividing the data size by the mean value of latency time E(T) (a markov process is assumed). The mean latency time E(T)is composed of: T_{ss} the latency time of the slow start phase, T_{loss} corresponding to the recovery time and RTO cost and T_{ca} representing the latency time of the steady state phase. Hence, the data rate is given by:

$$R = \frac{data}{E(T_{ss}) + E(T_{loss}) + E(T_{ca})} \tag{5.1}$$

Consequently, modeling the effect of TCP on HSDPA, requires estimates of the latency time of the slow start phase, the loss recovery, and the steady state phase (this is conducted respectively in sections 5.2.2, 5.2.3, and 5.2.4). The analysis of TCP timeouts needed in the latency times is presented in section 5.2.1.

5.2.1 Timeout

There are two ways that TCP detects losses: retransmission timeouts (RTOs) and triple duplicate ACKs. The retransmission timeouts (RTOs) of TCP can be caused by a congestion in the Internet Network or by a delay due to limited bit rate or to multiple retransmissions on the radio interface generated by the Automatic Repeat Request (ARQ) technique which increase Round Trip Time (RTT) and RTOs of TCP. In this section, the probability of RTOs due to the effect of the radio interface is derived.

Proposition

The probability of RTO due to the radio interface is given by the following equation:

$$q = Q\left(\frac{To - RTT_{wired} - \frac{1+P_e-P_eP_s}{1-P_eP_s}T_j}{\sqrt{\sum_m k_m \frac{W}{SF}\frac{(N\log 2(M)\tau)_{m,i}}{12000}TTI}\frac{\sqrt{P_e(1-P_e+P_eP_s)}T_j}{1-P_eP_s}}\right) \tag{5.2}$$

where To is the average duration of the first timeout in a section of one or more successive timeouts, RTT_{wired} is the average round trip time of the wired part of the network, P_e is the Probability of errors after decoding the information block via FEC and P_s is the probability of errors after soft combining two successive transmissions of the same information block. K_m is the probability of selection of a Modulation and Coding Scheme (MCS) m. Note that a MCS is the combination of a modulation order M, a channel coding rate τ and a number of parallel HS-DSCH channel codes N. TTI is the Transmit Time Interval (=2ms), SF is the spreading factor (SF=16) and W is the CDMA chip rate (3.84Mchips/sec). Parameter T_j is the transmission time of a segment on the radio interface. This transmission time depends upon the scheduler used in the MAC-hs entity to share the HS-DSCH channel among users. The analysis conducted in this section supposes that a basic fair throughput scheduler is implemented in the system. Introduction of better schedulers can only enhance performance.

Proof

In HSDPA, each TCP segment is transmitted using several predefined Transmission Time Intervals (TTIs), each lasting 2ms. The size of a TCP segment is 1500 octets. Transmitting a TCP segment requires between 12 and 60 TTIs (depending upon the modulation and coding schemes used on the radio interface). Let S_i be the data size transmitted over each TTI. The number of retransmission required to deliver the data of size S_i is a random variable due to varying radio channel conditions. The time

needed to transmit an error free TCP segment is:

$$RTT = \frac{\sum_{i=1}^{n_s} N_{TTI}(i)}{n_s} T_j + RTT_{wired} \tag{5.3}$$

Variable n_s is the number of TTIs needed to transmit a TCP segment when no errors occur on the radio interface and $N_{TTI}(i)$ is the number of transmissions of TTI i due to HARQ. The use of scheduling on a shared channel makes the errors on each TTI independent (the successive TTIs are allocated to various users). The number of retransmission of each TTI data is independent from the other TTIs. Using the central limit theorem, the sum of a large number of independent and identically distributed (iid) symmetric random variables can be considered as a gaussian variable. Hence, the number of transmissions of a TCP segment $N_i = \frac{\sum_{i=1}^{n_s} N_{TTI}(i)}{n_s}$ can be modeled by a gaussian variable. Consequently, the time needed to transmit a TCP segment (RTT) is a gaussian variable. The probability of timeout RTO expressed as prob(RTT=gaussian>To) with the gaussian assumption leads to: $Q(\frac{To-E(RTT)}{\sigma(RTT)})$. By evaluating and replacing $E(N_i)$ and $\sigma(N_i)$ by their values, E(RTT) and $\sigma(RTT)$ are obtained and the probability of RTO has the form provided previously in (5.2).

5.2.2 Slow Start

The TCP connection begins in slow start mode where it quickly increases its congestion window, to achieve best effort service, until it detects a packet loss. In the slow start phase, the window size cwnd is limited by a maximum value W_{max} imposed by the sender or receiver buffer limitations. To determine $E(T_{ss})$, the number of data segments $E(d_{ss})$, the sender is expected to send before losing a segment, is needed. From this number, one can deduce $E(W_{ss})$, the window one would expect TCP to achieve at the end of the slow start, where there is no maximum window constraint. If $E(W_{ss}) \leq W_{max}$, then the window limitation has no effect, and $E(T_{ss})$ is simply the time for a sender to send $E(d_{ss})$ in the exponential growth mode of the slow start. On the other hand, if $E(W_{ss}) > W_{max}$ then $E(T_{ss})$ is the time for a sender to slow start up to $cwnd = W_{max}$ and then send the remaining data segments at a rate of W_{max} segments per round.

Let e be the probability of retransmission (congestion+RTO). Probability e can be evaluated using the following equation:

$$e = p + q - pq \tag{5.4}$$

The term $E(d_{ss})$ can be calculated using the following expression:

$$\begin{aligned} E(d_{ss}) &= \left(\sum_{k=0}^{d-1}(1-e)^k e.k\right) + (1-e)^d.d \\ &= \frac{(1-(1-e)^d)(1-e)}{e} \end{aligned} \tag{5.5}$$

where d is the number of segments in the file. Using the same demonstration as in [34], the mean value of the latency time can be evaluated as follows:

$$E(T_{ss}) = \begin{cases} RTT\left[log_\gamma(\frac{W_{max}}{W_1} + 1 + \frac{1}{W_{max}}(E(d_{ss}) - \frac{\gamma W_{max} - W_1}{\gamma - 1})\right] & \text{When } E(W_{ss}) > W_{max} \\ RTT.log_\gamma(\frac{E(d_{ss})(\gamma-1)}{W_1} + 1) & \text{When } E(W_{ss}) \leq W_{max} \end{cases} \tag{5.6}$$

γ is the rate of exponential growth of the window size during the slow start. $E(W_{ss})$ is given by:

$$E(W_{ss}) = \frac{E(d_{ss})(\gamma - 1)}{\gamma} + \frac{W_1}{\gamma} \tag{5.7}$$

5.2.3 Recovery time of the first loss

The slow start phase in TCP ends with the detection of a packet loss. The sender detects a loss in two ways : negative ack (triple duplicate) or retransmission timeouts (RTO). The RTO could be caused by a congestion in the wired network or by the retransmissions on the radio interface. After an RTO, the window size decreases to 1, however the loss detected by the triple duplicate acks decreases the window size to a half. In this section, we evaluate the recovery time of this first loss. The probability of loss in a file of d TCP segments is:

$$loss = 1 - (1-e)^d \tag{5.8}$$

The loss between segments could be considered independent [32, 33]. Let $Q'(e, w)$ be the probability that if a loss occurs it is a RTO. This probability can be evaluated as follows: Let *cong* and *wirel* be respectively the probabilities that there is a congestion loss in the transmission of the file and there is a RTO due to radio interface conditions.

$$cong = 1 - (1-p)^d \tag{5.9}$$

$$Wirel = 1 - (1-q)^d \tag{5.10}$$

Where q is evaluated in section 7.4.1 by (5.2). References [32, 33] derive the probability that a sender in congestion avoidance will detect a packet loss with an RTO, as a function of congestion rate p and window size w. This probability is denoted by F(p,W):

$$F(p,W) = min\left(1, \frac{(1+(1-p)^3(1-(1-p)^{w-3}))}{(1-(1-p)^w)/(1-(1-p)^3)}\right) \tag{5.11}$$

The probability of RTO is simply obtained through:

$$RTO = cong.F(p,W) + Wirel - Wirel.cong.F(p,W) \tag{5.12}$$

Hence, the probability $Q'(e,w)$ is derived as:

$$\begin{aligned} Q'(e,w) &= \frac{RTO}{loss} \\ &= \frac{cong.F(p,W) + Wirel - Wirel.cong.F(p,W)}{1-(1-e)^d} \end{aligned} \tag{5.13}$$

The probability of loss via triple duplicate is $loss(1 - Q'(e,w))$. It is assumed that fast recovery for a triple duplicate takes one RTT [34]. However, it takes more time for an RTO. The RTO cost, derived in [32, 33], does not take into account the radio interface effects. Using the mean expected cost of an RTO

$$E(z^{TO}) = \frac{1+e+2e^2+4e^3+8e^4+16e^5+32e^6}{1-e}To \tag{5.14}$$

and combining these results, the mean recovery time at the end of the initial slow start is obtained:

$$E(T_{loss}) = loss\Big(Q'(e,w)E(z^{TO}) + (1-Q'(e,w))RTT\Big) \tag{5.15}$$

5.2.4 Steady State phase

The time needed to transfer the remaining data can be derived in the same way as in [34]. Indeed, the amount of data left after the slow start and any following loss recovery is approximately:

$$E(d_{ca}) = d - E(d_{ss}) \tag{5.16}$$

This amount of data is transferred with a throughput $R(e, RTT, To, W_{max})$. The latency time is then given by:

$$E(T_{ca}) = \frac{E(d_{ca})}{R(e, RTT, To, W_{max})} \tag{5.17}$$

In [32, 33], the throughput $R(p, RTT, To, W_{max})$ is evaluated without the radio interface effects. By using the same demonstration as in [32, 33] and by introducing e, RTT and $Q'(e, w)$ provided in this section, the derivation of the throughput expression leads to the following equation:

$$R(e, RTT, To, W_{max}) = \begin{cases} \frac{\frac{1-e}{e} + \frac{W(e)}{2} + Q'(e,W(e))}{RTT(\frac{b}{2}W(e)+1) + \frac{Q'(e,W(e))G(e)To}{1-e}} & \text{When } W(e) < W_{max} \\ \frac{\frac{1-e}{e} + \frac{W_{max}}{2} + Q'(e,W_{max})}{RTT(\frac{b}{8}W_{max}+2+\frac{1-e}{eW_{max}}) + \frac{Q'(e,W_{max})G(e)To}{1-e}} & \text{When } W(e) \geq W_{max} \end{cases} \tag{5.18}$$

where b is the number of TCP segments acknowledged by one ACK and $W(e)$ is given by:

$$W(e) = \frac{2+b}{3b} + \sqrt{\frac{8(1-e)}{3be} + \left(\frac{2+b}{3b}\right)^2} \tag{5.19}$$

Finally, once the total latency time is calculated, the bit rate for each service, at TCP layer can be evaluated using equation (5.1).

5.3 Simulation and Results

The derived analytical expressions of the TCP bit rate and the HSDPA cell throughput are resolved via a Monte Carlo simulation. The simulated area is a regular hexagonal cell surrounded by 18 cells with a radius of 2km (macro cell). The distribution of mobiles in the cell is uniform.

In addition, a network simulation is also conducted to assess the accuracy of the proposed analytical model.

5.3.1 NS-2 Simulation

The simulated area is a regular hexagonal cell surrounded by 18 cells with a radius of 2km (macro cell). The distribution of mobiles in the cell is uniform. The target SIRs for the modulation and coding schemes are taken from [35] for a BLER of 10%. Mobile positions are changed independently of each other to obtain the average value of the throughput.

Concerning the NS-2 simulation, the same simulator described in the previous chapter is used. FTP/TCP services are generated for the all users. In the wired network, a congestion rate varying from

0 to 9% is introduced. At the TCP level, the initial congestion window size is equal to 6kbytes (since the increase of initial window size results in an increase of system performance). The TCP segment size is assumed to have a value of 1.5kbytes and the maximal congestion window size of 18kbytes.

5.3.2 Results

The analysis conducted in this chapter can be used to characterize the interaction between TCP and HSDPA MAC-hs layer and thereby to determine the performance of RR, FT, Max C/I, PF or SB schedulers at the TCP layer. Since the PF scheduler represents an acceptable trade-off between fairness and capacity (compared to the others algorithms cited above), we present in this chapter the results corresponding to this scheduler only. One can use the proposed model to evaluate the performance of the other schedulers. In order to assess the effect of TCP on the performance of the PF scheduler, figures 1 and 2 show respectively the CDF of user bit rate at the TCP level for users situated respectively at 200 and 800m from the node B. The TCP congestion rate is assumed to be at 3% (which is an acceptable mean value [1-27]). The radio channel is assumed to be a composite multipath/shadowing channel with amplitude following a Rayleigh distribution. One can use the same models, described in this chapter and chapter 3, to determine the TCP performance in the cases of dense multipath or Nakagami fading channel. The objective of this chapter is to show that the PF scheduler is not the optimal solution for non real time data services and that it can be improved as we show in the next section. Compared to the results obtained in chapter 3 with the same radio conditions, figures 1 and 2 show that the TCP interaction with the MAC-hs layer results in a loss of 24% of the user bit rate for the user at 800m and a loss of 15% for the user at 200m. This results in more loss of fairness of the PF scheduler and loss of efficiency of the system. Besides, results obtained by simulation assess the accuracy of those obtained by the analytical model. Even though the deviation between the results of analytical model and simulation is around 10%, the loss of system efficiency is proved by simulation. A loss of user bit rate respectively of 26% for the user at 800m and 14% for the user at 200m are obtained via simulation.

In addition to these results, figure 3 depicts the overall cell throughput according to the TCP congestion rates. The results show that the cell throughput decreases of about 20.5% when p increases from 0 to 3%. These results show the need of more efficient schedulers suitable for TCP protocol and capable to improve the user bit rate and the system performance.

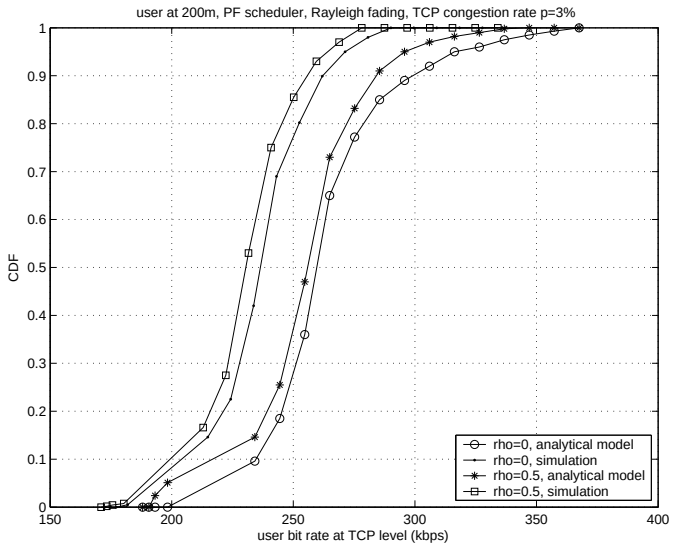

Figure 5.1: CDF of user bit rate at the TCP level for user at 200m when the proportional fair scheduler is used, in the presence of Rayleigh fading channel with rho=0, 0.5

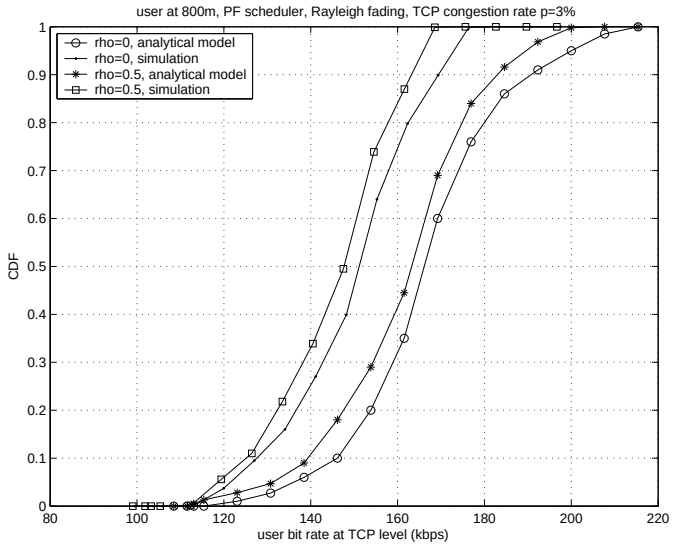

Figure 5.2: CDF of user bit rate at the TCP level for user at 800m when the proportional fair scheduler is used, in the presence of Rayleigh fading channel with rho=0, 0.5

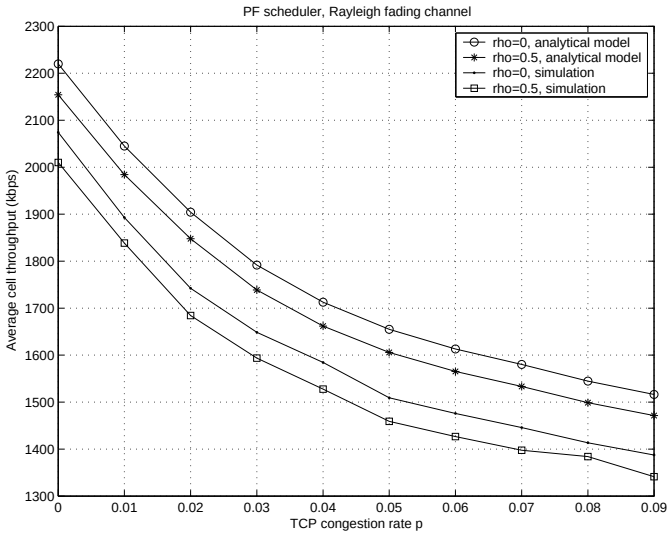

Figure 5.3: HSDPA cell throughput at the TCP level when the proportional fair scheduler is used

5.3.3 Discussions and Proposals to improve the TCP performance

Proposal 1

The results shown in the figures 1, 2 and 3 lead us to propose a method to achieve a higher flow bit rates and reduce the degradation in TCP flow rates induced by the radio interface. The schedulers used in HSDPA must therefore be adapted to take into consideration the interaction with TCP in order to improve the TCP bit rate.

In fact, the reason of user throughput degradation at the TCP level is the delay variation of receiving packets at the TCP level. The existing schedulers used in HSDPA do not consider to presence of the TCP protocol at the transport layer. Users at the cell border (e.g., 800m) have lower bit rates than users near the node B which results in more delays of receiving TCP packets for these users (i.e. at the cell border). This generates more TCP timeouts and results thereby in more user throughput degradation. One of the possible solution to reduce this interaction and throughput degradation is to consider the achieved bit rate at the TCP level in the scheduler. For example, when a Proportional Fair scheduler is used, the scheduler allocates the channel to the user which has max(r/S) where S in this case is the mean TCP bit rate instead of the mean radio interface bit rate. This solution needs more signalling between layers at the mobile user.

By changing the PF scheduler as above, we use the NS2 simulation to evaluate the performance of this scheduler at the TCP level. Figures 4 to 6 depict respectively the CDF of TCP user bit rate for users at 200 and 800m and the variation of the average cell throughput according to the TCP congestion

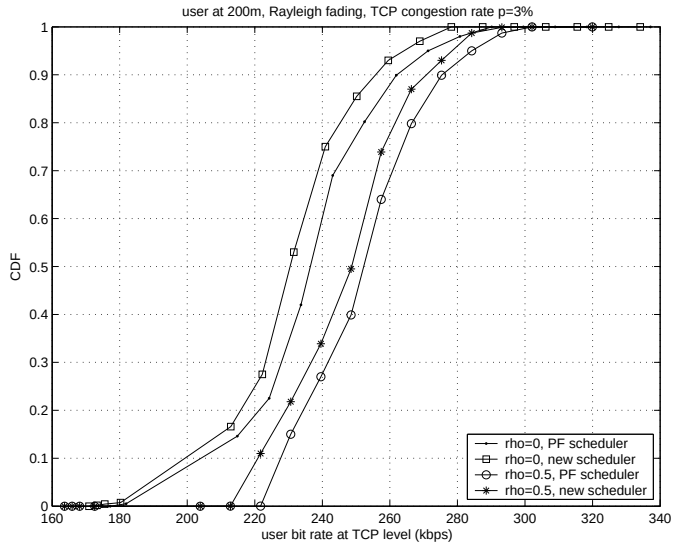

Figure 5.4: CDF of user bit rate at the TCP level for user at 200m when the proportional fair and modified proportional fair are used, in the presence of Rayleigh fading channel with rho=0, 0.5

rate. Compared to PF, these results show an improvement of user bit rate respectively of 9% for user at 800m and 4% for user at 200m at a congestion rate of 3%. The cell throughput is also improved of approximately 7.5%. The number of TCP segment retransmissions due to unnecessary TCP timeouts are reduced with the modification introduced to the PF scheduler.

Proposal 2

The previous method requires cross layer signalling between TCP and MAC layers. This results in more complexity in the system. In this section, we propose a new scheduler that provides similar TCP performance than with the previous method without requiring any signalling between TCP and MAC layers. This scheduler consists of allocating the HS-DSCH channel to the users according to the following priority:

$$max\{-log(\delta)\frac{r}{\overline{CQI}}\left(1-\frac{R}{\sum_{j=1}^{N_u}R_j}\right)\} \tag{5.20}$$

where R is the achieved bit rate. The advantage of this algorithm is that it allocates the channel to the user having a compromise between the actual channel conditions (represented by the bit rater), the mean statistical channel conditions ($\overline{CQI}$) and the achieved bit rate. In chapter 6, this scheduler is generalized to allow the transmission of streaming services over HSDPA without losing much cell capacity.

Using the NS2 simulation, we evaluate the performance of this scheduler at the TCP level. Figures 7 to 9 depict respectively the CDF of TCP user bit rate for users at 200 and 800m and the variation

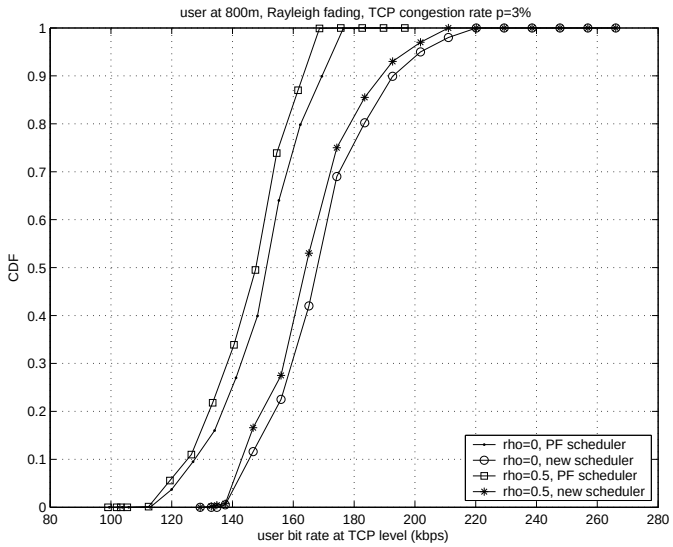

Figure 5.5: CDF of user bit rate at the TCP level for user at 800m when the proportional fair and modified proportional fair are used, in the presence of Rayleigh fading channel with rho=0, 0.5

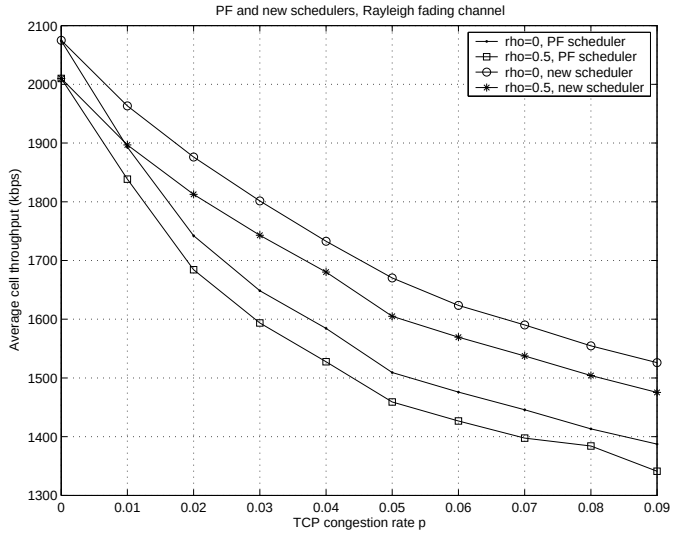

Figure 5.6: Improvement of the HSDPA cell throughput at the TCP level when the modified proportional fair scheduler is used

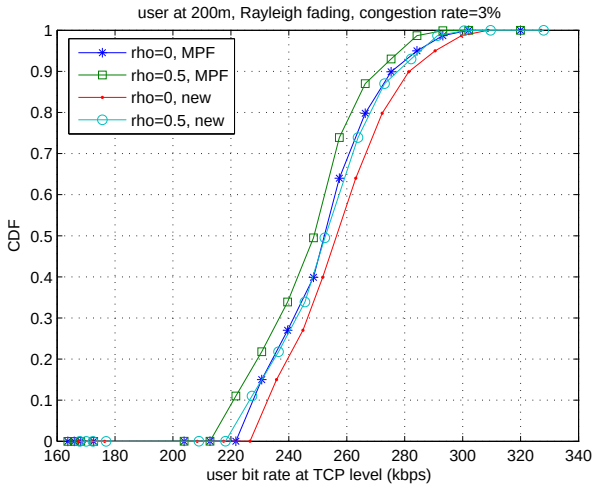

Figure 5.7: CDF of user bit rate at the TCP level for user at 200m when the modified proportional fair and the new scheduler are used, in the presence of Rayleigh fading channel with rho=0, 0.5

of the average cell throughput according to the TCP congestion rate. These figures show that this new scheduler provides TCP performances similar to those obtained using the previous method (modified proportional fair). A deviation of 1.5 to 2.5% is observed between the performances of these two schedulers.

Consequently, this new scheduler is simpler and more practical to be implemented in HSDPA than the modified PF since it does not require any signalling between TCP and MAC-hs layers.

5.4 Conclusion

This chapter proposes analytical models to determine the effect of TCP on the UMTS-HSDPA system performance. Cell capacity and user bit rate are evaluated analytically by combining the analytical model proposed in this chapter to the analysis conducted in the chapter 3. Even though the proposed model can be applied in the cases of RR, FT, Max C/I, PF and SB schedulers, we are focusing in this chapter on the PF scheduler since it represents an acceptable trade-off between fairness and cell capacity (compared tot the other schedulers). Network simulation is also conducted to assess the accuracy of the analytical model. Additional insight on the HSDPA system behavior and interactions with TCP is provided. The effect of TCP on application performance results in a loss of efficiency and fairness of the proportional fair scheduler. A loss of user bit rate of 24% and 15% respectively for the user at 800 and 200m at a TCP congestion rate of 3%. The overall cell throughput presents a loss of 20.5% at a congestion rate of 3%. Analyzing the results, a new scheduler is proposed at the end of this chapter.

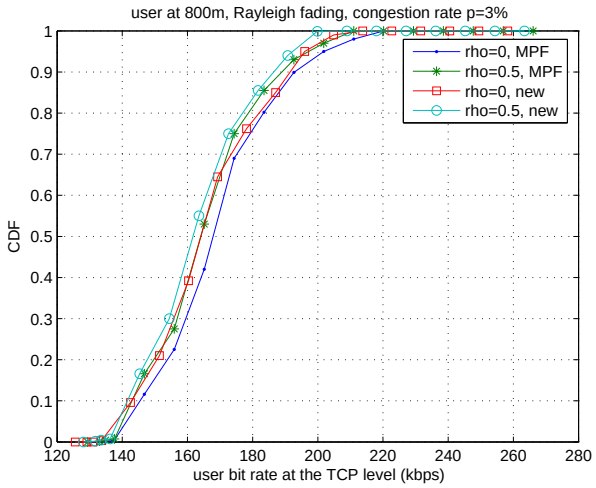

Figure 5.8: CDF of user bit rate at the TCP level for user at 800m when the modified proportional fair and the new scheduler are used, in the presence of Rayleigh fading channel with rho=0, 0.5

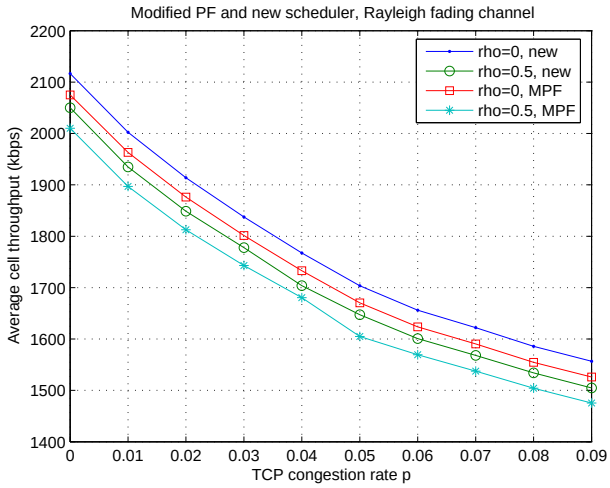

Figure 5.9: HSDPA cell throughput at the TCP level when the modified proportional fair and the new scheduler are used

This scheduler allows to mask as much as possible the radio impairments and reduce the unnecessary TCP timeouts resulting thus in reducing the TCP throughput degradation. Results afforded by this scheduler indicate a loss in cell capacity not exceeding 10% for a TCP congestion rate of 3% and a loss of user bit rate lower than 16% for a user at 800m and 9% for a user at 200m for a congestion rate of 3%. Finally, the results obtained in this chapter shows that in HSDPA it is possible to reduce the effect of TCP in a Wireless system, by using the shared channel with an appropriate scheduler.

Bibliography

[1] M. Allman et al., "TCP congestion control", RFC 2581, April 1999.

[2] S. Floyd and T. Henderson, "The NewReno Modification to TCP's Fast Recovery Algorithm", RFC 2582, April 1999.

[3] A. Gurtov, "Making TCP Robust Against delay Spikes", University of Helsinki, Department of Computer Science, Series of publications C, C-2001-53, Nov 2001. ¡http://www.cs.helsinki.fi/u/gurtov/papers/report01.html¿

[4] H. Balakrishnan et al., "TCP Performance Implications of Network Asymmetry", RFC 3449, Dec. 2002.

[5] M. Allman and V. Paxson, "On estimating end to end Network Path Properties", ACM SIGCOMM 99, Sep. 1999.

[6] A. Gurtov and R. Ludwig, "Responding to Spurious Timeouts in TCP", IEEE INFOCOM'03, March 2003.

[7] R. Ludwig and R.H. Katz, "The Eifel Algorithm: Making TCP Robust Against Spurious Retransmissions", ACM Computer Communication Review 30(1), Jan. 2000.

[8] M. Mathis, J. Mahdavi, S. Floyd, and A. Romanow, TCP Selective Acknowledgment Options. RFC 2018, April 1996.

[9] M. Allman, S. Floyd and C. Partridge, "Increasing TCPs Initial Window", RFC 3390, Oct 2002.

[10] K. Pentikousis, A survey of TCP in wired-cum-wireless environments

[11] H. Balakrishnan, V. Padmanabhan, S. Seshan, M. Stemm, and R. H. Katz, "TCP behavior of a busy Internet server: Analysis and improvements", in Proceedings of IEEE INFOCOM, pages 252–262, March 1998.

[12] M. Mathis and J. Mahdavi. "Forward acknowledgement: Refining TCP congestion control", in Proceedings of the ACM SIGCOMM, August 1996.

[13] A. Bakre, B. R. Badrinath, I-TCP: indirect TCP for mobile hosts, Proceedings - International Conference on Distributed Computing Systems, Vancouver, Canada, pp. 136-146, 1995.

[14] R. Cceres and L. Iftode, "Improving the Performance of Reliable Transport Protocols in Mobile Computing Environments", in IEEE Journal on Selected Areas in Communications, Vol. 13, No. 5, June 1995.

[15] H. Balakrishnan, S. Seshan, and R.H. Katz, "Improving reliable transport and handoff performance in cellular wireless networks", ACM/Baltzer Wireless Networks J., vol. 1,no. 4, Dec. 1995.

[16] J.H. Hu and K.L. Leung, "Hierarchal cache design for enhancing TCP over heteregeneous networks with wired and wireless links", in proc. Globecom 2000, Nov. 2000.

[17] M. Meyer. Analytical Model for TCP File Transfers over UMTS, 3Gwireless'01, 2001.

[18] R. Ludwig, B. Rathonyi, A. Konrad and A. Joseph, "Multi layer tracing of TCP over a reliable wireless link", ACM Sigmetrics 99, May 1999.

[19] M. Yavuz and F. Khafizov, "TCP over Wireless Links with Variable Bandwith", proc. of IEEE VTC, Sep. 2002.

[20] G. Xylomenos, G.C. Polyzos, P. Mahonen and M. Saaranen, "TCP Performance issues over Wireless Links", IEEE Commun. Mag., pp 52-58, Apr. 2001.

[21] H. Balakrishnan, V. Padmanabhan, S. Seshan, M. Stemm, and R. H. Katz, "A Comparison of mechanisms for improving TCP performance", IEEE/ACM Transactions on Networking, vol.5, pp. 756-769, Dec. 1997.

[22] N.M. Chaskar, T.V. Lakshman and U. Madhow, "TCP over wireless with link level error control: Analysis and design methodology", IEEE/ACM Trans. Networking, vol.7, pp. 605-615, Oct. 1999.

[23] J.W.K. Wong and V.C.M. Leung, "Improving end to end performance of TCP using link layer retransmissions over mobile internetworks", in proc. ICC, 1999, pp.324-328.

[24] Y. Bai, A.T. Ogielski and G. Wu, "Interaction of TCP and radio link ARQ Protocol," in proc. IEEE VTC, 1999, pp. 1710-1714.

[25] K.Y. Wang and S.K. Tripathi, "Mobile end transport protocol: An alternative to TCP/IP over wireless links", in proc. INFOCOM, 1998, pp. 1046-1053.

[26] E. Hossain, D.I. Kim and V.K. Bhargava, "Analysis of TCP Performance under joint rate and power adaptation in multi cell multi rate WCDMA Packet data Systems", IEEE Transactions on Wireless Communications, vol. 3, no. 3, May 2004.

[27] J. Peisa and E. Englund, "TCP Performance over HS-DSCH", pro. of VTC'02, vol. 2, pp. 987-991, May 2002.

[28] P.J. Ameigeiras Gutierrez, "Packet Scheduling And QoS in HSDPA", Ph.D. Thesis, Aalborg University, Oct. 2003, ISBN: 8790834380.

[29] R. Bestak, "Reliability Mechanisms (Protocols ARQ) and their Adaptation in 3G Mobile Networks", (French title: "Les mcanismes de fiabilisation (protocoles ARQ) et leur adaptation dans les rseaux radiomobiles de 3G"), Ph.D. Thesis, ENST Paris, 18 Dec. 2003. http://pastel.paristech.org/archive/00000514/01/RBestakThese.pdf

[30] Mun Choon Chan and Ram Ramjee, Improving TCP/IP Perfornance over Third Generation Wireless Networks, INFOCOM04, Hong Kong, March 2004.

[31] Mun Choon Chan and Ram Ramjee, TCP/IP Performance over 3G Wireless Links with Rate and Delay Variation, ACM Mobicom02, Atlanta, GA, Sep. 2002

[32] J. PADHYE, V. Frnoiu, D. TOWSLEY, and J. KUROSE, "Modeling TCP throughput: A simple model and its empirical validation," In Proc. of ACM SIGCOMM (1998).

[33] J. PADHYE, V. Frnoiu, D. TOWSLEY, and J. KUROSE, "Modeling TCP throughput: A simple model and its empirical validation," IEEE/ACM Transactions on Networking, vol. 8, issue 2, April 2000, pp. 133-145.

[34] N. Cardwell, S. Savage, T. Anderson, "Modeling TCP Latency", In Proceedings to IEEE INFOCOM 2000, Volume 3, 26-30 March 2000, pp. 1742-1751.

[35] Finalising TFRC reference list and uplink signalling definition, 3GPP input paper TSGR1 24(02) 2002.

Chapter 6

Scheduling of Streaming Services in HSDPA

Streaming is a popular technology widely developed and used in the internet to convey multimedia application (e.g., audio, video clip, etc.) to mobile users. This type of application is supposed to occupy a large share of the third generation system bandwidth. The fundamental characteristic of this applications class is to maintain traffic jitter under a specific threshold. Jitter relates to the time relation between received packets. This threshold depends on the application, the bit rate and the buffering capabilities at the receiver. The use of a buffer at the receiver smoothes traffic jitter and reduces the delay sensitivity of the application. At the receiver, the client plays at a constant rate the video sequences stored in the buffer. A typical buffer capacity at the receiver is 5 s. This means that the application streams could not be delayed in the network more than 5 s. If the buffer is empty, due to jitter and delay latency, the application will be paused until enough packets to play are stored in the buffer. Typical examples of the streaming application softwares are Real Player and Windows Media Player that are able to play audio and video streaming.

In the UMTS release 99, streaming services are conveyed over dedicated channels which guarantee the respect of the delay and jitter constraints. In HSDPA, streaming applications are transmitted over the HS-DSCH channel which requires the use of an appropriate scheduler suitable for this kind of applications.

In the literature, only few studies have been conducted in order to enable the transmission of streaming services over HSDPA (e.g., [1-3]). The most significative contributions in this context are presented in section 6.2.

In this chapter, we have conducted a study on the scheduling algorithms for streaming services in the UMTS HSDPA system. The objective is to see if these algorithms are suitable for streaming services. Suitable for streaming means that these algorithms can achieve an acceptable cell capacity while offering streaming services with fixed reading rates (i.e. CBR 128kbps). In addition, a new scheduler, more appropriate for handling streaming services, has been suggested in this study to alleviate the weaknesses observed and encountered for the existing schedulers. Due to the traffic nature and time constraints of streaming data, it is very complicated to conduct this scheduling analysis by statistical models. This study is consequently achieved via network simulations developed for and conducted using NS2 (an open source network simulator). Selected sources in the simulations operate at 128 kbps as CBR streaming traffic. The entire end to end path from the applications in the UE to the source side (in the network) is implemented. Since a 5 second buffering capability in the UE terminal is assumed, particular attention was given to the evaluation of the average bit rate over 5 second intervals in order to decide if the connection can handle streaming services or not. Results show that the proportional fair is not suitable for streaming traffic. The bit rate fluctuations over time do not allow offering streaming services with acceptable cell capacity. In addition, simulations conducted assess the performance of this new scheduler and show that it can outperform the existing schedulers in terms of achieving a better trade-off between scheduler efficiency and cell capacity, in other words guaranteeing the QoS constraints of streaming services without losing much cell capacity.

These studies has been conducted in the context of a research project with France Telecom Research and Development (FTR&D). The studies described and presented in this chapter correspond only to the public part of this project.

6.1 Streaming Services

The most suitable protocol stack to handle streaming services is RTP/RTCP/UDP (Real Time protocol, Real Time Control Protocol) since it can achieve low delays and jitter. However, streaming is carried in certain cases over TCP protocols (e.g., network containing fire- walls requiring use of TCP, non live streaming applications which are completely downloaded before being played, etc..). The use of retransmission mechanisms is acceptable as long as the number of retransmissions and the overall delay are limited. The use of Hybrid Automatic Repeat Request (HARQ) mechanism in the Medium Access Control - high speed (MAC-hs) sublayer in HSDPA (High Speed Downlink Packet Access) is acceptable. The ARQ protocol of the Radio Link Control (RLC) sublayer is however not suitable for this class

of applications due to the important delays introduced in the received information. Concerning the tolerated error rates at the receiver, the target or limit Bit Error Rate (BER) can vary between 5.10^{-2} and 10^{-6} depending on the application as indicated in the 3GPP specifications [4-5].

6.1.1 Streaming Session protocols

A Streaming Session is enabled by a set of protocols in charge of session establishment, set-up, session control, data transport and session release [3-4].

The session establishment consists of a primary Packet Data Protocol (PDP) context request sent by the application in the UE. This primary PDP context will convey the session control signalling (Real Time Streaming Protocol, RTSP). The client shall initiate the provisioning of a bearer with appropriate QoS for the streaming media. The set up of the streaming service is done by sending an RTSP SETUP message for each media stream chosen by the client. Then, a secondary PDP context is set-up with a UMTS QoS profile for streaming class. Through this PDP context, the streaming data flow (Real Time Protocol, RTP) and signalling feedback with the quality of the distributed data (Real Time Control Protocol, RTCP) will be conveyed (see [3]). Then, the client sends a RTSP PLAY message to the server that starts to send one or more streams over the IP network. To stop the stream delivery from the media server, a teardown request shall be sent by the client. Note that the Transport layer protocol used during the packet streaming transmission and control is the User Datagram Protocol (UDP) (for more details see [3-5]).

The User Datagram Protocol (UDP) is a transport protocol provided by the IP protocol stack and used in data networks to carry various application services. UDP transmits segmented data, provided by the application layer, as independent datagrams. UDP is a datagram-oriented protocol. In addition, UDP is connectionless and does not implement connection establishment and connection termination. There is no flow control which may generate buffer overflow in UDP either. UDP is not a reliable transport protocol as it does not implement any retransmission or recovery mechanisms. Hence, errors or datagram losses during transmission are not corrected.

The major use of UDP is in the transport of real time multimedia services, due essentially to the tight delay constraints that characterize this type of applications. Since no error recovery mechanisms are used in UDP, robustness has to be built into the application and the source encoder. In this context the Real Time Protocol (RTP) has been developed for real time interactive communications (e.g. streaming). RTP includes a sequence number field to the RTP packets in order to detect packet

losses and to restore the packet sequence. In addition, RTP frames the data to be delivered to UDP, allows the synchronization at the receiver and removes the delay jitter caused by the network.

6.1.2 Streaming Video Encoding

Rate control strategies for video coding can be classified into constant bit rate (CBR) and variable bit rate (VBR) [3,5]:

- Constant Bit Rate (CBR) Encoding: this video encoding strategy smoothes out the bit rate variations from the video source and generates therefore constant bit rate data flows. This technique is suitable for low end-to-end delay communications since it does not require any Pre decoder or Post decoder buffering at the receiver. Due to the variable rate nature of video compression and to the attempt of trying to maintain a constant rate, CBR rate controls try to limit the number of bits used for compressing each picture in a video sequence. The final quality of the compressed video stream depends then on the complexity of the content. Consequently, CBR encoding works fine for constant complex scenes and presents a degraded perceived quality for scenes with varying coding complexity.

- Variable Bit Rate (VBR) Encoding: this video encoding strategy generates variable bit rate data flows. However, it provides a constant user's perceived image quality for arbitrary video sequences containing scenes with varying coding complexity.

In this thesis, we are focusing in our study on the 128Kbps CBR video streaming since it is the most streaming service used. The UE buffer size is fixed to a 5 sec (i.e. 80 Kbytes for 128Kbps) to absorb the bit rate variation from video stream.

6.2 Related Work and proposed scheduler

A scheduling algorithm provides successfully streaming application to a user if the following two conditions are respected: 1) the transfer delay and the GBR (Guaranteed Bit Rate) requirements are achieved; 2) the Service Data Unit (SDU) error ratio is kept below a certain threshold manageable for the application (e.g., 1%). Traditional schedulers, such as Proportional Fair or Score Based, do not consider these constraints streaming services. These schedulers are then not suitable for streaming services (this aspect will presented later in section 6.4), and new schedulers should be conceived to offer streaming connections without losing much cell capacity.

In the literature, few references have considered the streaming traffic constraints in the scheduling study over HS-DSCH [1-3]. The most significative studies propose improvements of the proportional fair algorithm. In [1], Barriac and Holtzman propose an improvement of the proportional fair algorithm by introducing a delay dependent priority. For users with a delay "D" below a certain threshold "τ" (e.g. 60% of the deadline) the priority is computed according to the Proportional Fair algorithm, while for users with a delay larger than the threshold, the priority of the Proportional Fair algorithm is modified as follows:

$$\begin{cases} \frac{r}{R} & \text{When } D < \tau \\ \frac{r}{R}\frac{max_j\overline{CQI}_j}{\overline{CQI}_i} & \text{When } D \geq \tau \end{cases} \tag{6.1}$$

where r is the transmission rate in the current TTI (according to the transmission scheme selected) and R is the mean bit rate transmitted in the previous TTIs and evaluated through an exponentially smoothed average according to the PF algorithms. $\overline{CQI}_i$ is the average of the CQI of user "i" and $max_j\overline{CQI}_j$ is the maximum average CQI between the other users.

This scheduler priorities flows with delays larger than the threshold "τ" which reduces the percentage of discarded packets in the node B [3].

In [2], Andrews proposes an interesting solution to deal with the streaming conveyance over shared channel by keeping the probability of the packet delay exceeding the due time below the SDU error ratio δ:

$$max\{-log(\delta)\frac{r}{R}\frac{D}{T}\} \tag{6.2}$$

where "T" is the due time. This solution does not control the user throughput, which, without any further rate control, is fully determined by the input traffic load of the user and the SDU error ratio. This implies that data flows, for example VBR video streams, temporarily raising their bit rate over the GBR would subsequently increase their cell resources consumption without any restriction, which could cause the starvation of the remaining flows in the cell (see [3] for details).

In [3], Ameigeiras propose to combine these two solutions as follows:

$$max\{-log(\delta)\frac{r}{R}\frac{max_j\overline{CQI}_j}{\overline{CQI}_i}\frac{D}{T}\} \tag{6.3}$$

This scheduler takes advantage of the both scheduler strengths and uses them jointly to compensate the drawbacks of each one. The disadvantage the modified PF [1] is compensated by the use of the fraction D/T and the disadvantage of the second scheduler [2] is compensated by the faction $\frac{max_j\overline{CQI}_j}{\overline{CQI}_i}$.

6.2.1 Proposed scheduler

In this thesis, we have proposed a new scheduler for streaming services. The objective is to increase as much as possible the cell capacity while guaranteeing the quality of service of streaming connection. The proposed scheduler consists of modifying the priority as follows:

$$max\{-log(\delta)\frac{r}{\overline{CQI}}\left(1-\frac{\frac{R}{\overline{GR}}}{\sum_{j=1}^{N_u}\frac{R_j}{\overline{GR_j}}}\right)\} \tag{6.4}$$

where R is the achieved bit rate and GR is the required bit rate. The advantage of this algorithm is that it allocates the channel to the user having a compromise between the actual channel conditions (represented by the bit rate), the mean statistical channel conditions ($\overline{CQI}$) and the achieved bit rate according to the required bit rate. To better explain the advantages of this scheduler, we consider the following cases:

- When all the users have the same achieved rate and the same required bit rate, the channel is allocated to the user having the $max(r/\overline{CQI})$ which allows to take advantage of the instantaneous peak in the received signal i.e. to keep track of the fast fading peak in the radio channel.

- When all the users have the same channel conditions, the TTI is then allocated to the user having the most need in bit rate (i.e. highest required bit rate or lowest achieved bit rate) according to the need in bit rate of the other users.

Note that the fraction $\frac{\frac{R}{\overline{GR}}}{\sum_{j=1}^{N_u}\frac{R_j}{\overline{GR_j}}}$ allows to smooth the effect of "the need in bit rates" on the priority evaluation of each users and therefore to improve the cell capacity.

6.3 Network Simulation

In this section, we describe the simulation model adopted in our simulations to evaluate the scheduling performance of the different algorithms described above and show how much they contribute to improve both the overall cell throughput and the user data rates while achieving fairness among users.

The topology used in our simulation consists of both link level and network level simulation. The link-level simulator implements all physical layer aspects of HSDPA as specified by 3GPP (release 5). The network level simulator implements end to end sessions between applications on UE and the core network side. The simulator focuses on MAC (Medium Access Control) and RLC (Radio Link

Control), where high-speed versions of these protocols are implemented for HSDPA according to the 3GPP W-CDMA standard, release 5.

The users are supposed to be uniformly distributed in the cell. Since the network simulator is static, several scenarios are simulated to cover all the possible cases or scenarios (10000 scenarios simulated). Each simulation was run for 500 s giving us 500 s long traces.

Note that the correlation distance of the shadowing is set to 40m and that the users are assumed to move around their geographical position within a short range and the environment is assumed to be variable, which is modeled by a fast fading with independently fading Rayleigh processes, whose power delay profile is described by the ITU Pedestrian A model. A speed dependent Doppler spectrum as given by Clarke and Jakes [6-10] is included in every tap of the power delay profile, and the user default speed is 3 km/h.

The link-level simulator estimates the performance of each single TBS (Transport Block Size). The simulator considers radio communication between the Node-B and the UE using the HS-DSCH, and follows the 3GPP specifications. The simulations assume a full Rake receiver.

The node B transmission power is 42dBm and its antenna gain is 17dBi. The SNR/BLER Matrix file is also an important input file for our simulations. The values in this file correspond to the BLER values 0.0005:0.001:0.9995 and 30 columns, corresponding to CQI values 1 to 30. The values are the SNR values as a function of BLER and CQI. The input file is then fed into the network level simulation (NS2) where the RLC and the MAC-hs are implemented.

The source uses CBR streaming traffic for the simulation. The L2 PDU Header/Payload size is 40 Bytes. The wired core links between GGSN and node B are 20 Mb/s in bandwidth and 10ms in propagation delay. The switching and the processing delays in the SGSN and GGSN are around 5ms. The physical layer encodes PDUs in a TTI and thus bit errors happen per TTI.

6.4 Results

First, it is important to note that we have fixed the geographical positions of two users: one at 200m and the other at 800m from the node B. The other users are selected in such a way to have a uniform distribution in the cell. The radio channel is assumed to be a composite uncorrelated multipath/shadowing channel with amplitude following a Rayleigh distribution. The simulation is repeated for 10000 scenarios where each scenario corresponds to a given distribution of the users in the cell. To get the maximum number of streaming users, we evaluate the average bit rates over 5 seconds and we plot the CDF of

these bit rates variation. For example, for each user and each scenario, the simulation duration is 500 s (i.e. 100 of 5 s intervals). By evaluating the mean bit rate over 5 s, we can get 100 values of the mean bit rate. By repeating the simulation 10000 times (for 10000 scenarios), we can get 1000000 values of 5 seconds average bit rates. We plot then the CDF to see the number of times the bit rate during 5 s is less than a given value (128 kbps). To get the maximum number of users, we repeat this procedure for several number of users. The CDF of the user at 800 m is decisive since it indicates whether the streaming can be used for this user or not. If not, the number of users should be then decreased.

First, the mean cell throughput in the case of streaming services experiences great losses compared to the case when FTP services are used (around 35%). The reason is that the streaming source is limited at 128kbps which results in lack of packets in the transmission buffer for users having good channel conditions. Sometimes the channel is not allocated to the best user (e.g. having the best r/R in the case of PF) since no packets are present in the transmission buffer.

Results, depicted in figures 6.1 to 6.9, show that PF scheduler can not be used for streaming services unless a low capacity and low data rates are accepted in the cells. The bit rate fluctuations for users at 800 m (having relatively bad channel conditions) do not guarantee a normal reading (behavior) of the streaming video at the user UE. The use of higher buffer capacity (more than 5 s) at the receiver and a higher discard timer at the RLC level will increase eventually the number of streaming users but not as much as one would hope. The scheduler described in [3], which an improvement of the modified proportional fair proposed in [1], presents better performance than the PF algorithm. 13 streaming connections can be handled instead of 11 in the case of PF. Figures 6.7 to 6.9 shows that our proposed algorithm outperforms the existing schedulers by handling 14 streaming connections (128kbps) over the HS-DSCH channel.

6.5 Conclusion

The natural conclusion, based on the obtained results in this chapter, is that traditional schedulers such as PF and SB, that achieve a reasonable trade-off between fairness and cell throughput and that are used basically for non real time data, are not suitable for streaming services and a new scheduler is required to deal with the real time constraints of these services. In this context, the new scheduler proposed in this chapter seems to be an interesting approach to handle streaming connections over HSDPA without losing much cell capacity. Results, depicted in section 6.4, show that this scheduler outperforms the existing scheduler in the literature. More research and studies should be pursuing

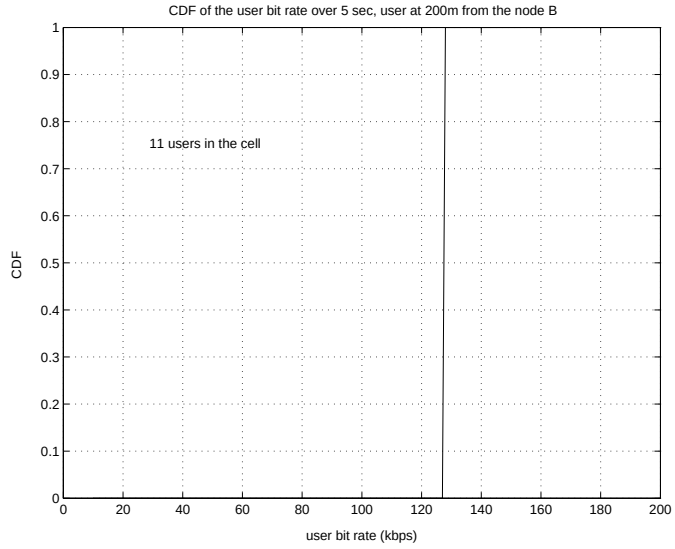

Figure 6.1: CDF of the bit rate over 5 sec of a user situated at 200m from the node B in the case of PF scheduler, 11 users in the cell

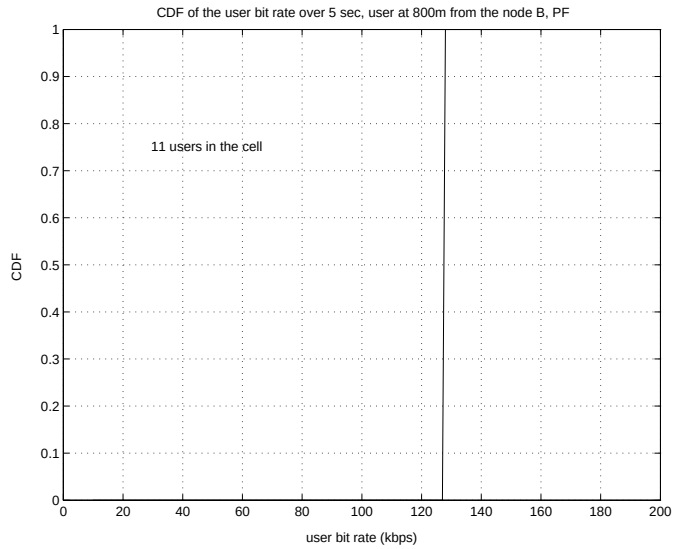

Figure 6.2: CDF of the bit rate over 5 sec of a user situated at 800m from the node B in the case of PF scheduler, 11 users in the cell

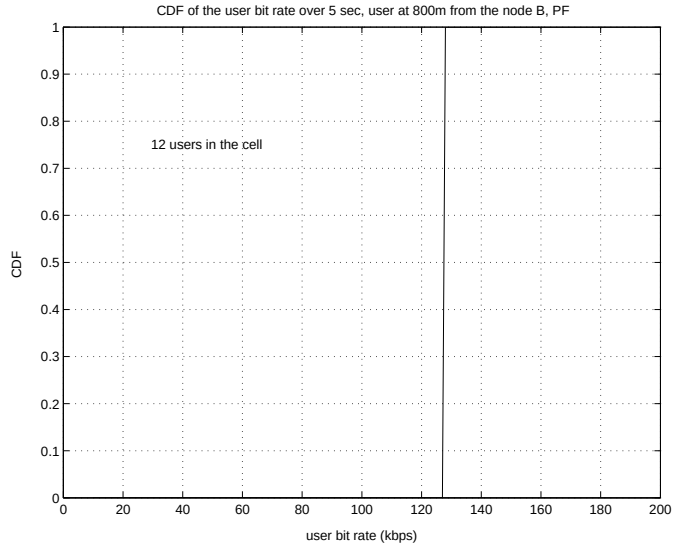

Figure 6.3: CDF of the bit rate over 5 sec of a user situated at 800m from the node B in the case of PF scheduler, 12 users in the cell

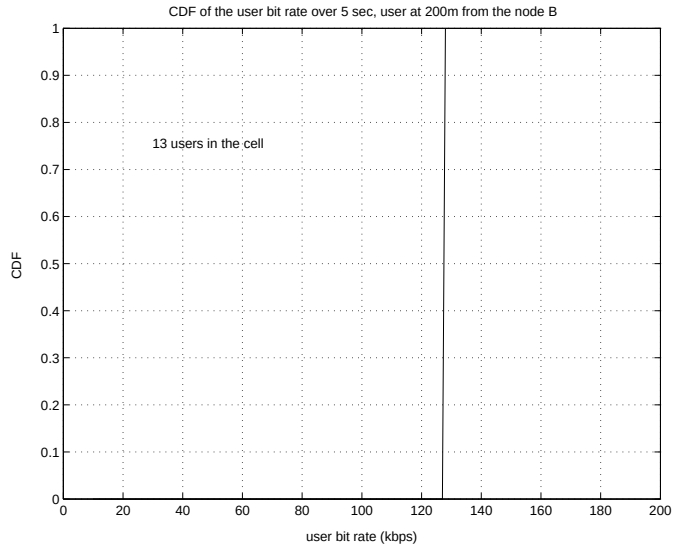

Figure 6.4: CDF of the bit rate over 5 sec of a user situated at 200m from the node B in the case of the scheduler proposed in [], 13 users in the cell

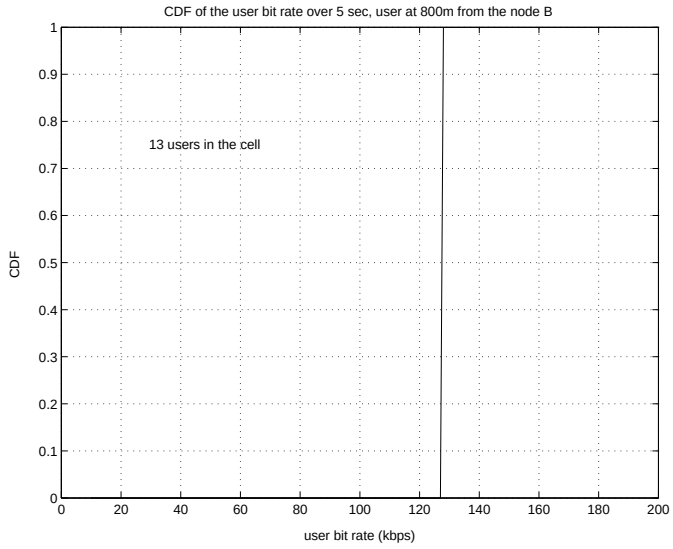

Figure 6.5: CDF of the bit rate over 5 sec of a user situated at 800m from the node B in the case of the scheduler proposed in [], 13 users in the cell

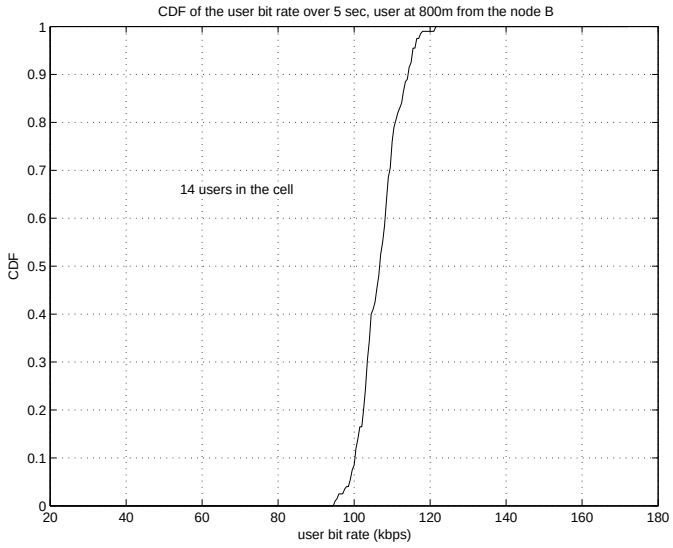

Figure 6.6: CDF of the bit rate over 5 sec of a user situated at 800m from the node B in the case of the scheduler proposed in [], 14 users in the cell

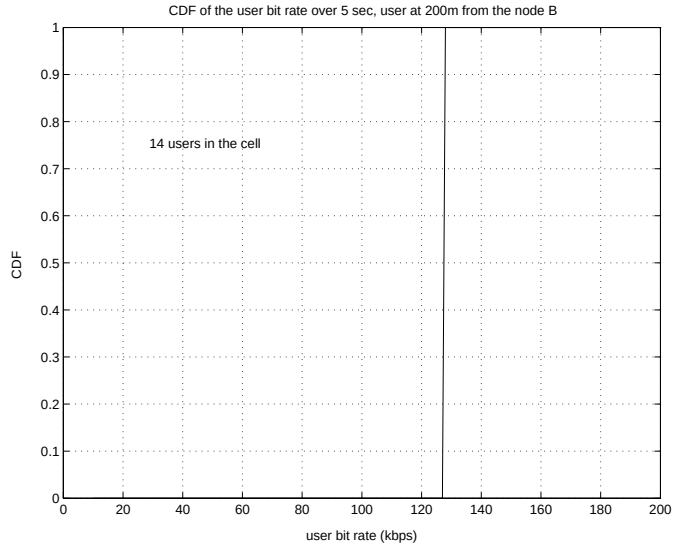

Figure 6.7: CDF of the bit rate over 5 sec of a user situated at 200m from the node B in the case of our proposed scheduler, 14 users in the cell

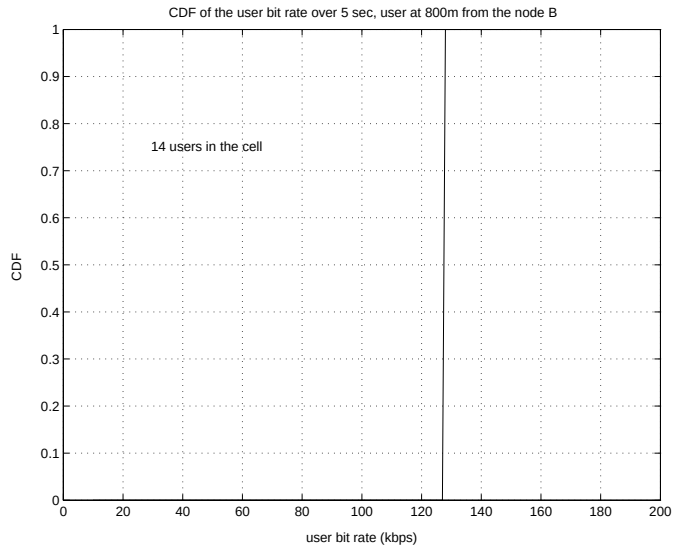

Figure 6.8: CDF of the bit rate over 5 sec of a user situated at 800m from the node B in the case of our proposed scheduler, 14 users in the cell

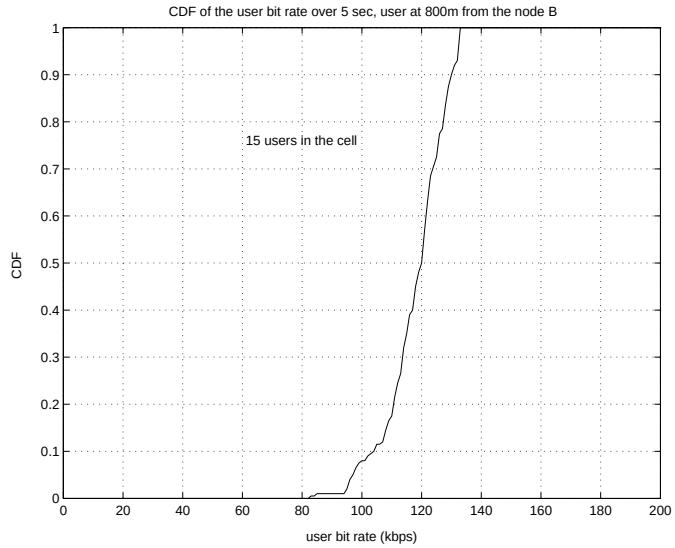

Figure 6.9: CDF of the bit rate over 5 sec of a user situated at 800m from the node B in the case of our propose scheduler, 15 users in the cell

in this direction in order to optimize the resource allocation in HSDPA system with respect to the traffic QoS constraints. Besides, the case of multi-services (simultaneous use of non real time data and streaming services) should be considered also.

Bibliography

[1] G. Barriac and J. Holtzman, "Introducing Delay Sensitivity into the Proportional Fair Algorithm for CDMA Downlink Scheduling," IEEE Seventh International Symposium on Spread Spectrum Techniques And Applications, ISSSTA 2002 , Volume 3, 2002, pp. 652-656.

[2] M. Andrews, K. Kumaran, K. Ramanan, A. Stolyar, P. Whiting, and R. Vijayakumar, "Providing quality of service over a shared wireless link," IEEE Communications Magazine, vol. 39, no. 2, pp. 150-154, Feb. 2001.

[3] P.J. Ameigeiras Gutierrez, "Packet Scheduling And QoS in HSDPA", Ph.D. Thesis, Aalborg University, Oct. 2003, ISBN: 8790834380.

[4] 3GPP TS 26.233 version 4.2.0, "Transparent end-to-end Packet-switched Streaming Service (PSS); General Description".

[5] 3GPP TR 26.937 version 1.2.0, "Transparent end-to-end Packet switched Streaming Service (PSS); RTP usage model".

[6] W. C. Jakes, Ed., Microwave Mobile Communications, John Wiley and Sons, New York, 1974.

[7] Theodore S. Rappaport, Wireless Communications: Principles and Practice, Prentice Hall, 2002, ISBN 0-13-042232-0.

[8] J. D. Parsons, Radio Wave Propagation, in Land Mobile Radio Systems, R. J. Holbeche, ed. London: Peter Peregrinus, Ltd., 1985.

[9] J. D. Parsons, The Mobile Radio Propagation Channel, John Wiley and Sons, 1992.

[10] ITU Recommandation, Guidelines for Evaluation of Radio Transmission Technologies for IMT-2000 ITU-R M.1225, 2450,1997.

Chapter 7

Conclusions and Future Work

In this chapter, we summarize the research presented in this dissertation and present directions for future work.

7.1 Summary of Research

The study of the cross layer interactions in HSDPA system has formed the focus of the conducted research during this thesis. HSDPA or High Speed Downlink Packet Access is an evolution of the UMTS standard to achieve higher aggregate bit rates on the downlink and offer Internet and multimedia based services. A number of enhanced techniques such as Hybrid ARQ, Adaptive Modulation and Coding or AMC and fast scheduling over time shared channels are introduced into the standard to achieve this evolution and enable flexible and adaptive packet transmissions. The performance and efficiency of these introduced techniques depends upon the radio channel conditions and the interaction of these techniques with the upper layers (TCP, application). Retransmission mechanisms relying on ARQ and scheduling interact with higher layer protocols, especially the Transport Control Protocol (TCP) used in conjunction with IP to offer non real time services, as well as with the stringent QoS constraints of the streaming services conveyed on RTSP/RTP/IP. These cross layer interactions can have a drastic impact on overall throughput and capacity. Care are taken in this thesis to characterize these interactions and suggest ways of preventing or at least reducing any negative effects resulting from these interactions. The following sections draws the conclusions of the main contributions and investigations in each chapter.

7.1.1 Effect of radio channel models on HSDPA performance (chapter 3)

This chapter studied analytically the effect of wireless fading on the performance of various schedulers in HSDPA system. This study has been conducted using statistical models of wireless channel fading. The proposed analytical models estimate cell throughput and user bit rate and enable performance comparisons between schedulers.

The user bit rate and cell capacity estimation requires the introduction into the model of the techniques used in HSDPA, in particular AMC, HARQ and scheduling. In addition, derivation of the analytical expressions requires the description of the channel model, the receiver type and an approximate expression of SIR (Signal to Interference Ratio). Several statistical channel models are considered in the study. The cases of composite uncorrelated and correlated (correlation equal to 0.3, 0.5 and 0.7) multipath/shadowing channels with path amplitude following Rayleigh and Nakagami (m=2 and 4) distributions are investigated. The case of composite dense uncorrelated and correlated multipath/shadowing channel is also studied. This last case considers the presence of Wide-sense Stationary channel, constant Power Dispersion Profile (PDP) and frequency selective fading following a Rayleigh distribution.

Results obtained of the Cumulative Distribution Function (CDF) of user bit rate and average cell throughput indicate a decrease of system performance of 5% when the correlation increases from 0 to 0.7 without as much affecting the degree of fairness of the studied schedulers. In addition, when the Nakagami parameter m increases from 2 to 4, the system performance increases of approximately 6%. Consequently, the comparison between the schedulers in HSDPA, conducted for a given fading model, can still be valid in other wireless conditions and fading models even if the user bit rate and cell throughput change in these new conditions. Besides, the obtained results show that the proportional fair algorithm is the best trade-off between fairness and cell throughput compared to the other schedulers studied in this chapter. finally, the results obtained by the analytical models are compared to those obtained via simulation. A deviation of 5 to 8% between these results allow to assess the accuracy of the analyses conducted in this chapter.

7.1.2 Interaction of HSDPA services with Circuit Switched services transmitted on UMTS R99 (chapter 4)

The 3GPP specifications allow the use of CS services on the Dedicated Physical Channels (DPCHs) in parallel to HSDPA users. This requires the introduction of priority policies between CS and HSDPA

services. Such policies can be found according to the effect that CS services have on the capacity of HSDPA. The analysis conducted in this chapter can assess such effects and can be used to deduce such appropriate policies. This chapter characterizes analytically the interaction of CS services conveyed on the dedicated DPCH channels of the release 99 on the HSDPA performance. A network level simulation, implemented in NS-2, is used to evaluate the accuracy of the analytical models. HSDPA throughput variations according to the number of CS users and soft handover margins (MSH) are reported. In addition, the CDF of user bit rate in the presence of simultaneous CS users and for various radio fading channel models are depicted. The results of the analytical model are close to those obtained via simulation.

7.1.3 Interaction of MAC-hs and schedulers with TCP protocol (chapter 5)

The introduction of new features in HSDPA such as HARQ and scheduling unavoidably interact with higher layer protocols, especially the Transport Control Protocol (TCP) used in conjunction with IP to offer non real time services. TCP that relies on a retransmission mechanism and flow control (variable transmission window size and congestion control mechanism) misinterprets the delays generated by the HARQ and scheduling techniques on the HS-DSCH channel as network congestion. This results in transmission window size shrink and unnecessary packet retransmissions and consequently in drastic decrease of user throughput.

This chapter proposes analytical models to determine the effect of TCP on the UMTS-HSDPA system performance. Cell capacity and user bit rate are evaluated analytically by combining the analytical model proposed in this chapter to the analysis conducted in the chapter 3. Even though the proposed model can be applied in the cases of RR, FT, Max C/I, PF and SB schedulers, we are focusing in this chapter on the PF scheduler since it represents an acceptable trade-off between fairness and cell capacity (compared tot the other schedulers). Network simulation is also conducted to assess the accuracy of the analytical model. Insight on the HSDPA system behavior and interactions with TCP is provided. The effect of TCP on application performance results in a loss of efficiency and fairness of the proportional fair scheduler. A loss of user bit rate of 24% and 15% respectively for the user at 800 and 200m at a TCP congestion rate of 3% (an acceptable value). The overall cell throughput presents a loss of 20.5% at a congestion rate of 3%. Analyzing the results, a new scheduler is proposed at the end of this chapter. This scheduler allows to mask as much as possible the radio impairments and reduce the unnecessary TCP timeouts resulting thus in reducing the TCP throughput degradation. Results afforded by this

scheduler indicate a loss in cell capacity not exceeding 10% for a TCP congestion rate of 3% and a loss of user bit rate lower than 16% for a user at 800m and 9% for a user at 200m for a congestion rate of 3%. Finally, the results obtained in this chapter shows that in HSDPA it is possible to reduce the effect of TCP in a Wireless system, by using the shared channel with an appropriate scheduler.

7.1.4 Interaction of MAC-hs and schedulers with Streaming services (chapter 6)

Streaming, a popular technology widely developed and used in the internet to convey multimedia application (e.g., audio, video clip, etc.) to mobile users, is supposed to occupy a large share of the third generation system bandwidth. The streaming services are generally characterized by stringent Quality of Service QoS requirements (e.g., delay, jitter, etc.). This chapter focuses on the possibility to transmit streaming traffic on the HS-DSCH channel using an appropriate scheduler. Therefore, the interaction of MAC-hs and existing schedulers (in particular the proportional fair scheduler) with Streaming services have been studied and the results are reported. Analyzing these results, we can conclude that traditional schedulers such as PF and SB, that achieve a reasonable trade-off between fairness and cell throughput and that are used basically for non real time data, are not suitable for streaming services. The stringent real time constraints of these services generate a drastic loss in the cell throughput. Consequently, a new opportunistic scheduler is proposed in this chapter to deal with the real time constraints of these services without losing much cell throughput. Results afforded for this scheduler are promising. This algorithm outperforms the existing scheduler in the literature.

7.2 Future Research

Many avenues are open to pursue the research carried out in this thesis. The analytical framework developed in this thesis opens the path for additional investigation and modeling. Herein some lines of possible investigations:

- Introduction of the HTTP traffic model for non real time data in the analysis and modeling of the scheduling performance to obtain an end-to-end analytical model (PHY,MAC, RLC, TCP and traffic model).
- Introduction of real power control for circuit switched services while studying the effect of CS services on HSDPA is an extension of the thesis results to move beyond an assumed perfect power control.

- Analysis and characterization of the effect of mobile speed on the performance of AMC and scheduling in HSDPA. A sensitivity analysis should be done in this case since the radio channel will change more quickly. During the delay between the radio conditions estimation and the transmission over the HS-DSCH channel, the radio conditions can vary which results in a loss of HSDPA performance.

- The studies on the impact of variable delays, caused by schedulers over reliable (ARQ) time shared channels, on TCP performance appear as a promising approach to effectively reduce the TCP throughput degradation in wireless systems. These types of analyses should be pursued to exploit even further user diversity (users experience different random short term channel variations), to maximize the overall system throughput, reduce TCP performance degradations and achieve fairness among TCP flows. Accomplishing this joint optimization remains a challenge that requires an extended definition of metrics to achieve overall tradeoff in terms of efficiency and fairness.

- The results of the thesis provide a good basis to define ways forward for HSDPA systems that introduce multiple antenna systems and especially MIMO systems. The same holds for the introduction of multi-user detection in the analytical framework. The framework lends itself easily to this extension by replacing the RAKE receiver by a multi-user detector. Adapting the SIR expression is envisaged to extend the analytical model.

- Finally, call admission control can also be introduced in the analytical expression for the scheduling studies.